Appendix C

Geotechnical, Subsidence and Caving Assessment for 918 Panel (SCT 2026)

EMM
creating opportunities

SCT OPERATIONS PTY LIMITED

Strata Control Technology

CENTENNIAL COAL COMPANY PTY LTD

Geotechnical, subsidence and caving assessment for 918 Panel

CLR5894

SCT Operations Pty Ltd PO Box 824 Wollongong NSW 2520 Australia
Phone: +61 2 4222 2777 Email: sctnsw@sct.gs Website: www.sct.gs
ABN: 23 078 328 953

REPORT TO Peter Corbett
General Manager Technical Operations
Centennial Coal Company Pty Ltd
1384 Castlereagh Highway
Lidsdale NSW 2790

TITLE Geotechnical, subsidence and caving assessment for 918 Panel

REPORT NO CLR5894

PREPARED BY Yvette Heritage

DATE 24 April 2026

Yvette Heritage
Managing Director/
Principal Geotechnical Engineer

Report No	Version	Date	Revisions
CLR5894	Draft	19 May 2025	
CLR5894	Draft V2	24 June 2025	
CLR5894	Draft V3	15 July 2025	
CLR5894	Final	22 July 2025	
CLR5894	Rev1 Draft	21 November 2025	
CLR5894	Rev1 Draft2	17 February 2026	
CLR5894	Final Rev1	19 February 2026	
CLR5894	Final Rev2	24 April 2026	

EXECUTIVE SUMMARY

Centennial Coal Company Pty Ltd are applying for an Extraction Plan approval under development consent DA 504-00 and federal approval under the Environmental Protection Biodiversity Conservation (EPBC) Act to extract second workings from 918 Panel within the Katoomba Seam. 918 Panel is proposed to be extracted using the shortwall mining method. Clarence Colliery has a subsidence impact assessment criteria of 100mm vertical subsidence in the DA-504-00 development consent area. This report assesses the proposed 918 shortwall mining layout geometry in relation to caving, subsidence, groundwater interaction and pillar stability.

Centennial has chosen a conservative approach to not undertake secondary extraction directly below most of the swamps above the 918 Panel. As such, 918A Panel is shortened in the North, and 918B is split into B1 and B2 panels. 918B1 Panel has a panel void width of 83m, while the adjacent 918A and 918B2 have 75m void widths. The panels are separated by a spine pillar system with a minimum combined pillar and roadway width of 83m.

Numerical modelling estimates a maximum surface subsidence of 76mm ± 20mm tolerance due to natural variability and survey tolerance. The numerical model used for this assessment of two shortwall panels has been validated with Clarence 910-906 Panels. Numerical modelling has been successful in understanding the subsidence mechanisms and informing mine design at Airly Mine. An addendum with updated subsidence modelling to address model geometry improvements, key geotechnical assumptions and an uncertainty analysis produced subsidence less than the original maximum subsidence. It is recommended that the original subsidence outcomes in this report be used for ongoing assessment as the more conservative outcome of the modelling assessments.

The groundwater system at Clarence Colliery consists of an upper (shallow and perched) water table and a lower (deep) water table. The groundwater data indicates that the Mt York Claystone forms the lower boundary of the upper water table. The lower water table shows a hydraulic head above the Katoomba Seam well below the Mt York Claystone. There is however a hydraulic connection between the upper and lower water tables that suggests downwards flow/recharge from the upper water table to the lower water table. This is inferred by the non-hydrostatic pore pressure observed in piezometers located between the Mt York Claystone, and the hydrostatic component of the lower water table. The Mt York Claystone is approximately 110m above the 918 Panel mining horizon in the Katoomba Seam.

The modelling assessments indicates mining induced caving fractures extending to a maximum of 90m above the mining horizon. The vertical conductivity is not expected to change significantly above this caving height. Horizontal bedding fractures are likely to occur above the height of caving and often present in groundwater monitoring as a short-term volumetric pore pressure reduction that recovers.

A height of total depressurisation of 46m ± 25m is estimated using the Tammetta (2012) empirical approach. The Ditton and Merrick (2014) approach of determining the A-Zone, where water freely drains, estimates a height of 52-66m, slightly greater than Tammetta's height of total depressurisation and within range of the model caving height (60-90m).

Clarence experience and groundwater observations of from partial pillar extraction using single and double-sided lifting indicates that these mining methods do not reduce the pore pressure in the upper water table with similar panel widths. It is anticipated that pore pressure reduction is likely to occur below the Mt York Claystone however, pore pressure is not anticipated to reduce in the upper water table. A level of downwards flow, similar to pre secondary extraction levels, is anticipated to occur from the upper water table via the existing natural joint network and geological structures.

It is understood that Centennial experience of mining below the Pagoda Swamp above 906 Panel has not produced a discernible reduction in the Swamp water table with vertical subsidence of 100-130mm at the surface.

The pillar stability assessment indicates an appropriate pillar design to meet the objectives of subsidence and serviceability, with adequate consideration of long term stability.

TABLE OF CONTENTS

PAGE NO

1. INTRODUCTION

Centennial Coal Company Pty Ltd (Centennial) own Clarence Colliery (Clarence) in the Western Coalfield, NSW, operated by Clarence Colliery Pty Ltd. Clarence Colliery is located approximately 10km East of Lithgow and mines coal underground within the Katoomba Seam. Clarence Colliery is primarily a bord and pillar - partial pillar extraction operation with some historic, full pillar extraction and longwall areas.

Centennial are applying for state Extraction Plan and federal Environmental Protection Biodiversity Conservation (EPBC) approval to undertake secondary extraction of the 918 Panel in its DA-504-00 development consent area. 918 Panel is proposed to be extracted using the shortwall mining method. Clarence has a 100mm subsidence limit in its DA-504-00 development consent area approved for partial extraction and, as such, Clarence are taking a cautious approach to prove the mining method and resulting subsidence effects.

The proposed mine plan for 918 Panel and DA-504-00 area are presented in Figure 1. The adjacent 906, 908 and 910 Panels within council development consent IRM.GE.76 are also presented in Figure 1.

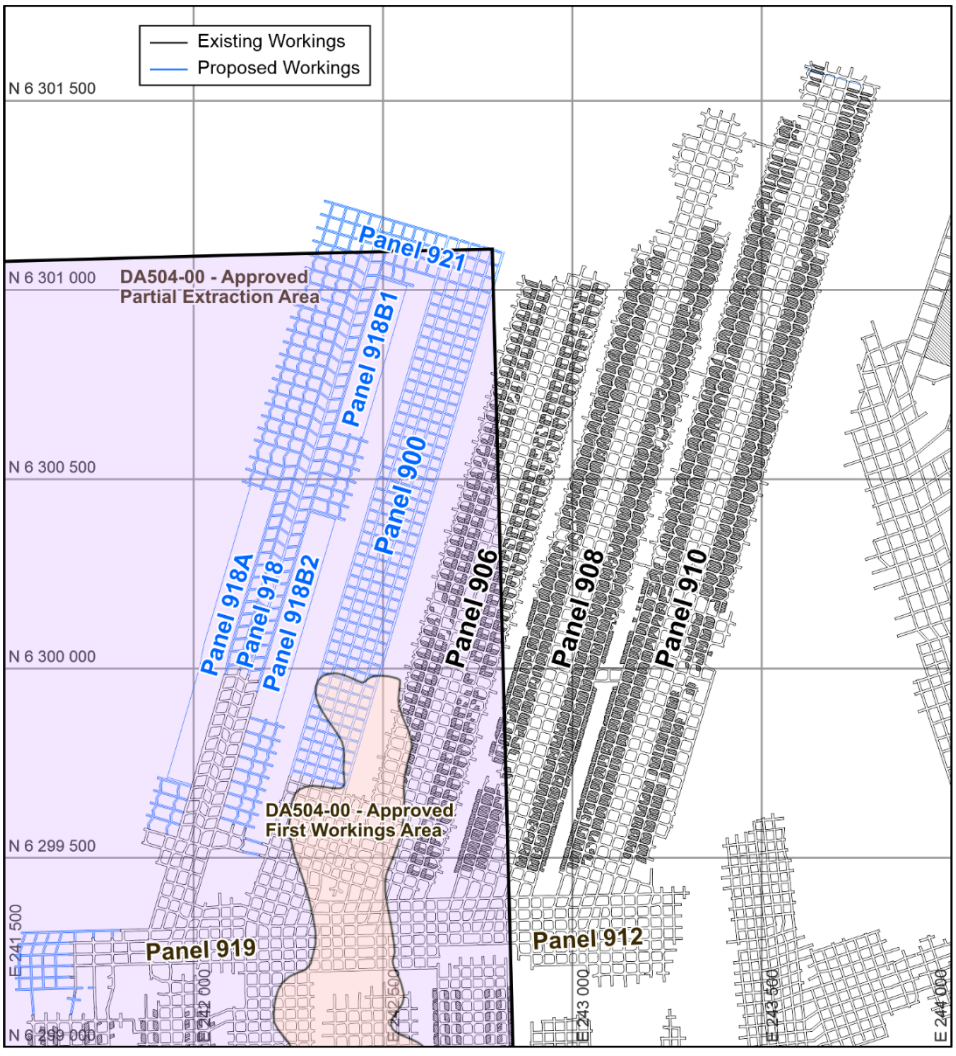

Figure 1: Mine plan showing existing 906, 908 and 910 panels and proposed 900s and 918 panels.

1.1 Scope

SCT Operations Pty Ltd (SCT) were asked to provide a geotechnical assessment of their proposed mining geometry for 918 shortwall and first workings panels for environmental assessment and mining approval processes. Specifically, SCT were engaged to conduct a numerical modelling exercise to assist Centennial in designing a panel geometry for 918 Panel that abides by the maximum 100mm subsidence limit of DA-504-00.

The geotechnical assessment of 918 shortwall panel includes:

- Geological Setting.
- Geotechnical Characterisation.
- Pillar Stability Assessment.
- Literature Review of relevant overburden caving, conductivity and groundwater interaction.
- Overburden Caving and Hydraulic Conductivity Assessment.
- Surface Subsidence Estimates – to feed into a separate subsidence prediction and impacts assessment.

The adjacent 906-910 Panels have been used for comparison and model validation to the 918 Panel assessments given their proximity and similar panel geometries with pillar extraction using double sided lifting.

2. CONCLUSIONS AND RECOMMENDATIONS

This geotechnical report presents assessments supporting the proposed 918 shortwall mine design in relation to caving, subsidence, groundwater interaction and pillar stability.

Centennial has chosen a conservative approach to not undertake secondary extraction directly below most of the swamps above the 918 Panel. As such, 918A Panel is shortened in the North, and 918B is split into B1 and B2 panels. 918B2 Panel has a panel void width of 83m, while the adjacent 918A and 918B2 have 75m void widths. The panels are separated by a spine pillar system with a minimum combined pillar and roadway width of 83m.

Numerical modelling estimates a maximum surface subsidence of 76mm ± 20mm tolerance due to natural variability and survey tolerance. The numerical model used for this assessment of two shortwall panels has been validated with Clarence 910-906 Panels. Numerical modelling has been successful in understanding the subsidence mechanisms and informing mine design at Airly Mine.

The groundwater system at Clarence Colliery consists of an upper (shallow and perched) water table and a lower (deep) water table. The groundwater data indicates that the Mt York Claystone forms the lower boundary of the upper water table. The lower water table shows a hydraulic head above the Katoomba Seam well below the Mt York Claystone. There is however a hydraulic connection between the upper and lower water tables that suggests downwards flow/recharge from the upper water table to the lower water table. This is inferred by the non-hydrostatic pore pressure observed in piezometers located between the Mt York Claystone, and the hydrostatic component of the lower water table. The Mt York Claystone is approximately 110m above the 918 Panel mining horizon in the Katoomba Seam.

The modelling assessments indicates mining induced caving fractures extending to a maximum of 90m above the mining horizon. The vertical conductivity is not expected to change significantly above this caving height. Horizontal bedding fractures are likely to occur above the height of caving and often present in groundwater monitoring as a short-term volumetric pore pressure reduction that recovers.

A height of total depressurisation of 46m ± 25m is estimated using the Tammetta (2012) empirical approach. The Ditton and Merrick (2014) approach of determining the A-Zone, where water freely drains, estimates a height of 52-66m, slightly greater than Tammetta's height of total depressurisation and within range of the model caving height (60-90m).

Clarence experience and groundwater observations of from partial pillar extraction using single and double-sided lifting indicates that these mining methods do not reduce the pore pressure in the upper water table with similar panel widths. It is anticipated that pore pressure reduction is likely to occur below the Mt York Claystone however, pore pressure is not anticipated to reduce in the upper water table. A level of downwards flow, similar to pre secondary extraction levels, is anticipated to occur from the upper water table via the existing natural joint network and geological structures.

It is understood that Centennial experience of mining below the Pagoda Swamp above 906 Panel has not produced a discernible reduction in the Swamp water table with vertical subsidence of 100-130mm at the surface.

The pillar stability assessment indicates an appropriate pillar design to meet the objectives of subsidence and serviceability, with adequate consideration of long term stability.

2.1 Recommendations

It is recommended to install surface subsidence monitoring above the 918 Panels to measure the surface subsidence levels during development and extraction of the shortwall panels. Subsidence monitoring is recommended to include the centre of the shortwall panels and the centre of the spine pillar system to measure the typical maximum subsidence locations. It is also recommended to monitor subsidence outside an estimated half depth angle of draw to measure the effect of subsidence on adjacent workings, or proposed workings.

It is recommended to have a TARP based system in which to monitor and respond to any potential increases in subsidence greater than predicted.

3. EXPLANATION OF TERMINOLOGY AND CONCEPTS USED IN THIS REPORT

The terminology surrounding sub-surface ground movements and groundwater impacts is still evolving and different terminologies are used by different disciplines. The terms used by geotechnical engineers to differentiate zones of deformation within the overburden strata that have different characteristics are commonly confused with the terms that groundwater and other numerical modellers use to describe zones related to groundwater pressure. The terminology used in this report is explained in this section.

3.1.1 Characteristic Zones Based on Ground Deformation

The overburden strata above and adjacent to secondary extraction panels is recognised to be deformed as a result of the pillar extraction process. The shortwall extraction process occurs incrementally with the slice-by-slice retreat of the shortwall face. The deformations that occur also occur incrementally. The deformations from caving are observed to occur within a series of arch shaped zones above each panel as described by Mills (2022) as illustrated in Figure 2. The zones observed are consistent with observations of surface subsidence for a wide range of panel widths and overburden depths and the failure modes of rock strata observed in laboratory tests and are replicated in numerical models.

These zones, working upward from the mining horizon, can be characterised as:

1) A caving zone immediately above the mining horizon (goaf) where the rock strata is completely disturbed by downward movement of close to the full height of the extracted seam. In the proposed shortwall mining case, this zone extends for a few tens of metres above the mining horizon.

2) An arch-shaped zone of large downward movement (ZLDM) that extends to a height above the mining horizon equal to the extracted panel width. The incremental retreat of the longwall face causes fracturing within this zone to be pervasive and steeply dipping in a direction toward the longwall face and other solid goaf edges. Geological and stress variations within the overburden strata influence the height of the ZLDM but only slightly. Measurements of hydraulic conductivity within the ZLDM indicate an increase in vertical hydraulic conductivity above pre-mining conductivities in the range 100 to 1,000,000 times, largely depending on height above mining horizon, mining height and lithology. In this report, the ZLDM is referred to as the caving height.

3) An arch-shaped zone of bedding plane separation (ZBPS) that extends from above the ZLDM to a height above the mining horizon equal to 1.4-1.6 times panel width. The bedding planes separate as a result of rock splitting causing an increase in hydraulic conductivity in a horizontal direction but only a second order increase in a vertical direction.

4) An arch-shaped zone of elastic relaxation (ZER) that extends above the ZBPS to a height of three times the panel width. Hydraulic conductivity is increased as a result of elastic relaxation but only slightly.

5) A zone of compression that extends upward above each chain pillar and other solid coal abutments surrounding extracted longwall panels. Hydraulic conductivity is decreased as a result of this compression.

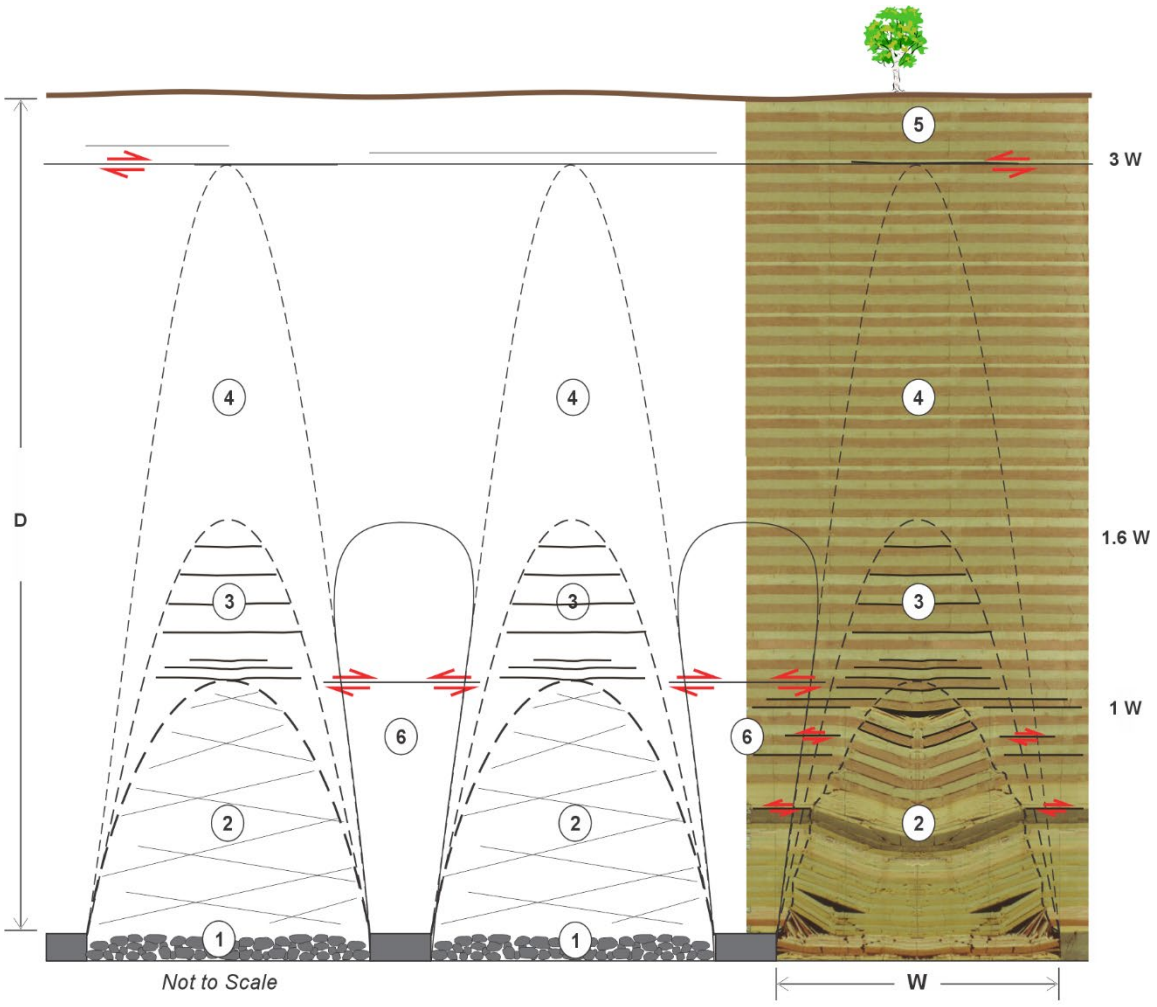

LEGEND

1. Zone of chaotic disturbance (goaf) immediately above mining horizon (0-20m).
2. Zone of large downward movement (≅1.0 x panel width).
3. Zone of vertical opening of bedding planes (1.0W - 1.6W).
4. Zone of vertical stress relaxation (1.6W - 3.0W).
5. Zone of no disturbance from sag subsidence (>3.0W) but shear along bedding planes for subsidence of multiple panels.
6. Zone of compression above chain pillars.

Figure 2: Overburden caving behaviour inferred from surface monitoring and other observations (Mills 2022).

Terms such as height of fracturing, height of conductive fracturing, height of connected fracturing and height of disconnected fracturing are not well-defined, mean different things to different people, and are to be avoided.

3.1.2 Characteristic Zones Based on Groundwater Observations

The pre-mining groundwater system for most coal mining operations is characterised by a profile of water pressure increasing linearly with depth from zero at a depth below surface referred to as the water table and increasing at a rate proportional to the density of water due to gravity. This pressure profile is referred to as a hydrostatic pressure profile meaning zero or minimal flow relative to recharge rate

Underground mining activity creates a zero-pressure horizon at the depth of the mining horizon. In the case of development / first workings, surface recharge from rainfall is usually more than sufficient to replace the small downward flows that occur through the undisturbed overburden strata into the mine and a hydrostatic profile is maintained throughout the overburden section. In some circumstances, such as below hydraulically conductive vertical structures, zero-pressure at the mining horizon is able to disturb the groundwater equilibrium and pore pressure changes are observed within the overburden section from first workings alone. This has not been observed in the Clarence/Springvale complex where there is a separate upper water table to the lower water table where the mining horizon is located.

The presence of a hydrostatic profile does not imply zero downward flow. When a downward gradient is created by the zero-pressure horizon, there is downward flow, with the magnitude of flow governed by the hydraulic conductivity of the strata and rate of recharge to maintain head pressure.

Figure 3 shows the pore pressure profile typically observed post-mining in a single water table scenario. Four groundwater zones are apparent above and to the sides of extracted panels. In the case of Clarence 918 Shortwall Panel, the panels are significantly subcritical where 1 x the panel width (W), Zone of Large Downward Movement (ZLDM) and Height of Depressurisation are below the Mt York Claystone and within the lower water table.

Working upward from the mining horizon, these zones are characterised as:

1) A zone of zero pore pressure that is connected to the zero-pressure horizon created at the mining horizon by mining. This zone extends upward through the fractured overburden strata to a height that Tammetta (2012) has shown can be estimated with a high degree of confidence. This zone, referred to as the height of depressurisation is observed to be proportional to panel width, extraction height raised to the power of 1.4 (effectively the level of ground disturbance caused by mining) and mining depth raised to the power of 0.2 (effectively the magnitude of horizontal stress).

   For most circumstances, in subcritical longwall and shortwall mining geometries, the height of depressurisation is well within the ZLDM, and sensitive to mining height. On this basis, other terms used in the literature such as the height of fracturing, the height of desaturation, height of connectivity, and the height of connected fracturing are confusing, and should be avoided.

   Within this zone of depressurisation, downward flow can occur under the influence of gravity alone if the strata is saturated. Chemical analysis and other considerations indicate that there are added complexities associated with partial saturation. Capillary forces provide an explanation of how water is stored within the partially saturated fracture network at zero pressure despite the action of gravity.

2) A transition zone occurs above the zone of depressurisation is characterised by an upward increase in pore pressure. This increased pressure is necessary to drive downward flow through the saturated, but increasingly less hydraulically conductive fracture network. Top of this zone generally coincides with top of ZLDM. Within this zone the pressure is reducing or "depressurising" with increasing depth. In the case of Clarence 918 Shortwall Panel the ZLDM is below the Mount York Claystone horizon.

3) A hydrostatic gradient above the transition zone indicates the zone where recharge is greater than the downward flow to the mining horizon through the fracture network created by mining. The natural fracture (joint) network and the intact strata is usually much less conductive than the mining-induced fracture networks of the ZLDM.

4) A zone of zero pressure above the groundwater table indicated by zero pore pressure. This zone may contain one or more perched water tables depending on the characteristics of the strata and the disturbance caused by mining.

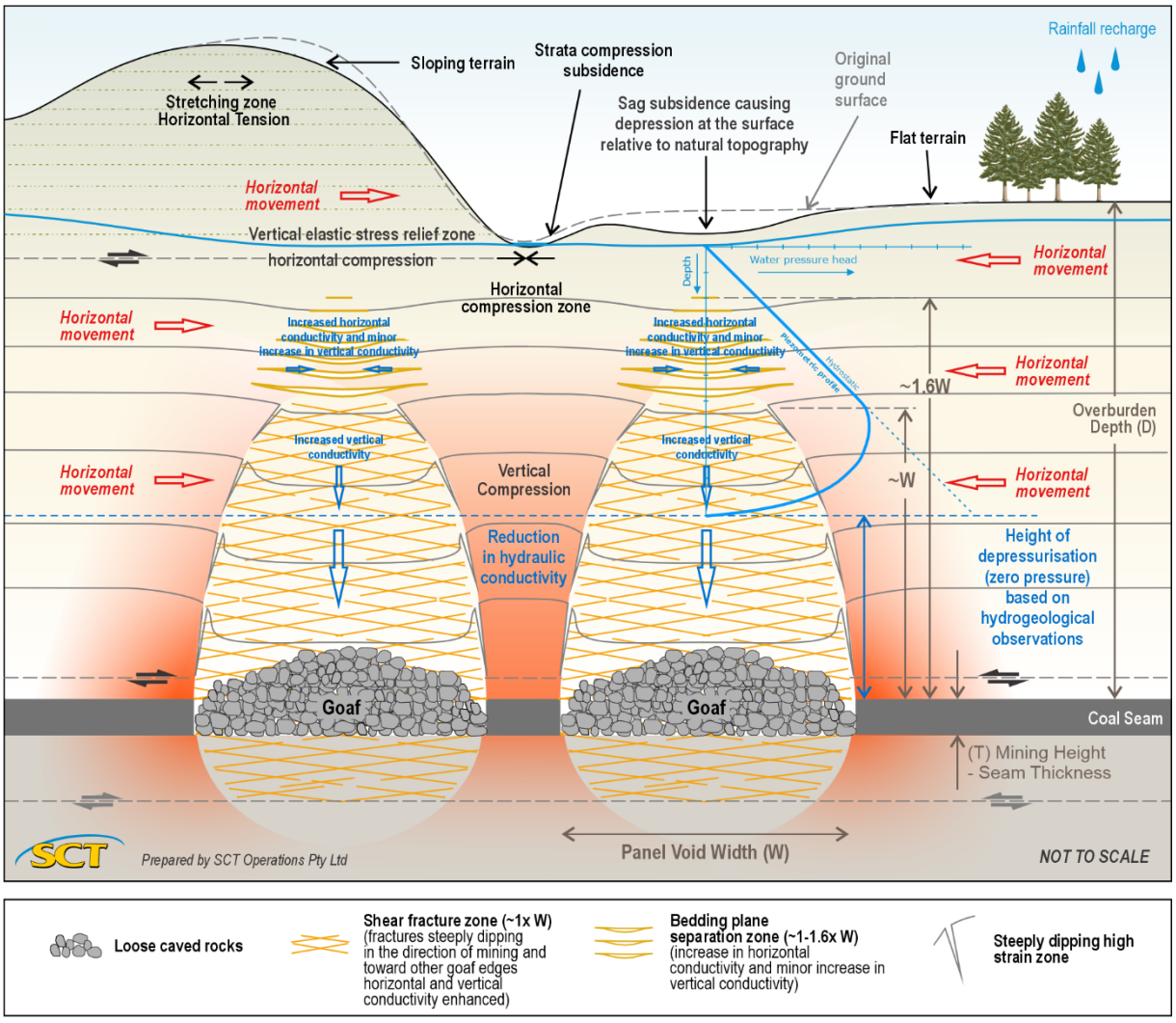

Figure 3: General overburden caving and groundwater behaviour around panels (Mills 2022).

Groundwater models are typically very coarse compared to the scale of individual longwall panels. This coarseness means they are unable to replicate the observed characteristics of these various zones. Artificial drains with zero pressure are turned on within the model to drain all water from the overburden strata to a predetermined height above the mining horizon and then selectively turned off again to match the inflows observed. These model limitations have tended to cloud interpretation of the mechanisms and processes that are observed in the field.

4. PROPOSED MINE GEOMETRY

The proposed mine plan is presented in Figure 1 and shows 918A and 918B shortwall panels separated by a four-heading and three pillar spine pillar system. Centennial has chosen a conservative approach to not mine directly below most swamps above the 918 Panel. As such, 918A Panel is shortened in the North, and 918B is split into B1 and B2 Panels. 918B2 Panel has a panel void width of 83m, while 918A and 918B2 have 75m void widths.

The mining geometry for 918 Panel is presented in Figure 4 for the double shortwall geometry, representing the greatest abutment loading scenario. The shortwall panels are separated by spine pillars with two pillar width scenarios separated by 5.5m wide roadways:

- Cut-throughs 1-20: 26.5m, 20m and 26.5m
- Cut-throughs 21-52: 21-26.5m, 26m and 26.5m.

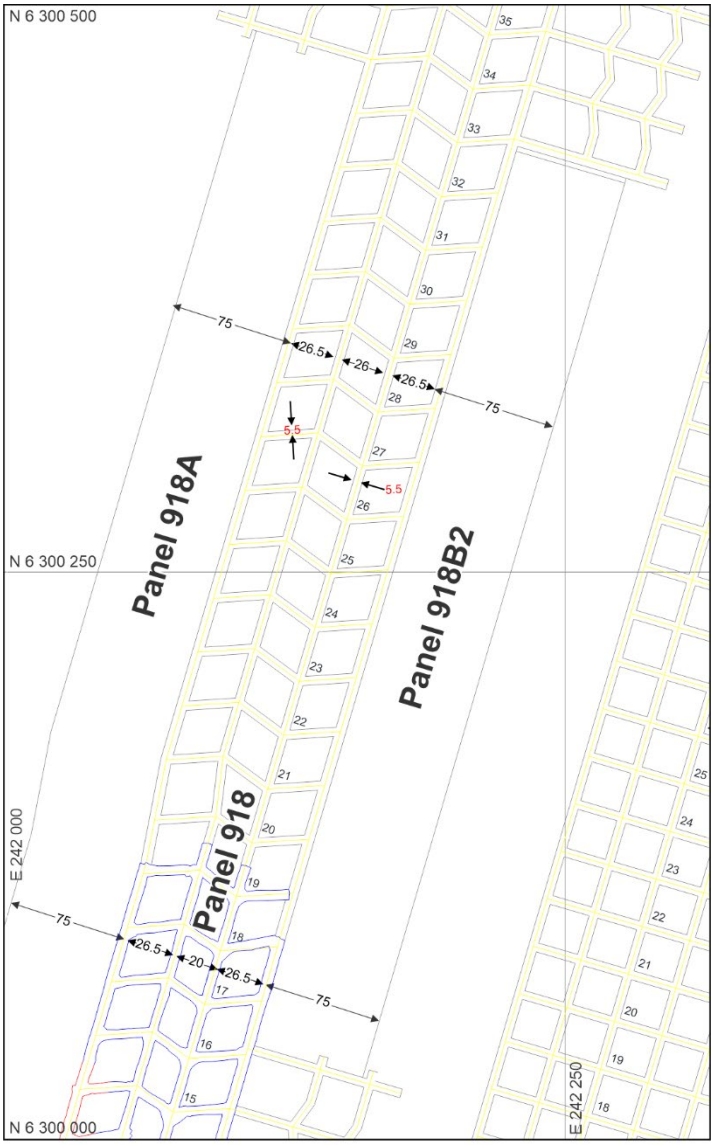

Figure 4: 918 Panel geometry.

5. GEOLOGICAL SETTING

5.1 Stratigraphy

The stratigraphic sequence is presented in Figure 5. The stratigraphy at Clarence includes Triassic sedimentary strata of the Narrabeen Group ranging from 160m to over 320m, where thickness is dependent on the eroded river systems through the surface. The Triassic strata includes the Burralow Formation at the top of the Newnes Plateau, the predominately massive Banks Wall Sandstone and the Burra Moko Sandstone which form the cliffs and pagodas of the Newnes Plateau, and the Caley Formation at the base.

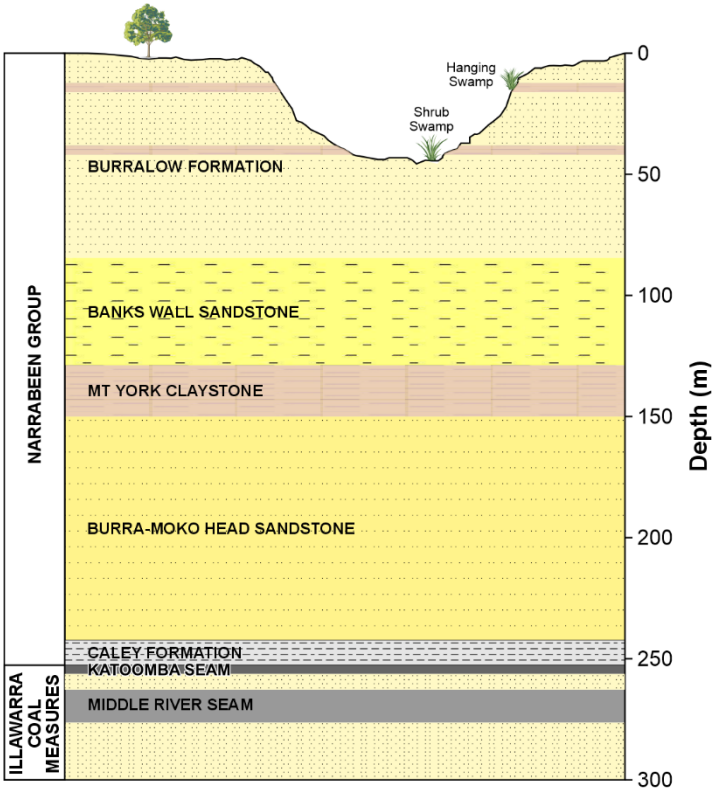

Figure 5: Stratigraphy at Clarence Colliery.

The Burralow Formation is an interbedded sandstone and claystone unit that forms the top of the Newnes Plateau. The Claystone horizons are understood to form aquitards in the sequence. The Burralow Formation Outcrop is presented in Figure 6 and shows the Burralow Formation is present above the proposed 918 Panel. Some portions over the first workings of 918 Panel in the south and east have eroded through the Burralow Formation to the underlying strata. Figure 7 presents fence sections through boreholes covering the 918 Panel area illustrating the eroded valleys into the Banks Wall Sandstone.

The Mount York Claystone separates the Burra Moko and Banks Wall Sandstones and is a key stratigraphic unit hydrologically (regional aquitard) and geotechnically. The Caley Formation is an interbedded siltstone, sandstone and claystone unit that underlies the Burra Moko Sandstone.

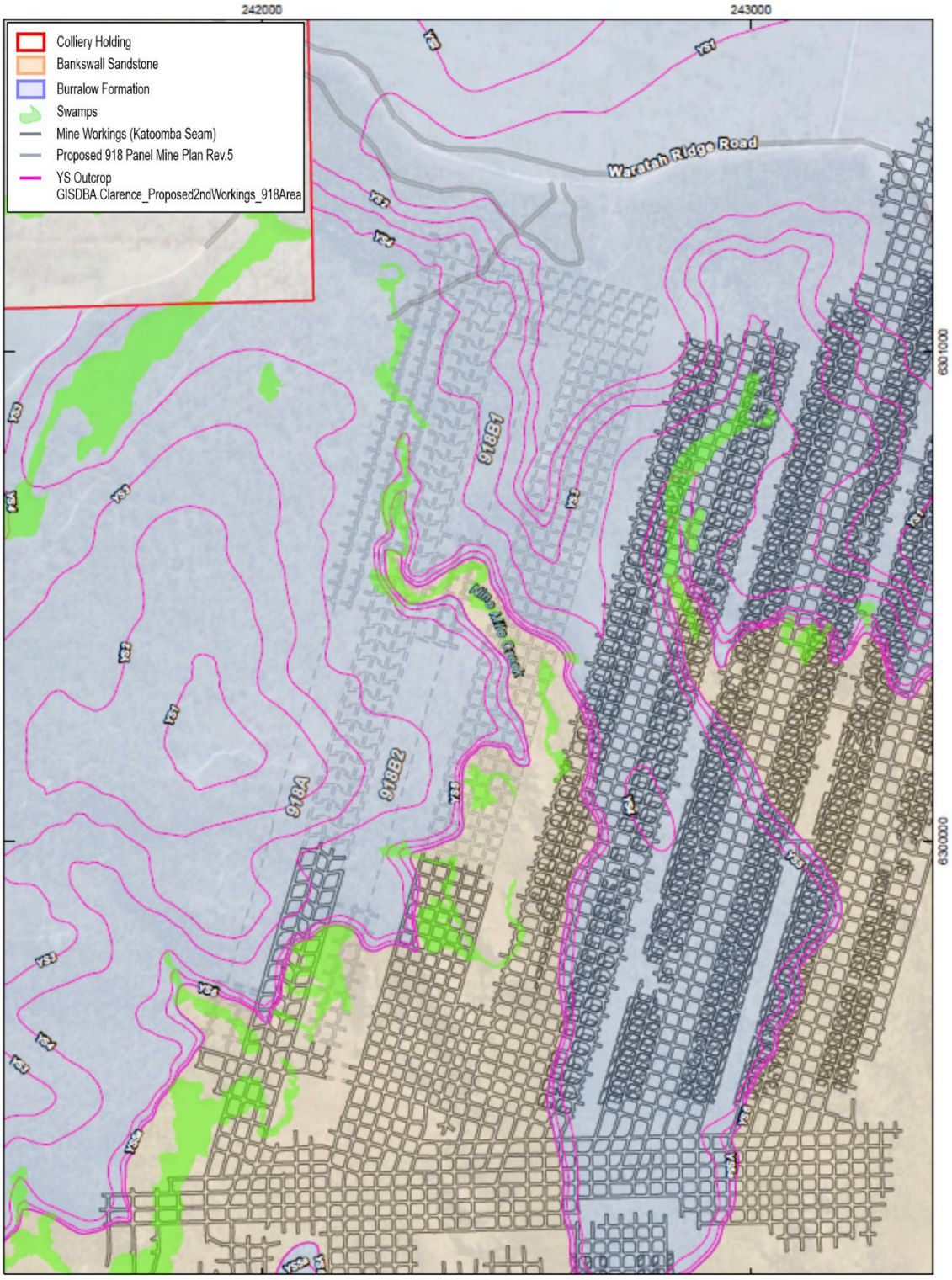

Figure 6: Outcrop of Burralow Formation.

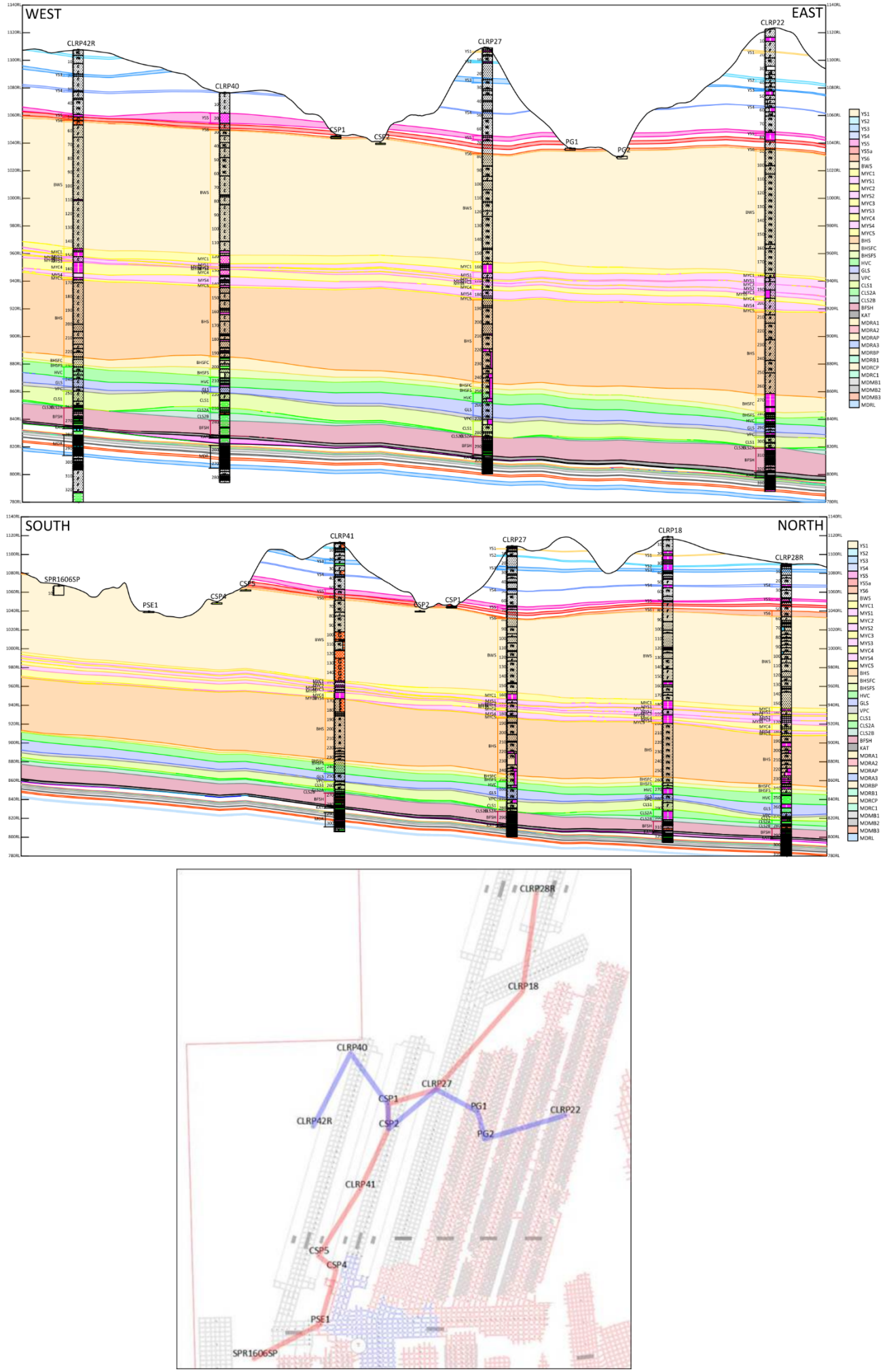

Figure 7: Fences of stratigraphy showing surface topography incising through the Burralow Formation.

The Permian (Illawarra Coal Measures) sedimentary strata underlies the Triassic strata, of which the Katoomba (KAT) Seam is the first economic seam in the Illawarra Coal Measures of the Western Coalfield. Beneath the Katoomba Seam is an interbedded siltstone, carbonaceous siltstone and claystone unit followed by the thick Middle River Coal Seam (MDR). Multiple coal seams exist beneath the MDR with varying interburdens of siltstone/sandstone/claystone. Boreholes supplied for this study extend down to the Lithgow Seam approximately 110m below the Katoomba Seam. Borehole CLRP41 stratigraphy is presented in Figure 8.

5.2 Topography

The topography above the Clarence underground workings has gully eroded river systems and steep gradients. The Newnes Plateau forms the top of the hilltops. Surface reduced levels over the 906-918 Panels are presented in Figure 9 which show an incised drainage system extending north from the start of 910 Panel and west over 910, 908 and 906 Panels. Another shallower incised valley exists over 900 Panel and partially over the southern and northern extents of 918 Panel. The topography grades up to the north and south of these incisions through the 900 Panels.

An east-west cross-section profile presented in Figure 10 shows the change in topography across the 918-910 Panels. The profile extends obliquely through the incised gully. Figure 10 shows the general increase in surface RL to the west as the surface transitions out of the gully towards higher ground. Figure 10 also shows the slight dip of the Katoomba Seam to the east.

5.3 Depth of Cover

The Katoomba Seam depth of cover over the 900 Panels is presented in Figure 11. All boreholes supplied for this assessment are also presented in Figure 11. Due to the change in topography over the area the depth of cover varies from 150m to 320m. The depth of cover variation is principally driven by the plateau topography with incised river gullies which overlies all the 900 Panels to varying degrees. A range of maximum and minimum depth of cover for each relevant panel is presented in Table 1.

Table 1: Depth of cover range over relevant 900 series panels

Panel (m)	Min depth of cover (m)	Max depth of cover (m)
910	150	325
908	240	320
906	160	295
918 study area	174	329
918 secondary workings	227	294

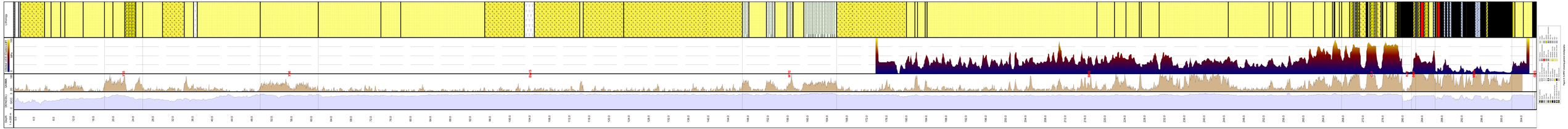

Figure 5.1 MD/TVD Mudlog plot of wellbore

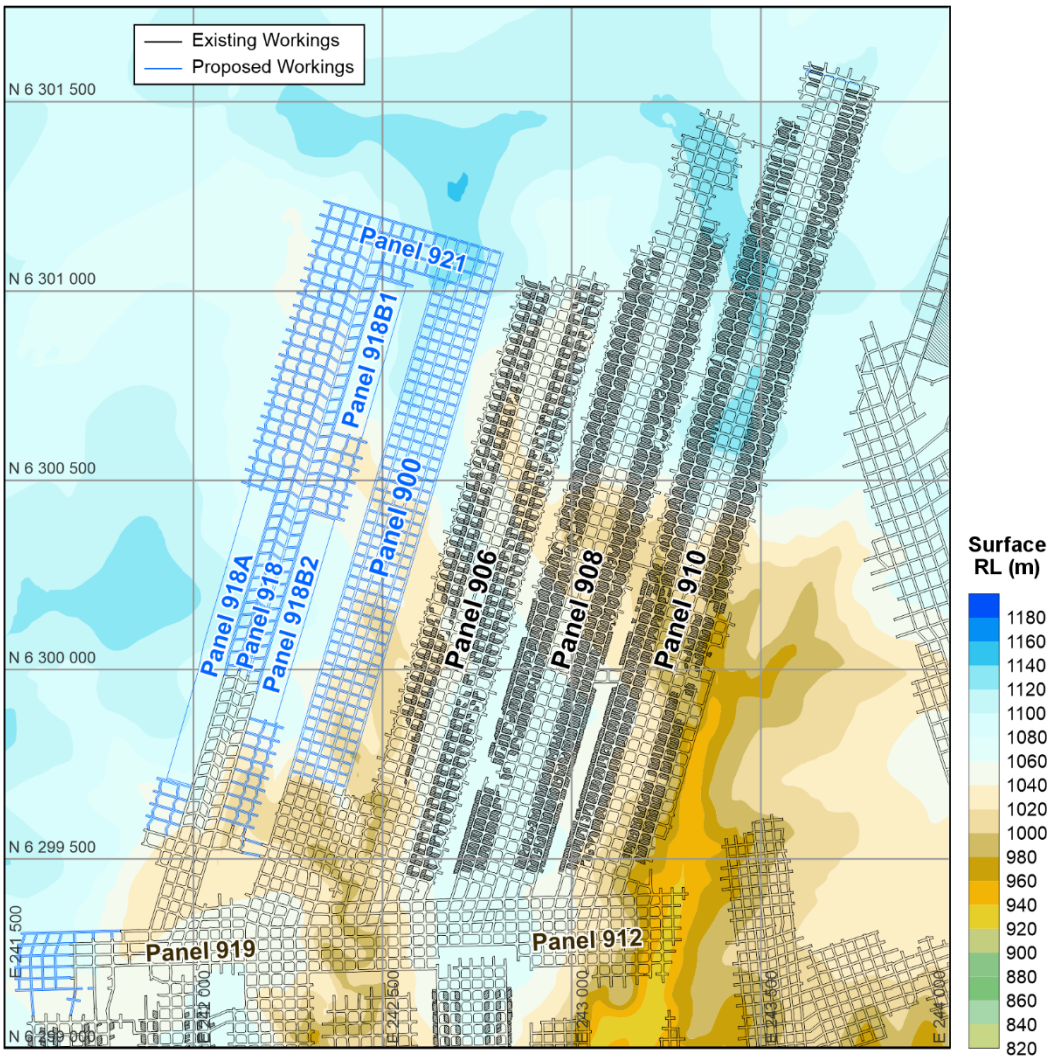

Figure 9: Clarence surface topography over 900 area.

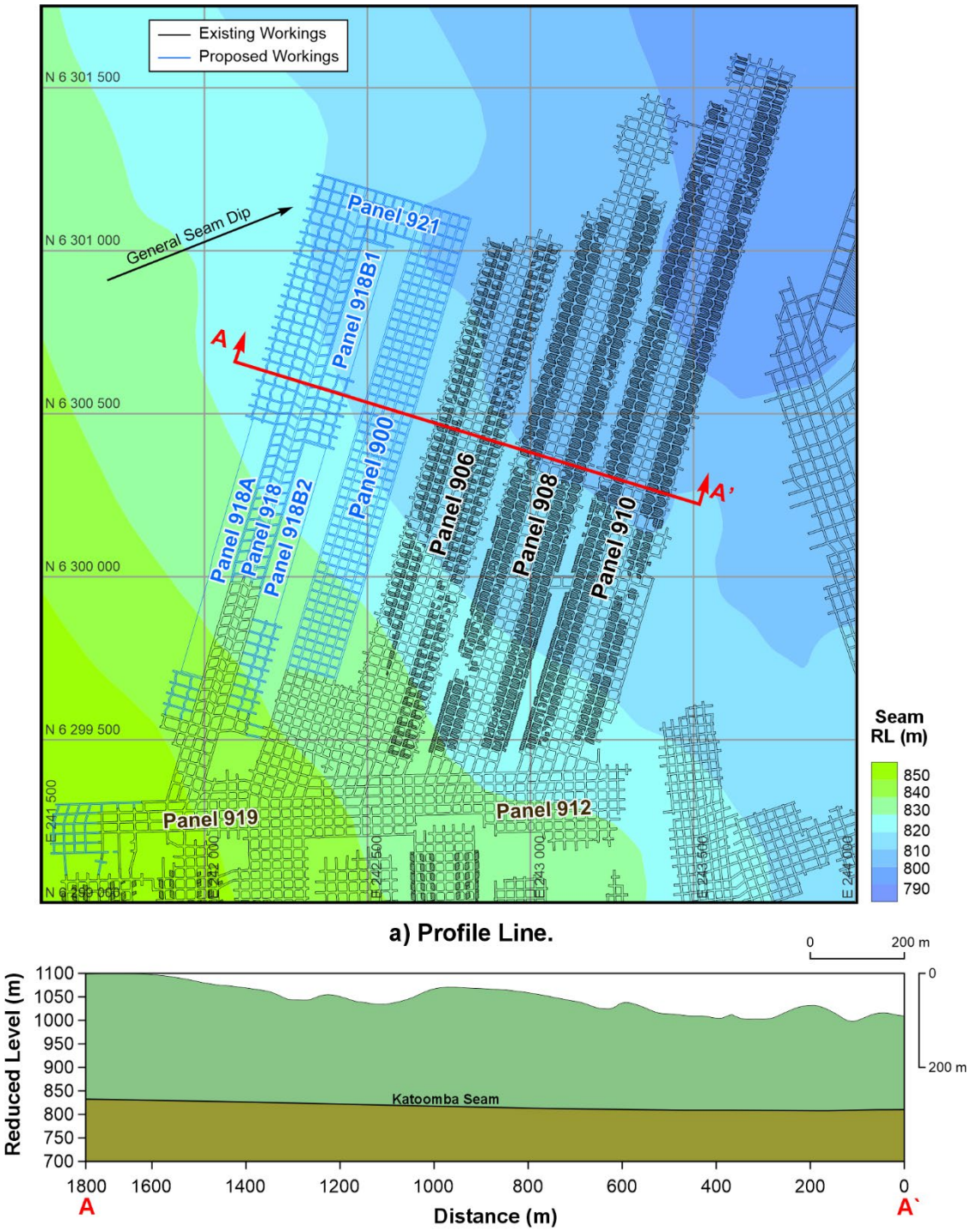

Figure 10: EW cross section showing profile of surface compared to gently dipping Katoomba Seam.

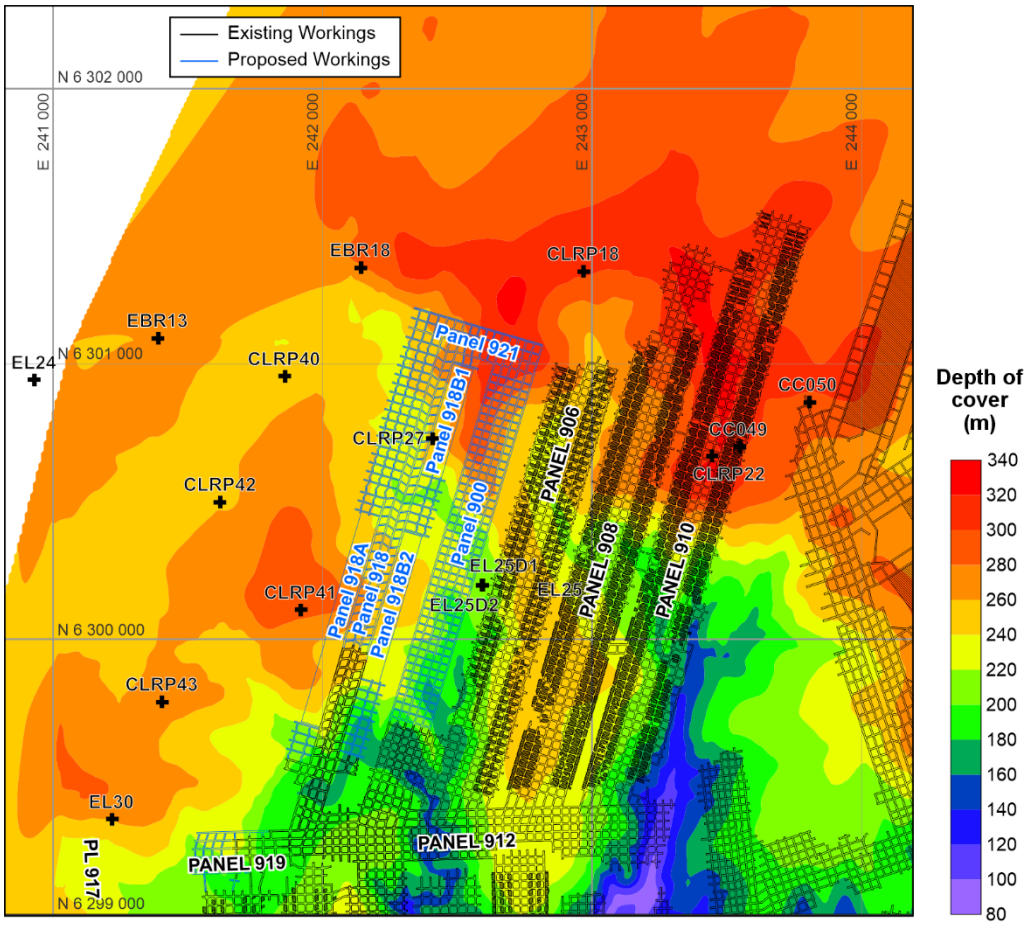

Figure 11: Katoomba Seam depth of cover for 900 Panels.

5.4 Seam Thickness

The Katoomba Seam thickness is presented in Figure 12. The Katoomba Seam is thickest in the east of the 900 area reaching 3.4m over 910 Panel. The thickness of the seam reduces to the west over 918 Panel where the minimum is 1.9m. A range of maximum and minimum seam thicknesses for each relevant panel is presented in Table 2.

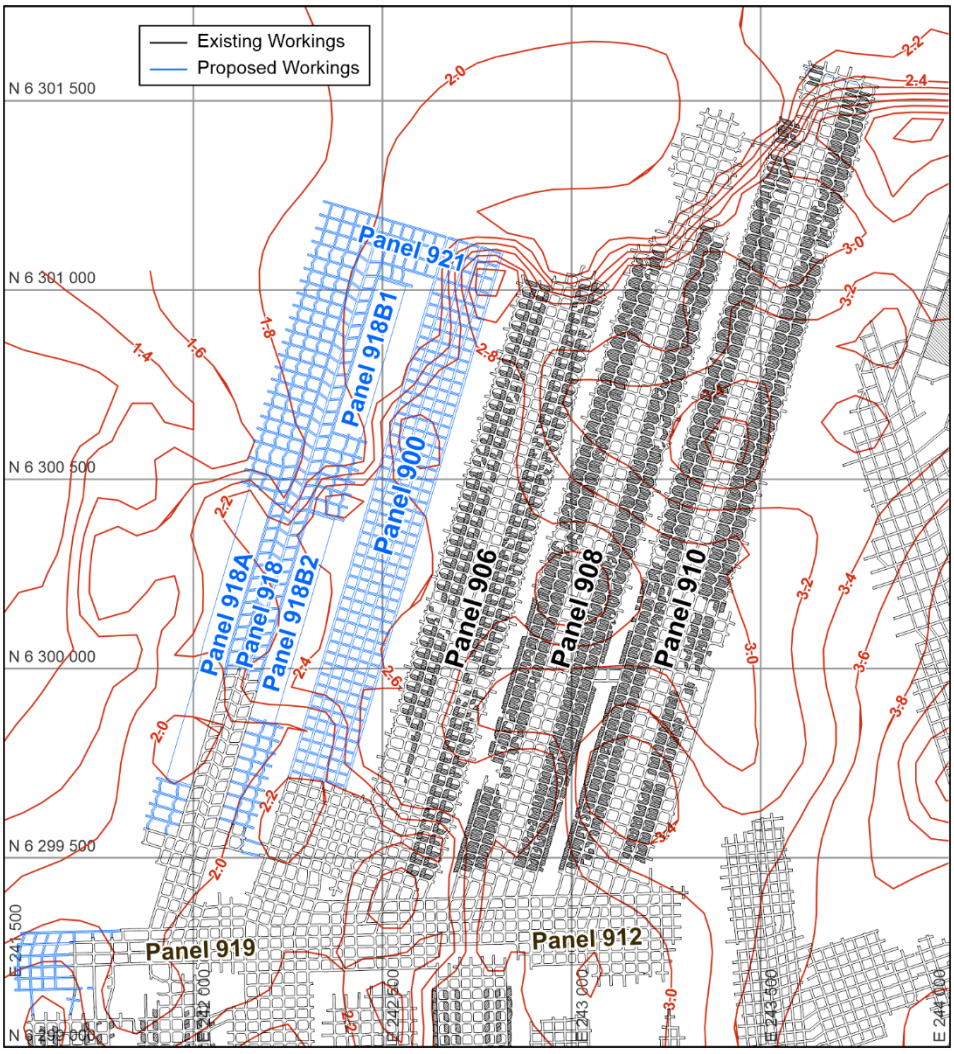

Figure 12: Katoomba Seam thickness.

Table 2: Katoomba Seam thickness range over key 900 Panels

Panel (m)	Min. Seam Thickness (m)	Max. Seam Thickness (m)
910	2.6	3.4
908	2.0	3.4
906	2.3	3.0
918	1.9	2.3

5.5 Faults

The faults at Clarence are typically in a NNW-SSE, NW-SE or NNE-SSW orientation. For 918 Panel, the projected faults have a NNW orientation. The mapped and projected faults for the Katoomba Seam level (provided by Centennial) are presented in Figure 13.

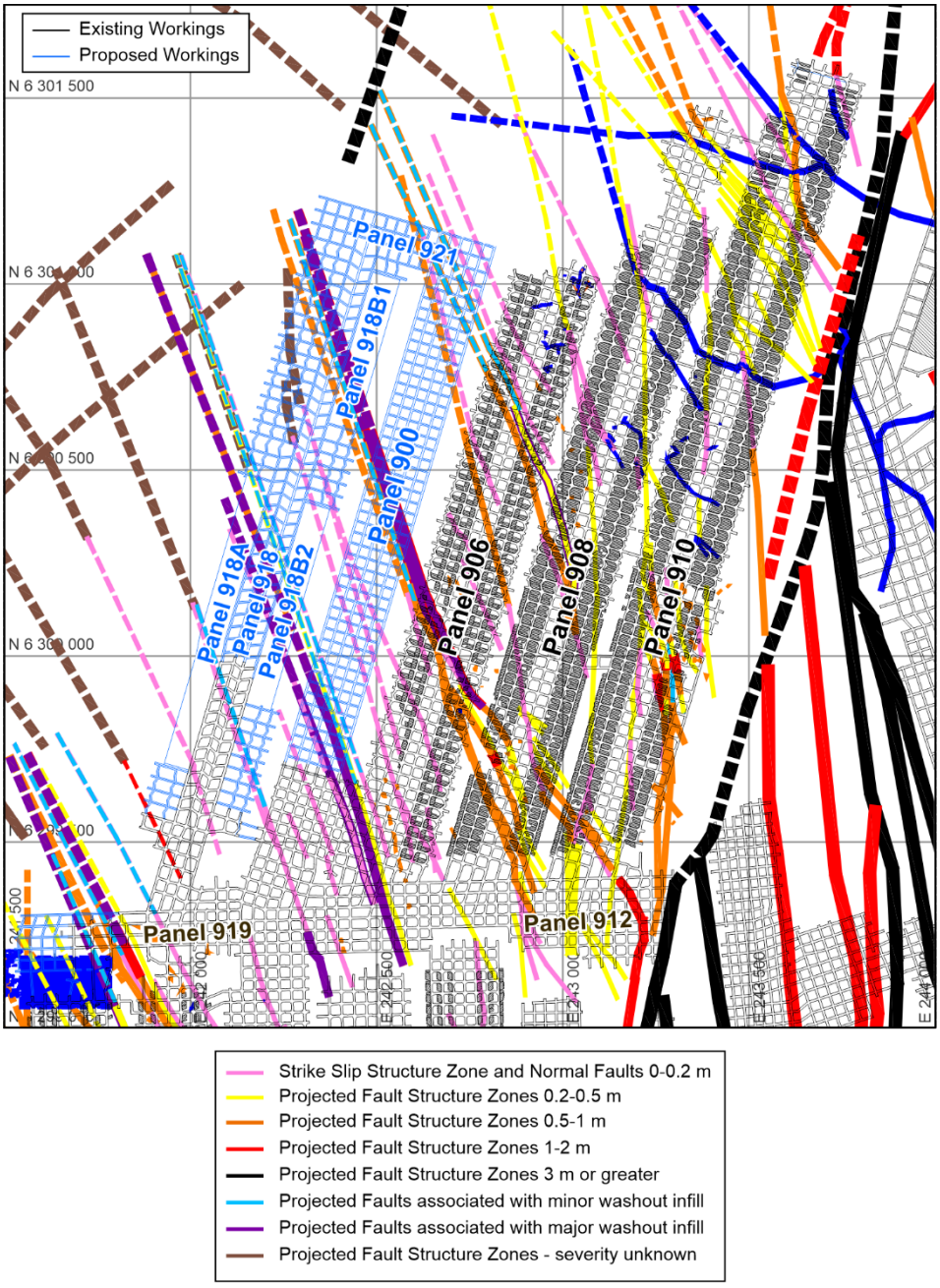

Figure 13: Mapped and projected faults.

Figure 13 shows a number of the projected faults transecting 918 Panel. The majority of projected faults in 918 Panel have been characterised as faults associated with minor and major coal seam washout. The faults up to 20ct in 918 Panel have been confirmed as minor faults in the spine roadway development. There are two minor fault zones in 10-20ct that transect 918A Panel. There is a pair of parallel faults transecting 918B1 Panel classified with 1-2m throw and potential for major washout.

The oblique orientation of these faults to the panel and pillar geometries is favourable for rib, face and pillar stability. There may be localised increase in rib spall associated with these faults, particularly the central spine pillar cut-throughs that are oriented at a lower angle to the faults.

Faults and lineaments may provide a connectivity pathway that is discussed in the connectivity section of this report.

6. GEOTECHNICAL CHARACTERISATION

6.1 Rock Properties

Geotechnical testing has been conducted for several boreholes at Clarence. The geotechnical testing database supplied for this assessment consists of Unconfined Compressive Strength (UCS) testing. Triaxial strength geotechnical testing at Springvale has been used to supplement this assessment.

6.1.1 Unconfined Compressive Strength

All UCS test data from Clarence provided for this assessment is presented in Figure 14 relative to Young's modulus. The rock types tested have been divided into predominant lithology. The general range of rock strength is 5MPa to 100MPa as indicated by geotechnical laboratory testing. The general range of rock stiffness is 3MPa to 35MPa based on the tangent Young's modulus.

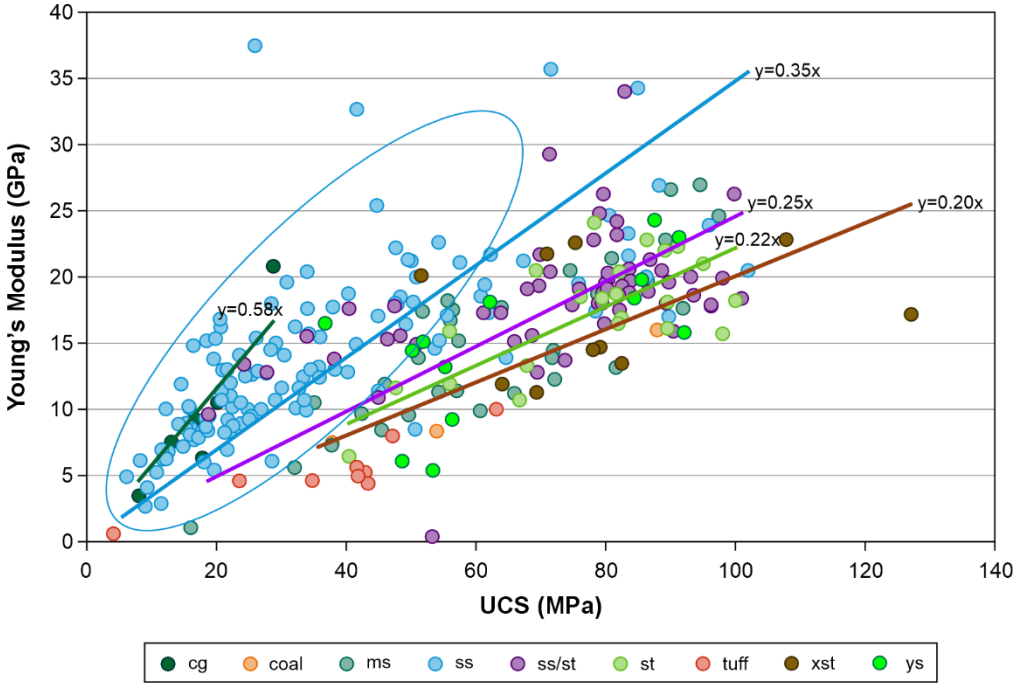

Figure 14: UCS relative to Young's Modulus for key lithologies at Clarence.

Figure 14 shows the relationships between rock type and stiffness. Rock types with larger grain size such as conglomerates and sandstones typically show a stiffer relationship to rock strength. The finer grained materials such as the siltstone and carbonaceous siltstones show a softer relationship to rock strength as illustrated by the relative strength to stiffness ratios in Figure 14.

The area highlighted in Figure 14 with the blue oval shows the majority of sandstone samples from the Caley Formation, Burra Moko Sandstone and Banks Wall Sandstone. The sandstones from these formations indicate a stiffer relationship to rock strength. This finding informed the model rock properties for the sandstone in these units where stiffness was increased from the average 0.35 to 0.38, which is representative of the sandstone samples from these formations.

UCS data relative to key stratigraphic formations is presented in Figure 15. The box and whisker plot assists in understanding the general range of UCS for each of these formations – noting that the amount of testing in the Burra Moko and Banks Wall sandstones is substantially less than the Caley and Farmers Creek formations as coring is generally focussed around the mining horizon.

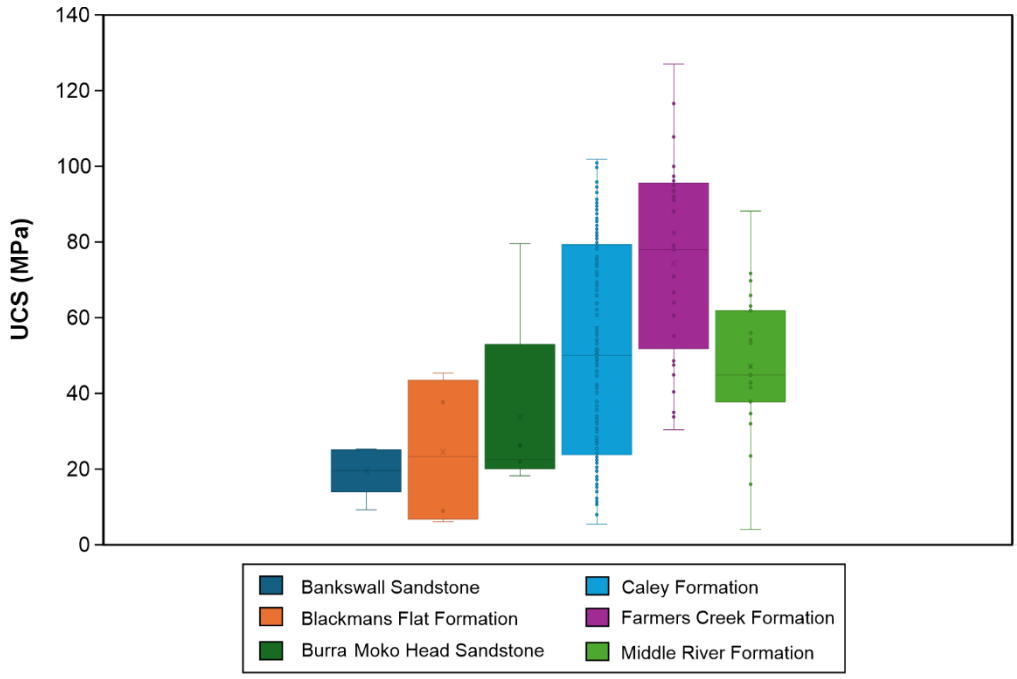

Figure 15: UCS range for rock samples in key stratigraphic units.

Figure 16 shows available results of UCS in the roof and floor strata of the Katoomba Seam observed in laboratory tests of samples from three boreholes at Clarence Colliery. In relation to pillar loading and rock failure, the in-situ strength is difficult to calculate with confidence from this data due to the large variability of rock strength. Bulk strength is typically lower than UCS determined from laboratory testing. Hoek and Brown (1980) suggests bulk strength is 0.68 of the UCS determined from laboratory testing for the test specimen sizes used. Confinement and Poisson's Ratio effects are expected to increase the strength of the rock strata. The numerical modelling approach assists in simulating the bulk rock strength with 1m high element rock property detail in the models.

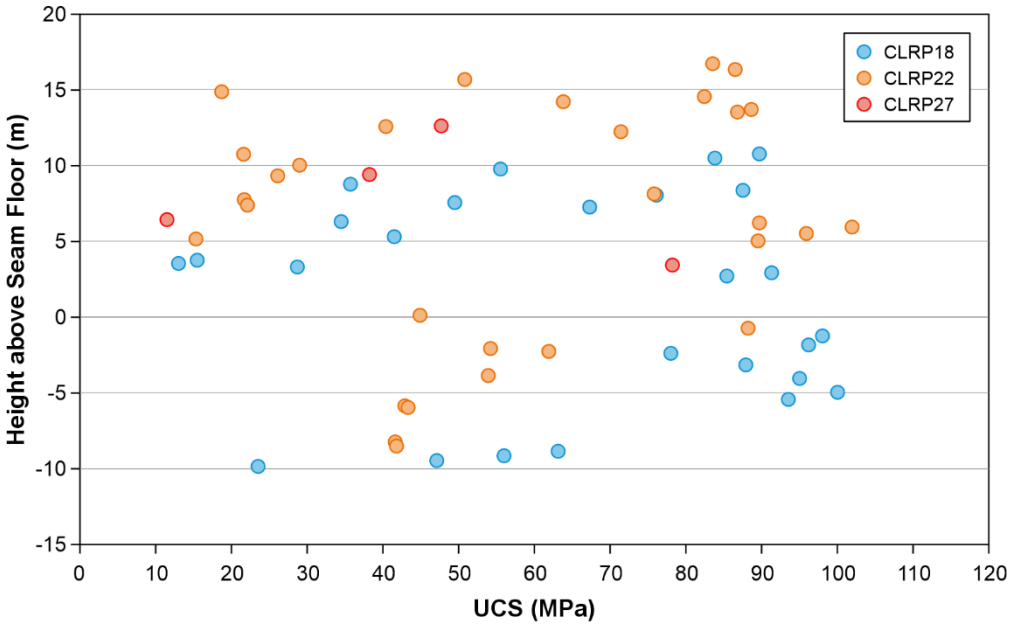

Figure 16: Laboratory UCS from boreholes relevant to Panels 908-910 and 918.

6.1.2 Inferred UCS

Downhole geophysical sonic velocity is commonly used to estimate the unconfined compressive strength (UCS) of clastic rocks (McNally, 1987). An empirical relationship can be derived between a rock sample tested for UCS in a geotechnical laboratory and the correlated downhole sonic velocity from borehole geophysics. Samples that fit the criteria of shear failure with a consistent corresponding sonic velocity are used for the relationship.

The relationship used to infer the UCS is presented in Equation 2 from Seedsman et al (2009). It is understood that Equation 2 is commonly used to derive strength from sonic velocity at Clarence. The relationship was supplied to SCT by Clarence for this assessment.

$$Inferred\ UCS\ (MPa) = 5785 * Exp\ (-\frac{17374}{velocity})$$

Velocity – sonic velocity (m/s)

[Equation 2] (Seedsman et al, 2009)

6.2 Joints and Cleat

The primary joint set strike direction is NNW-SSE with a minor, and significantly less prevalent, ENE-WSW joint set. The primary joint set orientation is oblique to the roadway ribs and pillars. The joint set orientation is also parallel with the fault strike direction, where joints are observed to increase in frequency adjacent to structure.

Figure 17 shows the mapped joints for the 900 and 918 Panels (provided by Clarence), together with the mapped and projected faults.

The cleat orientation is variable at Clarence, with cleat rosettes from surface borehole interpretation presented in Figure 18. The cleat trend in the area of 918 Panel is indicated to be NNW-SSE to NW-SE. This is typically consistent with the joint and fault orientation and is oblique to the ribs.

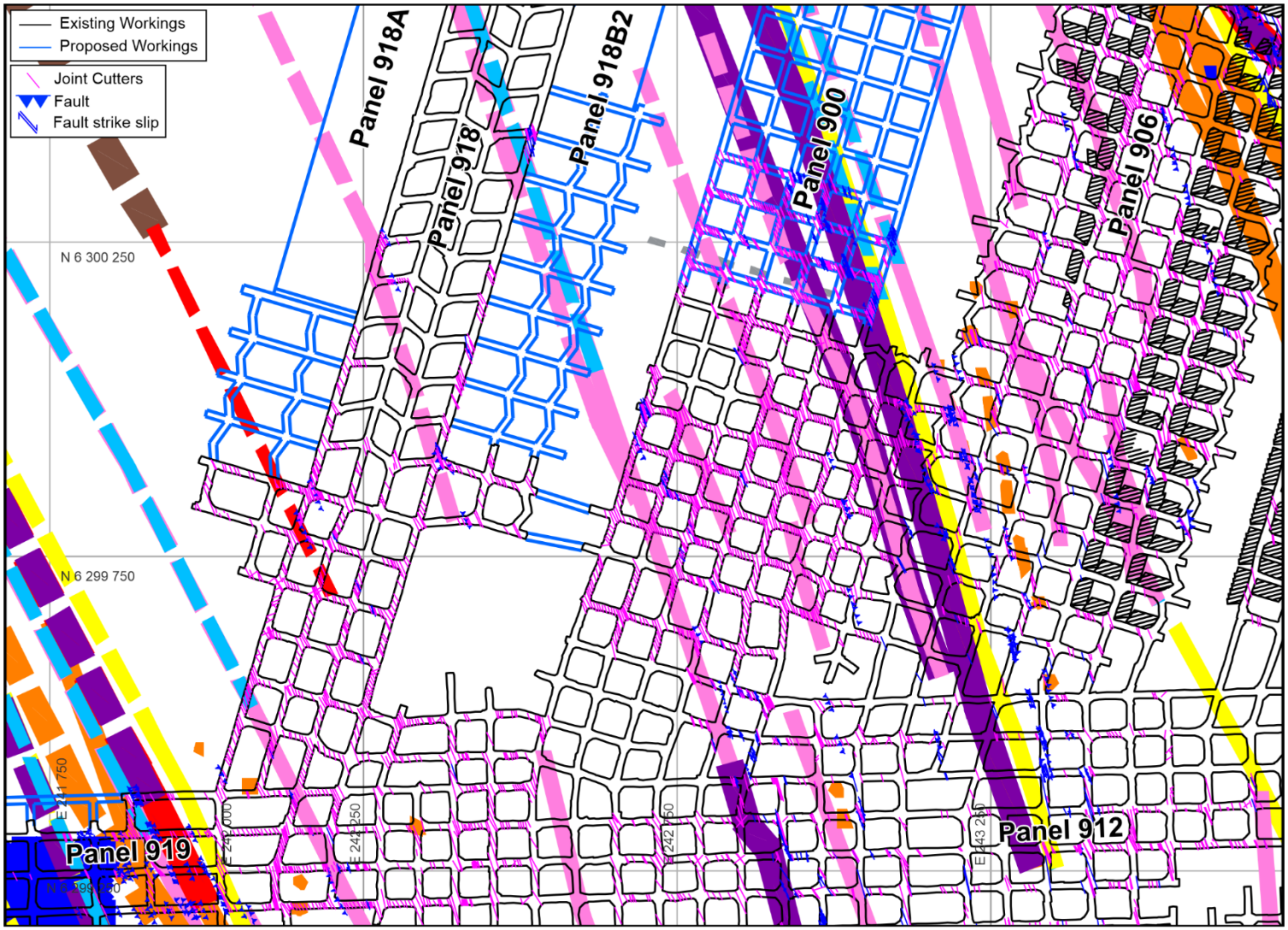

Figure 17: Underground mapping of joints and faults for Clarence Colliery (provided by Centennial).

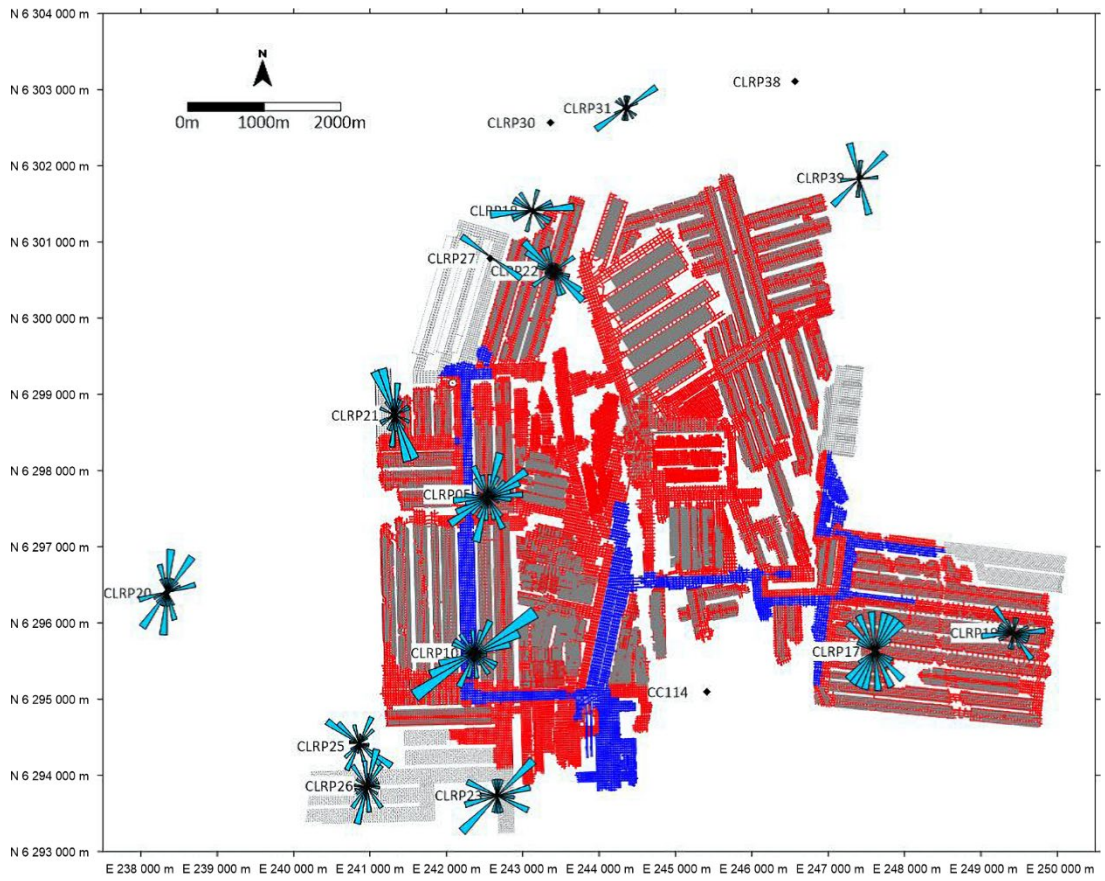

Figure 18: Cleat rosettes for Clarence Colliery.

The general oblique orientation of the joints, cleat and structure is oriented favourably to the ribs of the pillars and, as such, is beneficial for reducing rib spall in the pillars. The spine pillar cut-throughs are oriented at a lower angle to the joint, cleat and structure orientation and may produce a higher level of spall if unsupported. Although it is understood that all ribs are to be supported and meshed, which is anticipated to assist in providing resistance to rib spall.

6.3 Stress

Stress measurements from Clarence, Springvale and Angus Place mines have been compiled to supplement the limited Clarence Colliery database. Stress measurement results are presented as a Tectonic Stress Factor (TSF) which is a useful method of allowing stress measurements taken in different rock types and geotechnical properties to be compared. The stress measurements taken at Clarence, Springvale and Angus Place mines were compared with SCT's database of stress measurements in underground coal mines.

The TSF is a means of normalising the stress irrespective of the material stiffness and can be calculated using Equation 1 below:

$$\sigma'_H = v/(1-v) \times \sigma'_V + TSF \times E \qquad \text{[Equation 1] (Nemcik et al, 2006)}$$

σ'_H = Horizontal stress (MPa)
v = Poisson's Ratio
σ'_V = Horizontal stress (MPa)
E = Youngs Modulus (GPa)

SCT overcore stress measurements have previously been conducted at Clarence. The results from a stress measurement campaign in the roof of 408 Panel (SCT, 1992) are presented in Figure 19. Depth of cover was in the order of 200m. Noting the measurements were conducted at two sites (408 6CT and 7CT). Principal horizontal stress orientation was 29° to 76°, consistent with the regional northeast principal horizontal stress orientation. Stress measurements from Springvale (SCT, 1993) and Angus Place (SCT, 1996a and SCT 1996b) are included to supplement measurements at greater depth. The red Angus place data points represent SCT 1996a and the blue Angus place data points represent SCT 1996b.

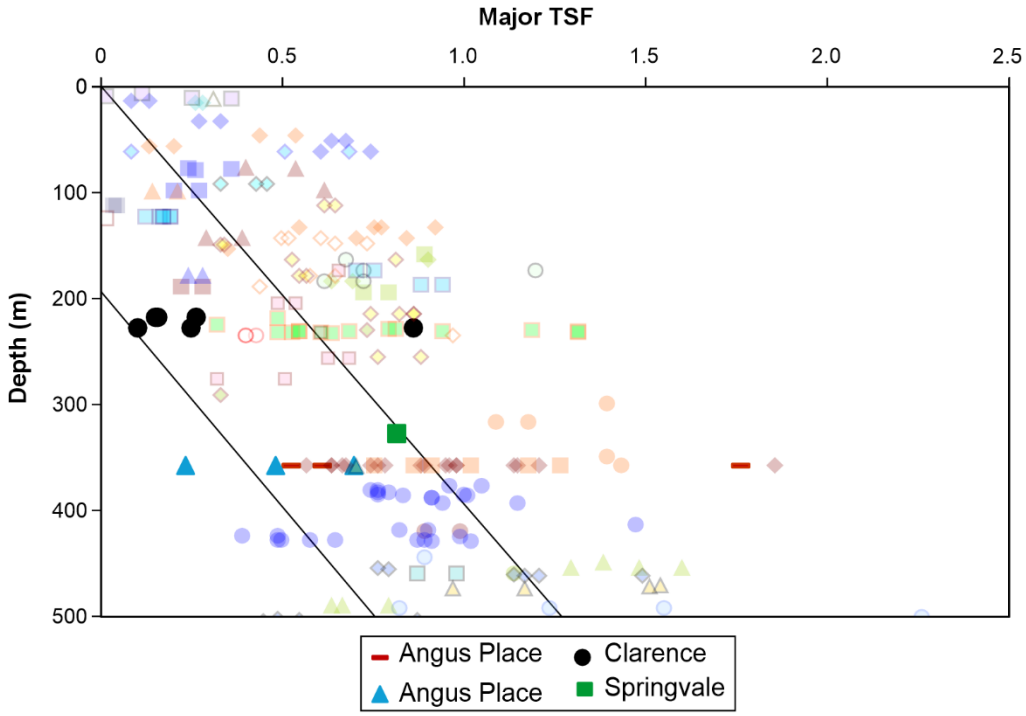

Figure 19: Stress measurements at Clarence, Springvale and Angus Place compared with SCT database for stress measurements in underground coal mines.

The stress measurements typically show a medium to low principal horizontal stress environment when compared with the SCT database for stress measurements in Australian underground coal mines. Noting some outliers at both Clarence and Angus Place which indicate the potential for elevated stress, however within the Australian experience. Further stress measurements in the Clarence 900 area would assist in refining the characterisation of the stressfield at depth.

6.4 Geotechnical Cross-Section

A geotechnical fence across multiple boreholes is presented in Figure 20. A borehole map can be found in Figure 11. The geotechnical fence includes geophysical logs (where available), lithological logs and stratigraphic logs. The geophysical logs are comprised of density (g/cm^3), gamma (API) and sonic inferred UCS (MPa).

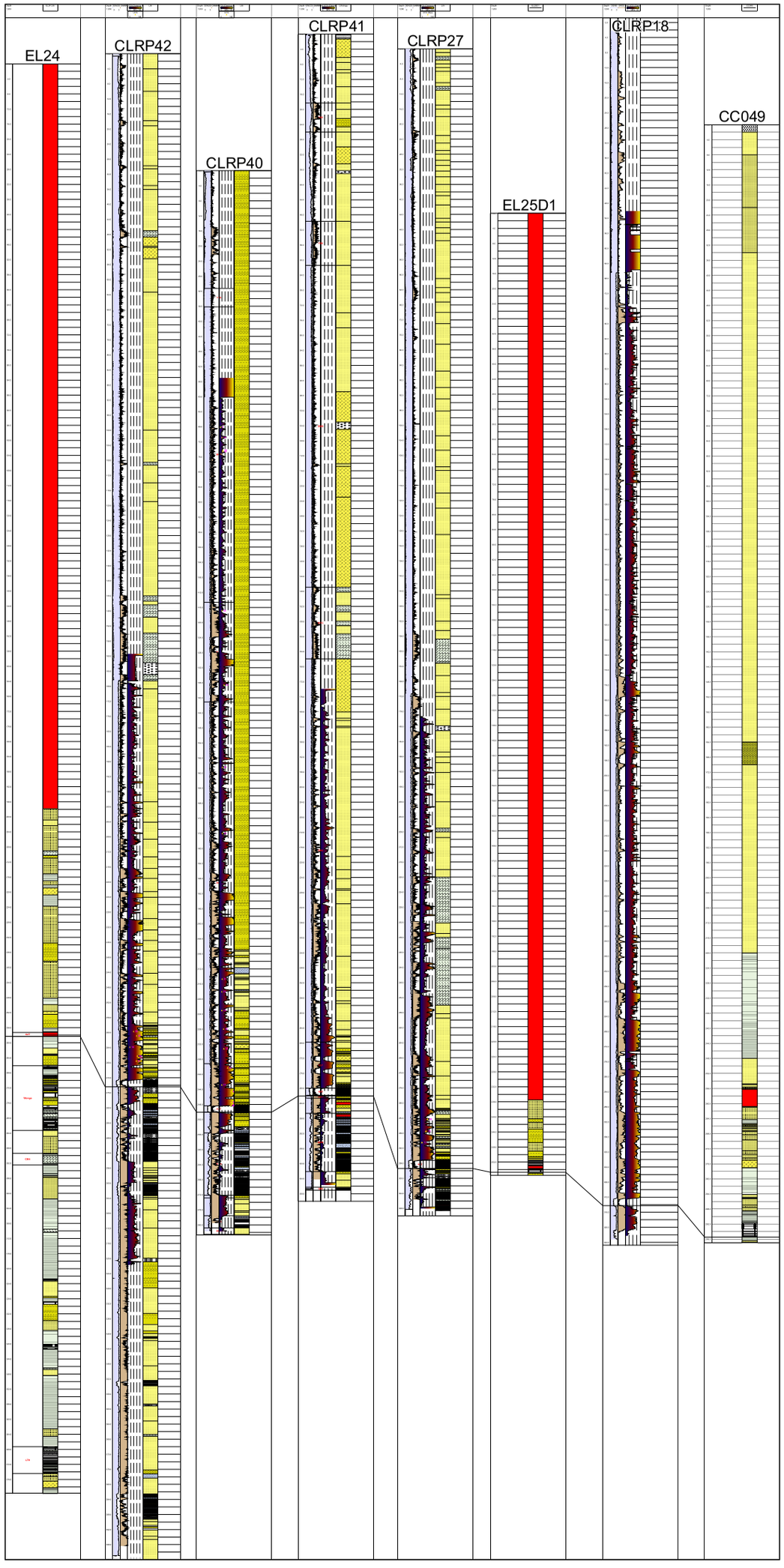

Figure 20: Geotechnical fence across 900 Panels.

Several key geotechnical characteristics are presented in the geotechnical fence and include:

- Immediate roof (initial 2m): Caley Formation
    - Strength: > 75MPa
    - Gamma: ~180 API
    - Lithology: interbedded siltstone/sandstone
- Above initial roof: Caley Formation
    - Strength: 25MPa to 100MPa
    - Gamma: 60 API to 180 API
    - Lithology: interbedded siltstone/sandstone/claystone (some shales and conglomerates may be present).
- Overburden: Burra Moko Sandstone (above Caley Formation)
    - Strength: 25MPa to 100MPa
    - Gamma: 45 API to 180 API
    - Lithology: predominantly sandstone
- Seam: The Katoomba Seam is thickest in the east and gradually thins to the west.
- Floor: The interburden between the Katomba Seam and MDR is generally ~4m thick and where the interburden increases, additional coal plies are observed.
    - A localised reduction in interburden thickness between the Katoomba and Middle River Seams is observed in borehole CLRP27 to < 2m.
    - The MDR is typically 16m thick over the 900 Panels.

The geotechnical fence suggests there is a general consistency in strength and stratigraphy across the 900 area. Noting the localised change in interburden between the Katoomba and MDR seams.

7. PILLAR DESIGN ASSESSMENT

7.1 Conditions in Consolidated Consent DA 504-00

The conditions of Consolidated Consent DA 504-00 (MOD10) for Clarence are relatively unique compared to similar approvals (project approvals or development consents) for other underground coal mining operations.

The standard definitions for subsidence, subsidence effects, subsidence impacts and environmental consequences (from subsidence impacts), first workings are not included.

A condition for first workings is also not included. A typical condition for first workings requires first workings to be designed to remain stable (or long-term stable) and non-subsiding, except insofar as they may be impacted by approved second workings and as such built to geotechnical and engineering standards sufficient to ensure long-term stability with negligible (or zero) resulting direct subsidence impacts (not subsidence effects).

The workings of the 918 panel are therefore considered partial extraction due to shortwall extraction and the pillar widths are less than the standard for the shortest horizontal dimension for conforming pillars designated in Schedule 3 of the Work Health and Safety (Mines and Petroleum Sites) Regulation 2022 (2022 Regs). The shortwall mining method is a form of panel and pillar partial extraction.

There is however a section within the Extraction Plan condition, not found in all approvals, for the extraction plan to include "*adequate consideration of mine roof and floor conditions, pillar width to height ratio, final pillar dimensions and long-term stability of pillars …".* Presumably, this is in recognition of the limitations of standard pillar strength formulae in certain geological settings (e.g. pillars with large width to height ratios in strong roof and floor conditions, soft roof and floor environments, geological structured ground) and consistent with the requirements of a Principal Hazard Management Plan for ground and strata failure in Schedule 1 of the 2022 Regs.

There are no subsidence impact performance measures for natural and built features commonly found in other approvals. There are however Subsidence Impact Assessment Criteria for first workings and partial extraction which are effectively limits for subsidence effects rather than impacts, presumably on the basis that any subsidence movements less than the low magnitudes of vertical subsidence, tilt and strain in these criteria would result in zero or negligible impacts and consequences.

In the context of DA 504-00, our assessment focussed on the potential subsidence outcomes and compliance with the subsidence effects limits from the ability of the remaining pillars to control subsidence, rather than a specific factor of safety (and associated probability of instability) derived from estimates of pillar strength and estimates of pillar loading.

From this perspective the numerical model created for Clarence and validated (not calibrated) against actual subsidence measurements for the various mining geometries is expected to provide a reasonable indication of pillar stability (and strata above the pillars) in both the short-term and over longer term.

7.2 Pillar Stability Assessment

The pillar geometry for 918 spine pillars consists of a four-heading layout with three pillars. The central pillar is the smallest pillar and used for the factor of safety (FOS) calculations. There are two central pillar widths of 20m and 26m; inbye of 21ct has 26m wide central pillar while outbye of 21ct has a 20m wide central pillar. Both these scenarios have left and right flanking pillars of 26.5m width. Both the 20m and 26m central pillar widths are considered in the FOS calculations for the relevant depth of cover and abutment loading scenarios.

The pillar design objective is to meet stability for serviceability and subsidence. Adequate consideration to long term stability is considered.

FOS calculations are based on tributary load and abutment load. Tributary load is based on a roadway width of 5.5m. An overburden density of 0.025MPa/m is assumed for the overburden weight.

An equal abutment load has been allocated across the three spine pillars. The abutment load uses the panel void width of 75m for cut-throughs 10-34 (918A and 918B2) and 83m for cut-throughs 39-52 (918B1) and a 12 degree caving angle, slightly more conservative than the pillar loads from the subsidence model.

For first workings, the depth of cover directly above the spine pillars is used. For single side abutment, the average depth of cover across the single panel is used. For double abutment loading, the average depth of cover across both panels is used.

Rib spall of 0.5m is included in all average load and pillar strength calculations. This creates an effective roadway 1m wider than the design roadway width, and an effective pillar size 1m smaller than the design pillar size. 0.5m of rib spall is considered realistic at these depths of cover ranging 180-280m.

The pillar strength calculations use the Mark-Bieniawski pillar strength formula for rectangular pillars (Mark and Chase, 1997). The Bieniawski formula (Bieniawski, 1992) is close to unity with the Mark-Bieniawski formula for square pillars. Given the range in pillar sizes between square and rectangular, the Mark-Bieniawski formula has been used for this assessment and is detailed below:

$$\text{Pillar Strength} = Sc\,(0.64+0.54(w/h)-0.18(w^2/lh))$$

where Sc = Coal strength
w = pillar width
h = pillar height
l = pillar length

A coal strength of 6MPa has been used. This is based on research in the UNSW/SCT ACARP (Gale and Hebblewhite, 2005) where 6MPa represents a strong contact, 5MPa represents a moderate contact, and 3-4MPa represents a weak claystone contact between the coal and the roof and floor material.

Bieniawski (1992) recommends the following relevant pillar size FOS:

- a FOS of 2 for pillars in retreat panels and mains
- a FOS of 1.3 for tailgate abutment loading for roadway serviceability
- a minimum FOS of 1.3 (noting all pillar failures in the Bieniawski database are at FOS less than 1.3).

Bieniawski (1992) also notes that *"For longwall mining, using the ALPS method developed at The Pennsylvanian State University by Mark and Bieniawski (1986), the recommended factor of safety is 1.3."*

The roadway height is 2.8m. The coal thickness is typically 2-2.1m for the 918 Panel, where a sandstone "cap rock" will form the upper part of the pillar. Mark et al (2011) states that the pillar height can be reduced by 50% of the "cap rock" height for pillar strength calculations. This 50% reduction in stone height has been applied to provide an effective pillar height for the pillar strength calculations.

The UNSW pillar strength formula is also included for comparison, as this is often used as an industry standard. In our opinion, the UNSW formula overestimates the pillar strength for larger width to height ratios. Pillars with W/H>8 strain harden and exhibit yielding behaviour, which is important for subsidence estimations. The Mark-Bieniawski formula includes coal strength behaviour that considers the mechanism of pillar yielding in the strain-hardening state of pillar loading.

The FOS calculations for the central spine pillar are presented in Table 3. The FOS results presented in Table 3 have a minimum FOS of 1.7 for 5 pillars and a FOS of >2.1 for the remainder of pillars with double abutment loading. A FOS of 1.63 has a UNSW probability of failure of 1 in 1000. The Mark-Bieniawski formula has a lower calculated strength and so will correlate with a lower FOS. There is no probability of failure for the Mark-Bieniawski approach and so probability of failure can be inferred from the UNSW approach.

The model pillar loads, in which we are comfortable to design the maximum level of subsidence from, show a lower pillar load than the calculated pillar load and correspondingly higher FOS. A comparison of the model loads and FOS for the realistic assumptions is presented in Table 4. It is also noted that the numerical rock failure model is based on the pillar geometry of 1-21 cut-through, and as such, the average model loads are conservative for the larger pillars from 21-52 cut-through.

All pillars in Table 3 have a pillar W/H ratio of greater than 8, with most having a W/H greater than 10. These pillars are therefore strain hardening and do not fail in a sudden brittle nature.

Regardless of nominal pillar strength and the calculated FOS pillar design methodology, large pillars in strong roof and floor conditions continue to build strength as they deform, a process referred to as strain hardening. This characteristic means that concepts of maximum strength and probability of failure, for pillars with large W/H in strong roof and floor conditions, become less meaningful.

AMIRA (1994) and ACARP (2005) provide details of strain hardening effects on pillar strength for larger W/H pillars where geological conditions allow frictional strength to be generated within the core of the pillar. For strength to build, pillar W/H needs to be greater than about six to eight and roof and floor conditions need to be strong enough to allow frictional confinement to be generated. As confinement builds, some low-level convergence develops and roof, rib, and floor conditions deteriorate, but the pillar is able to support increasingly higher loads as it deforms.

Additionally, the larger W/H pillars that are strain hardening tend to have larger loads that can create rock failure in both the coal pillar and the strata above the pillar which is more complex to unravel. Positively, the models do not indicate fracturing of the strata above the pillars, giving confidence in the long-term stability of the overall pillar system, including the strata above.

The pillar design approach is considered a conservative approach, without compounding the conservatism, and is supported by the model pillar loads.

Table 3: Pillar Design FOS Assessment

Central Pillar Calcs - TG Loading								Mark-Bieniawski		UNSW	
Cut-through	Depth	Pillar Width	Coal height	Pillar Height	W/H	Rib spall	Pillar load	Strength	FOS	Strength	FOS
16-21ct	230	20	2.1	2.45	8.2	0.5	11.8	23.1	2	22.4	1.9
16-21ct	240	20	2.1	2.45	8.2	0.5	**12.4**	**23.1**	**1.9**	**22.4**	**1.8**
21-34ct	230	26	2.2	2.5	10.4	0.5	11.4	26.2	2.3	29.5	2.6
21-34ct	240	26	2.2	2.5	10.4	0.5	12	26.2	2.2	29.5	2.5
21-34ct	250	26	2.1	2.45	10.6	0.5	12.6	26.7	2.1	30.6	2.4
21-34ct	265	26	2.1	2.45	10.6	0.5	13.4	26.7	2	30.6	2.3

Central Pillar Calcs - Double Loading								Mark-Bieniawski		UNSW	
Cut-through	Depth	Pillar Width	Coal height	Pillar Height	W/H	Rib spall	Pillar load	Strength	FOS	Strength	FOS
16-21ct	230	20	2.1	2.45	8.2	0.5	12.9	23.1	1.8	22.4	1.7
16-21ct	240	20	2.1	2.45	8.2	0.5	**13.6**	**23.1**	**1.7**	**22.4**	**1.7**
21-34ct	230	26	2.2	2.5	10.4	0.5	12.5	26.2	2.1	29.5	2.4
21-34ct	240	26	2.2	2.5	10.4	0.5	13.1	26.2	2	29.5	2.2
21-34ct	250	26	2.1	2.45	10.6	0.5	13.8	26.7	1.9	30.6	2.2
21-34ct	265	26	2.1	2.45	10.6	0.5	14.8	26.7	1.8	30.6	2.1

Central Pillar Calcs - Single Loading								Mark-Bieniawski		UNSW	
Cut-through	Depth	Pillar Width	Coal height	Equ. Pillar He	W/H	Rib spall	Pillar load	Strength	FOS	Strength	FOS
10-16ct	220	20	2.1	2.45	8.2	0.5	10.1	23.1	2.3	22.4	2.2
10-16ct	230	20	2.1	2.45	8.2	0.5	10.6	23.1	2.2	22.4	2.1
10-16ct	240	20	2.1	2.45	8.2	0.5	**11.1**	**23.1**	**2.1**	**22.4**	**2**
39-52ct	240	26	2.1	2.45	10.6	0.5	10.9*	26.7	2.4	30.6	2.8
39-52ct	250	26	2.1	2.45	10.6	0.5	11.5*	26.7	2.3	30.6	2.7
39-52ct	260	26	2.1	2.45	10.6	0.5	12.0*	26.7	2.2	30.6	2.6
39-52ct	270	26	2	2.4	10.8	0.5	12.5*	27.2	2.2	31.8	2.5
39-52ct	280	26	2	2.4	10.8	0.5	13.0*	27.2	2.1	31.8	2.4

Central Pillar Calcs - First Workings								Mark-Bieniawski		UNSW	
Cut-through	Depth	Pillar Width	Coal height	Pillar Height	W/H	Rib spall	Pillar load	Strength	FOS	Strength	FOS
7-21ct	180	20	2.1	2.45	8.2	0.5	6.5	23.1	3.5	22.4	3.4
7-21ct	200	20	2.1	2.45	8.2	0.5	7.2	23.1	3.2	22.4	3.1
7-21ct	220	20	2.1	2.45	8.2	0.5	8	23.1	2.9	22.4	2.8
7-21ct	240	20	2.1	2.45	8.2	0.5	**8.7**	**23.1**	**2.7**	**22.4**	**2.6**
21-52ct	200	26	2.1	2.45	10.6	0.5	7.2	26.7	3.7	30.6	4.3
21-52ct	220	26	2.1	2.45	10.6	0.5	7.9	26.7	3.4	30.6	3.9
21-52ct	240	26	2-2.1	2.45	10.6	0.5	8.6	26.7	3.1	30.6	3.6
21-52ct	265	26	2-2.1	2.45	10.6	0.5	9.5	26.7	2.8	30.6	3.2

*A panel width of 83m was used for the 39-51ct panels consistent with 918B1 Panel width

Table 4: Comparison of geometric load and model pillar load approaches for the double loading scenario

Geometric	Mark-Bieniawski		UNSW	
Pillar load	Strength	FOS	Strength	FOS
12.9	23.1	1.8	22.4	1.7
13.6	**23.1**	**1.7**	**22.4**	**1.7**
12.5	26.2	2.1	29.5	2.4
13.1	26.2	2	29.5	2.2
13.8	26.7	1.9	30.6	2.2
14.8	26.7	1.8	30.6	2.1

Model	Mark-Bieniawski		UNSW	
Pillar Load	Strength	FOS	Strength	FOS
10.7	23.1	2.2	22.4	2.1
11.0	**23.1**	2.1	**22.4**	2.0
10.7	26.2	2.5	29.5	2.8
11.0	26.2	2.4	29.5	2.7
11.4	26.7	2.3	30.6	2.7
11.9	26.7	2.2	30.6	2.6

7.3 Consideration of Faults on Pillar Stability

The faults at Clarence are typically in a NNW-SSE, NW-SE or NNE-SSW orientation. For 918 Panel, the projected faults have a NNW orientation. The mapped and projected faults (provided by Centennial) are presented in Figure 13. A summary of key faults is included below:

- The parallel faults transecting 918B1 Panel are classified with 1-2m throw and potential for major washout. At this location the pillars have a minimum W/H > 10 and a FOS > 2.2 with the single side abutment.

- The faults that are projected to transect 918A Panel and 918B2 Panel in the zone of double abutment zone are mostly in the zone where the central pillar has a W/H ratio of greater than 10. At this location the pillars have a geometric load minimum FOS of 1.7 and model load minimum FOS > 2.2.

- There is one projected fault that transects the central spine pillars at about 18ct. At this location the W/H ratio is > 8, and the load is likely to be closer to the tailgate load scenario with a geometric load FOS of 1.8 and a model load FOS likely to be higher.

Given the minor nature of most faults, oblique orientation to the pillar ribs and the strain hardening pillar geometries, the majority of pillars are considered to have minimal impact to pillar stability from the faults.

Large pillar W/H ratios and the resulting strain hardening is an important factor in assessing pillar stability. A fault located away from the pillar rib is subject to significant confinement and would not be anticipated to significantly impact pillar strength with pillars of 26m width.

A fault running obliquely through a pillar would not be anticipated to increase the rib or roof spall other than local effects due to the 26m pillar widths.

The worst fault location would be a fault paralleling the pillar rib line and within only a couple of metres of the rib. This may act to reduce the pillar size by a couple of metres. Given the orientation of the pillars to the fault strike, the faults are at an acute angle to the roadways for the cut throughs of the central spine pillars only. The effect of this could potentially be a reduction in pillar length by a couple of metres. Pillar length is not the key factor for pillar strength and as such, the conservative FOS for the pillars is anticipated to accommodate the event of a fault running parallel to, and close to, the rib line. Operational responses are also common at Clarence Mine, where pillar stability is actively improved by lengthening pillars and/or reducing lifts in response to the presence of geological structure.

Any minor increase to rib instability would be considered to be localised and therefore not inherently impact the stability of the pillar.

For the two faults projected through 918B1 panel with a 1-2m throw and major washout, the following notes are made:

- The pillar FOS is conservative due to the single abutment loading in this area.

- Any increase in roadway height from potential out of horizon drivage or cavities would be local or on one rib, and would therefore not ultimately alter the pillar strength.

- The worst case of increased rib spall would be aligned with the central spine pillar cut through rib i.e. impacting the pillar length (not width). Given the high FOS from single sided abutment, these pillars are considered stable with the presence of the projected faults.

The FOS of the pillars have an appropriate level of conservatism to allow for the projected faulting. Together with the primarily oblique nature of the faulting to the ribs and strain hardening design of the pillars, the potential for localised increased deformation is not anticipated to impact the stability of the pillars.

Although not a primary factor in pillar stability, the mine may choose to explore non-degradable/corrosive support strategies for supporting structured ground. However, given the conservative design of the pillars in the 918 panel, this may not be required.

8. OVERBURDEN CAVING AND HYDRAULIC CONDUCTIVITY

8.1 Review of Groundwater above 918 Panel

Figure 21 shows the current pre-development groundwater profile above 918A Panel indicated by a multi-string VWP arrays in Borehole CLRP41R. The profile indicates a separation between the shallow and deeper groundwater systems above the Mt York Claystone. The Mt York Claystone is located between the Banks Wall Sandstone and the Upper Burra Moko Head Sandstone. The reduction in pore pressure between the upper and lower groundwater systems suggests vertical downflow and/or lateral outflow into valleys, perhaps caused by a regional reduction in groundwater in the lower groundwater table due to mining.

The hydrostatic profile in the lower Burra Moko Head Sandstone suggests a pre-development equilibrium of flow at and about the Katoomba Seam, including the Burra Moko Head Sandstone and the Caley Formation.

8.2 Caving and Overburden Connectivity to the Shallow Aquifer

This section presents a summary of observations in relation to caving characteristics, overburden fracturing and connectivity to the overlying shallow aquifer.

EMM (2022) identifies the Mt York Claystone as the basal unit of the shallow aquifer system. Strata2 (2022) and UNSW (2022) indicate that the average combined thickness of the Caley and Burra Moko Head Sandstone is 110m. By maintaining the panel width less than 110m, experience presented in Mills (2012) would indicate that the zone of large downward movement where vertically connected shear fracturing predominates would be limited to below the Mt York Claystone, assuming adjacent panels remain isolated from each other by maintaining a large enough intermediate barrier pillar.

In effect, if panels remain isolated by a large enough barrier pillar, vertical connectivity through the Mt York Claystone to the Banks Wall Sandstone would be expected to remain unaffected by mining. The proposed panel width geometries of 75m and 83m are anticipated to maintain a caving height approximately 30m below the Mt York Claystone.

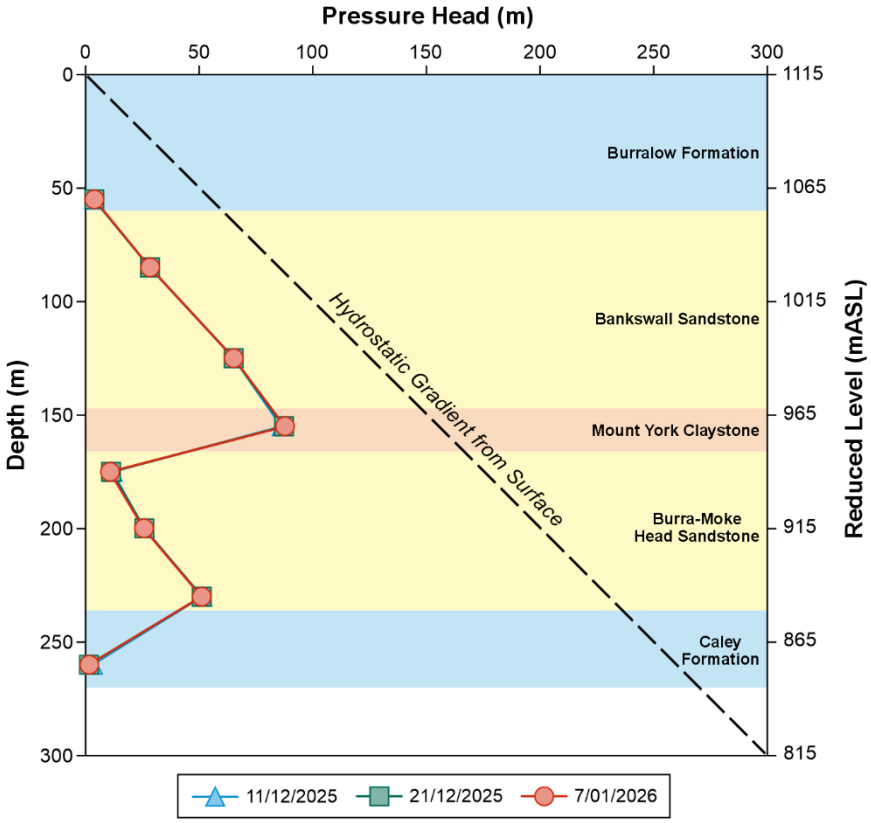

Figure 21: CLRP41R Piezometric Profile.

8.2.1 Caving Observations

8.2.1.1 300s Panels

The 308-311 Panels comprise 120m wide voids separated by 24m wide pillars. Strata2 (2021) reports "The available data from the 308 to 311 Panel area suggests that conditions deteriorated progressively as several adjacent panels were mined, which is indicative of the need to maintain sub-critical spans." This loading experience suggests that the geometry based on 120m voids and 24m chain pillars is not large enough to create isolated panels and that the load of the larger span of adjacent panels was experienced. This experience indicates the 24m pillars were not large enough to prevent non-elastic strata compression above these pillars. In this scenario, the lack of panel isolation would likely result in increased subsidence from chain pillar compression.

8.2.1.2 Airly Mine

Subsidence monitoring at Airly Mine showed a step increase in maximum subsidence from 200mm to 400mm when the overall width of extracted panels (each panel individually sub-critical) went from 240m to 330m during mining of the fourth panel. The overburden depth to the mining horizon is 250m. This step increase in subsidence suggests that the inter-panel pillars were not large enough to isolate the panels. Visible cracking of the Burra Moko Sandstone on the surface coincided with this subsidence increase, highlighting the potential span limit of the Burra Moko Head Sandstone when maximum subsidence reaches 300-400mm.

8.2.2 Piezometer Measurements

8.2.2.1 908-910 Panels

The 908-910 Panels used double-side lifting and are individually 80m wide and separated by a 40m wide barrier pillar. A multi-piezometer string is installed in Borehole CLRP22 midway along the 910 Panel (as shown on Figure 11), the first panel extracted. Figure 22 shows the piezometric profile measured in Borehole CLRP22 over the period of mining these panels. Figure 23 shows the piezometric pressure in Borehole CLRP22 plotted as a function of time.

Depressurisation at the top of the Burra Moko Head Sandstone is evident at 105m above the Katoomba Seam.

A drop in head pressure in the upper Burra Moko Head Sandstone piezometer is observed in April 2020 when 910 Panel extraction was mid-panel and just before commencement of mining in 908 Panel.

There is further reduction in pressure in the upper Burra Moko Head Sandstone piezometer as 908 Panel mines up to the piezometer. Strata2 report the piezometer installation failed due to a lightning strike in December 2020 while 908 Panel was still being extracted. Meaningful results were obtained from the upper piezometer when the readout was replaced but the deeper Burra Moko Head Sandstone piezometer remained unresponsive.

SCT have observed caving related fracturing and shearing from secondary extraction causing piezometer failures at sites. Although speculation in this instance, it is plausible that failure of the deeper piezometer may have occurred after the lightning strike and before the monitoring system was re-established.
The piezometer is located at 105m above the mining horizon. Numerical modelling suggests shear failure of strata up to 80-100m above the mining horizon with bedding shear connecting the caved zones above adjacent panels. The higher caving heights were modelled to occur above 908 Panel where the multi-panel effects are likely to have an impact on strata failure and caving. It is possible that the piezometer failure could have been caused by horizontal shearing of bedding planes within the strata.

Figure 22 suggests that the groundwater at the top of the Banks Wall Sandstone is recharging at a rate that maintains the shallow aquifer at pre-mining levels consistent with observation made in EMM (2022).

8.2.2.2 800s Panels

The majority of the 800s Panels are mined using single-side lifting. Two panels, 809 and 818A Panels, are mined using double-side lifting. The geometry of 818A Panel comprises 80m voids separated by a 54m wide spine pillar system and Panel 809 has 80m voids separated by a 56m spine pillar system.

Figure 24 shows the piezometric profile measured in Borehole CC115 above the 800s panels. This monitoring suggests substantial drawdown in the Burra-Moko Sandstone and low-level drop of up to approximately 10m water head in the Banks Wall Sandstone. This low-level drop may be due to volumetric change from bedding separation above the zone of large downward movement, or from reduced rainfall recharge.

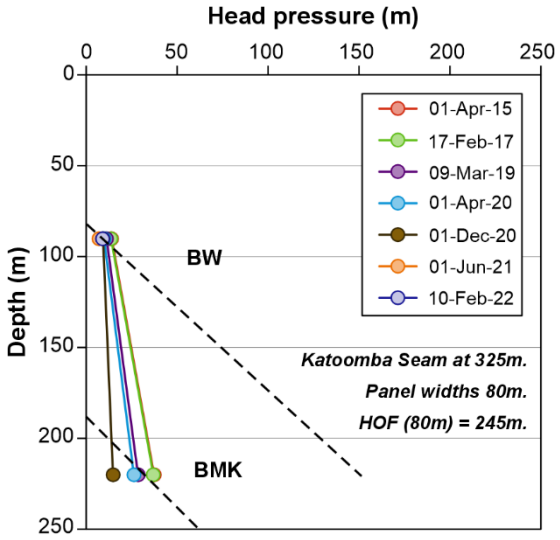

Figure 22: Piezometer profile for Borehole CLRP22 above Panels 908-910.

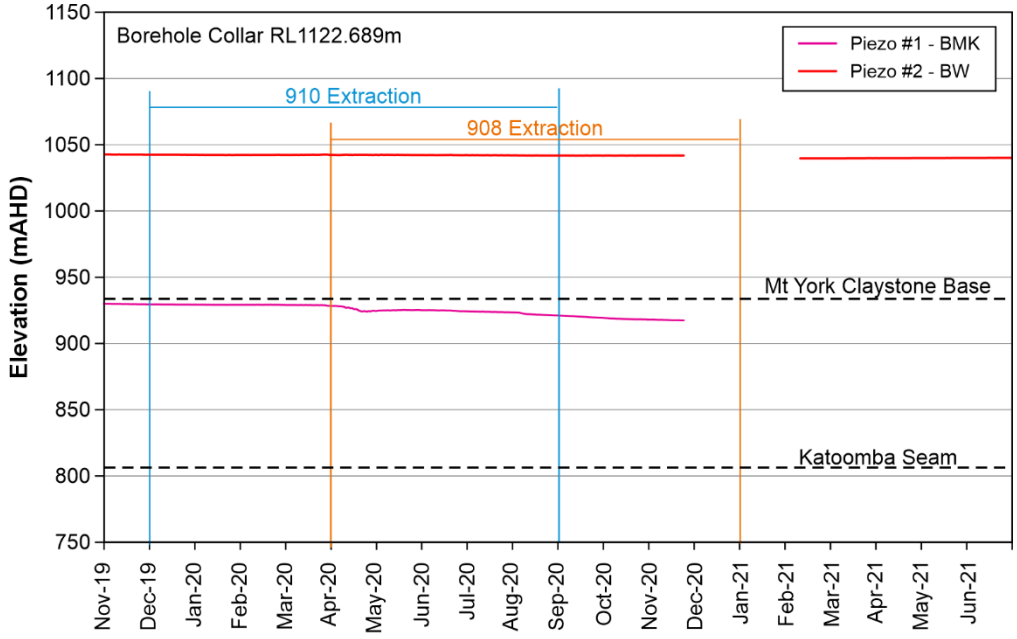

Figure 23: CLRP22 Vibrating wire piezometer hydrograph.

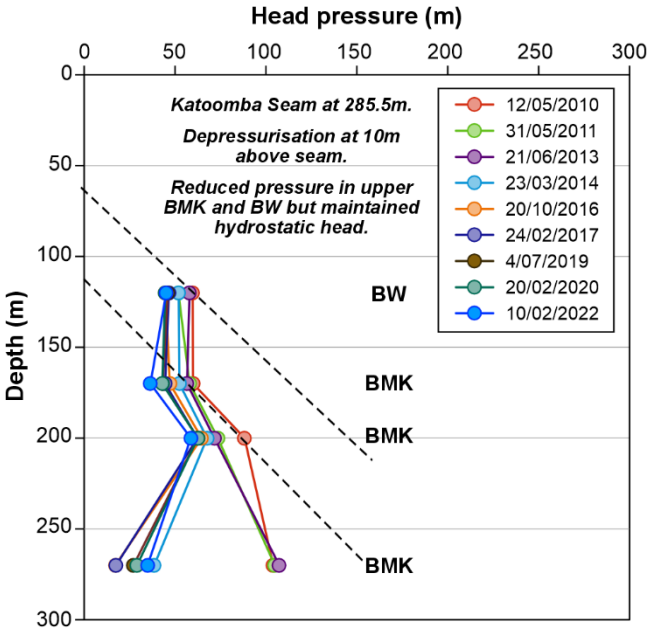

Figure 24: Piezometer profile for Borehole CC115 above Panel 812.

The upper Burra Moko Head Sandstone has maintained a hydraulic gradient which indicates that there is no mining induced hydraulic conductivity perceptible in this horizon at the resolution of the piezometer data. The observed reduction in head pressure could be due to reduced rainfall recharge prior to 2021, consistent with the relative drought in years 2017-2020.

Lowering of the water table is also measured by the piezometers at the Borehole CC114 control site. The data suggests the connection through the Mt York Claystone is minor and does not show indications of observable mining induced increase in conductivity.

The increase in piezometric pressure in the Banks Wall Sandstone in February 2023 is not observed in the upper Burra Moko Sandstone piezometers. This observation supports the inference that connectivity through the Mt York Claystone and the Banks Wall Sandstone is relatively low, and that recharge is greater than any minor flow or leakage that may be occurring through the Mt York Claystone.

8.2.3 Inflow Observations

8.2.3.1 Longwalls 1-6

The Strata2 (2021) report summarises inflows from longwall mining experience in LW1-LW6. Some key observations from this summary and mine geometry include:

- LW1 (182m wide, isolated panel, 160-300m DOC) – large water inflows
- LW2 (206m wide, 39m chain pillar to LW1, 160-300m DOC) – large water inflows
- LW3 (206m wide, 39m pillar to LW2, 160-280m DOC) – large water inflows

- LW4 (162m wide, isolated panel, 220-300m DOC) – no known incidents
- LW5 (206m wide, 39m chain pillar to LW4, 200-300m DOC) – inflows
- LW6 (150m wide, 39m chain pillar to LW5, 220-300m DOC) – no known incidents.

The above observations suggest that panels with a width greater than 180m have a high connection to the Banks Wall Sandstone aquifer and/or the surface and longwall panels with widths of 162m or less do not have a high connection through to the Banks Wall Sandstone aquifer.

These observations suggests that a span of 160m is adequate to preclude high inflows from the Banks Wall Sandstone or surface where the surface is less than 160m above the mining horizon. The Mt York Claystone is located about 110-120m above the mining horizon so it is plausible that the presence of the Mt York Claystone may be acting to reduce the mining induced hydraulic conductivity and therefore contributing to the lower inflows observed above narrower panels.

8.2.3.2 Mine Pumping Data

Figure 25 shows a correlation between water inflow into Clarence Colliery over the period 2017-2023 and cumulative rainfall deviation (CRD). EMM (2022) indicates that the shallow aquifer is recharged by rainfall and surface drainage lines. The correlation between inflow and CRD indicates the mining horizon is connecting to the shallow aquifer and/or the surface through mining-induced fractures and that the variation in mine water make corresponds with rainfall.

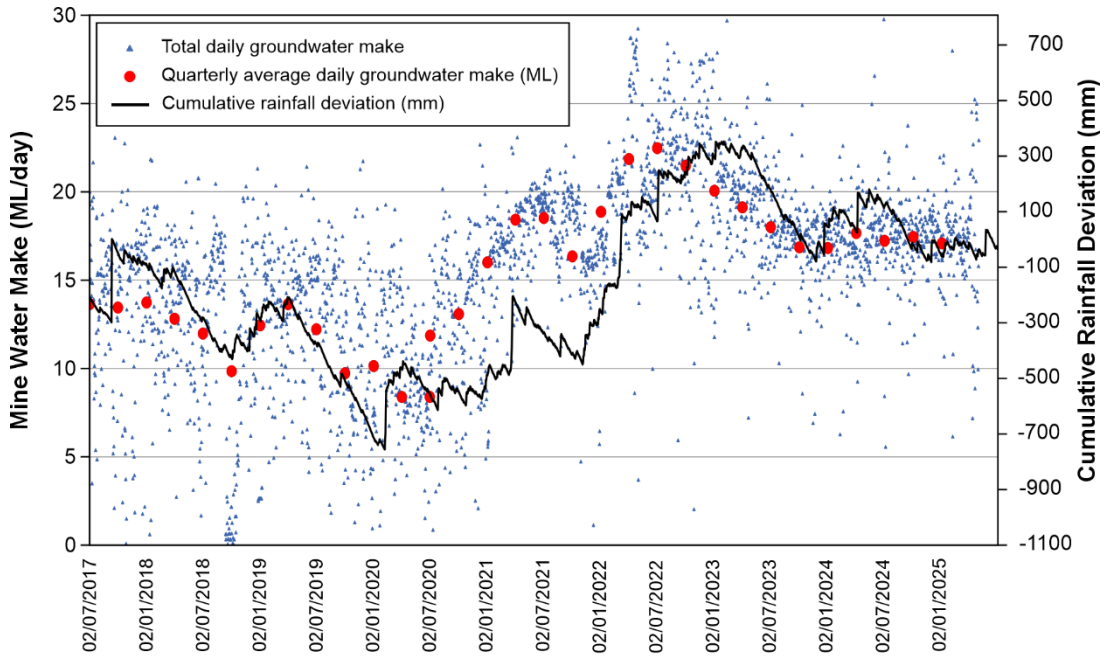

Figure 25: Clarence Mine water make.

Centennial provided mine pumping and inflow estimates for Clarence. Current total mine inflow estimates equate to 17.5ML/day of water make into the mine. The high inflows from the shallow longwall areas where panel width is greater than the overburden depth tend to overwhelm flows from other areas of the mine.

Corbett (2025) reports flows from 800 Area as being 4.2ML/day at completion of mining.

A summary of estimated inflow (from mine water storage) per area includes:

- All areas other than 908-910 and 800 area: 4-18ML/day dependent on rainfall.
- 800s Panels: 4.2ML/day measured over a 7km^2 extraction area and a 11km perimeter (28% of 800mm average annual rainfall for this period).
- 908-910 Panels: 0.7ML/day over a 1km^2 area and 5km perimeter (26% of 800mm average annual rainfall for this period).

The 908-910 Panels show similar inflow to the 800's Panels per area and less inflow per perimeter. This supports the evidenced theory of inflow per area for the adjacent Springvale Mine and other mines in the industry. Further analysis in relation to caving characteristics, horizontal flows and vertical flows may provide for a more detailed assessment on comparing the nature of inflows for the 800s and 908/910 Panels.

We recommend further analysis of mine pumping and storage data on a panel-by-panel basis to delineate the influence of individual panel geometries on mining induced fracturing and/or structure that may produce greater connectivity to the upper water table.

8.2.4 Implications for 918 Panel

The observations described above in this section indicate that the proposed panel geometry comprising of a 84-90m spine pillar system (3 pillars and 2 roadways) between 75m wide panels is unlikely to provide a substantial increase in mining-induced vertical connectivity through the Mt York Claystone.

With the Mt York Claystone at 110-120m above the mining horizon, the 75m and 83m panels are not anticipated to create vertically connected mining-induced fracturing to the Mt York Claystone, provided the 84-90m wide spine pillar system isolates each panel. It is anticipated that the 84-90m wide spine pillar system is wide enough to isolate the panels.

The numerical model results presented in Appendix 1 show the height of caving to extend above the mining horizon to a height of approximately 60-90m in the 280m depth model and 70-90m in the 180m depth model. The height of caving fractures are therefore a minimum of 20-30m below the Mt York Claystone.

8.3 Height of Depressurisation

SCT experience indicates Tammetta (2012) provides a reasonable first approximation for the height of total depressurisation above the 918 Panel. Tammetta's equation to estimate the height of total depressurisation is presented below:

$$H = 1438 \ln(4.315 \times 10{-}5u + 0.9818) + 26$$

where
u = wt1.4d0.2
t = seam thickness (m)
w = panel width (m)
d = depth (m)

Using the maximum depth of cover of 290m, maximum seam thickness of 2.3m and panel width of 75m, the maximum estimated height of total depressurisation from Tammetta's approach is 46m ± 25m.

Mining induced pore pressure drawdown can occur above the height of total depressurisation. This is observed in the piezometer data above 908-910 Panels and the 800s Panels, in Figures 22 and 24. The magnitude of drawdown and downward flow above the height of total depressurisation is dependent on the vertical hydraulic conductivity and the recharge (i.e. flow in vs flow out).

The caving height is anticipated to be about 60-90m above the mining horizon, based on modelling outcomes and consistent with a 1 x width/height ratio. The Mt York Claystone is a regional hydrological marker that appears to separate the upper water table and the lower water table. It is possible that some pore pressure reduction occurs up to the base of the Mt York Claystone. Pore pressure reduction is not anticipated to occur above the Mt York Claystone above the 918 Panel.

Ditton and Merrick (2014) propose the 95 percentile DGS height of fracture model where the "A Zone", labelled height of continuous fracturing, is estimated with the Geometry and Geology formulas below:

Geometry Model $A = 2.215\ W'^{0.357}\ H^{0.271}\ T^{0.372}$

Geology Model: $A = 1.52\ W'^{0.4}\ H^{0.535}\ T^{0.464}\ t'^{-0.4}$

where
W'= minimum of panel width and critical panel width (1.4H) (m)
H = cover depth (m)
T= mining height (m)
t' = effective width of strata within or above the "A Zone".

In DGS (2015), t' is noted to be 42m for Springvale and given the same strata lies between the Illawarra Coal Measures and the Burralow Formation, this would be considered representative. The massive portion of the Burra Moko Head Sandstone in Clarence borehole CLRP41 is 56m. Therefore, an estimate of t' ranging 42-56m is considered reasonable. Using a seam thickness of 2.3m, maximum depth of cover of 290m, panel width of 75m, the "A Zone" height is 66m and 52-59m for the geometry and geology models.

The DGS A-Zone is intended to refer to the zone in which the groundwater freely drains into the goaf above a panel, similar to Tammetta's height of total depressurisation. The A-Zone label of continuous fracturing is somewhat misleading as there is a mining induced and natural fracture network that extends above the height of depressurisation. The height of depressurisation depends on recharge and the conductivity of the natural and mining induced fracture networks.

The DGS A-Zone values of 52-66m are slightly greater than Tammetta's height of total depressurisation (46m ± 25m) and within range of the model caving height (60-90m).

The flow through the Mt York Claystone is a primary factor in determining the height of total depressurisation and the drawdown between the Mt York Claystone and this height of total depressurisation.

8.4 Conductivity

The majority of vertical conductivity increase from extraction of 918 Panel is anticipated to be within the height of caving up to 60-90m above the mining horizon. Some bedding separation may occur up to 120m above the mining horizon (1.6x panel width (Mills, 2022), however this is only anticipated to locally increase the horizontal conductivity and not the vertical conductivity. This volume change in the bedding separation zone is often observed as a small reduction in pore pressure, that then rebuilds with time. This has been observed at Clarence in borehole CC115 (Figure 24).

Gale (2009) formed a relationship between subsidence, overburden rock head and vertical hydraulic conductivity. This relationship is presented in Figure 26. For the low level of subsidence of less than 0.1m, the figures indicates that at the location of the Mt York Claystone at 110-120m above the mining horizon, the hydraulic conductivity is anticipated to be virgin hydraulic conductivity. This is consistent with the empirical and numerical model methods indicating the height of caving and height of depressurisation to be below the Mt York Claystone.

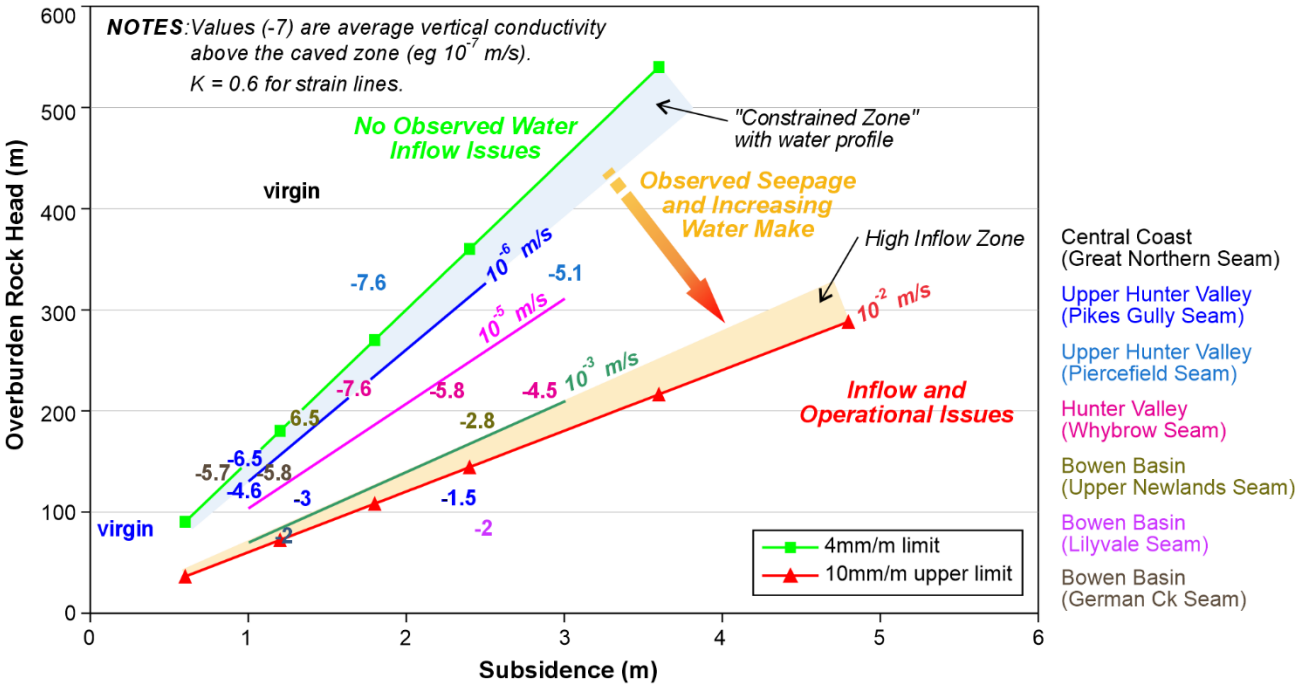

Figure 26: Average overburden conductivity characteristics relative to subsidence and depth criteria.

Vertical hydraulic conductivity of the caved zone was not directly modelled for this assessment; however, experience of modelling and research means that vertical hydraulic conductivity of the overburden above 918 Panel can be estimated:

- 0-45m above mining horizon 100-1,000,000 orders of magnitude greater than virgin
- 45-90m above mining horizon: 1-1000 orders of magnitude greater than virgin
- >90m above mining horizon: virgin.

The 100-1,000,000 times vertical hydraulic conductivity increase is the saturated hydraulic conductivity which most often corresponds with the zone of total depressurisation. This zone has a reduced saturation and therefore relative hydraulic conductivity orders of magnitude less than the saturated conductivity. This concept is being presented in a current ACARP project C33024 by Heritage (2025). The relative hydraulic conductivity of the zone of desaturated strata can be estimated from the saturated hydraulic conductivity of the last saturated layer (the limiting layer).

8.5 Faults and Connectivity

Faults and lineaments may provide for a connectivity pathway between the surface, upper water table and the lower water table. This pathway already exists in the unmined natural state and assists in the natural recharging of the lower groundwater table from the surface and upper water table.

The reduction in lower groundwater water table may facilitate additional flow along a fault from a change in pore pressure gradient. The Tammetta calculated height of depressurisation is significantly below the Mt York Claystone and the upper water table. The fault conduits are anticipated to continue to recharge the lower groundwater table in their natural state, thereby assisting to facilitate the recharge and presence of the pore pressure profile above the height of depressurisation.

Given the height of caving and the height of depressurisation being below the Mt York Claystone, the faults and lineaments are anticipated to provide water recharge to the lower groundwater table and have a low risk of reducing the pore pressure in the upper water table.

8.6 Experience of Mining Under the Pagoda Swamp

Pagoda Swamp is located above 906 Panel and was mined under with single sided lifting. The two adjacent 908 and 910 Panels were extracted with double sided lifting. D Line Subsidence survey line obliquely crosses 910 to 906 Panels and stops mid-way across 906 Panel. Figure 27 shows the location of the Pagoda Swamp over 906 Panel in relation to the D Line subsidence survey line and the seam geological structure.

The maximum subsidence across the 3 panels was 193mm. The subsidence under the Pagoda Swamp wasn't directly measured, however the first survey peg of D Line is located directly adjacent to the Pagoda Swamp and shows subsidence at this point of 130mm. Extrapolation of the subsidence trough along the location of the Pagoda Swamp infers the Pagoda Swamp was likely to experience subsidence of approximately 100-130mm.

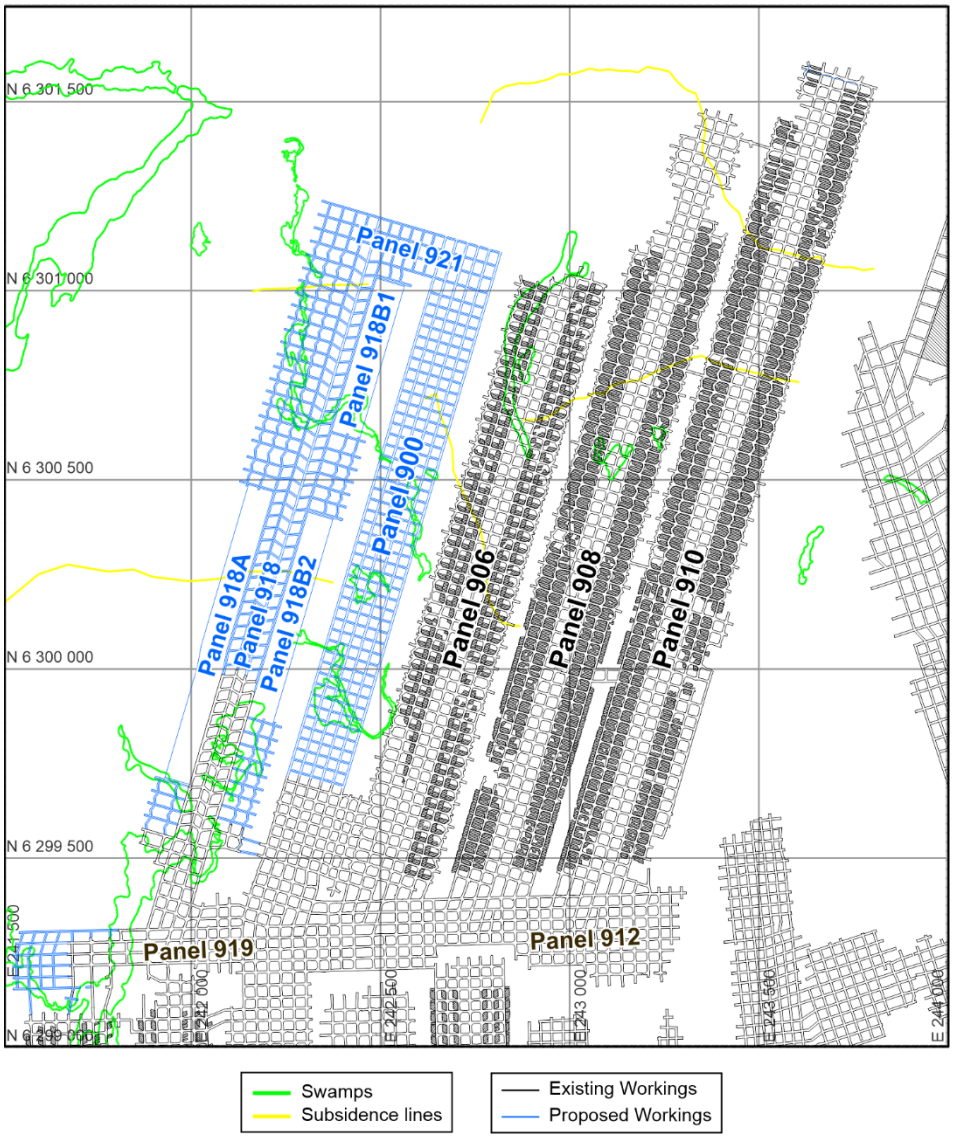

Figure 27: Location of Swamps with subsidence lines and seam structure.

A numerical modelling caving assessment of 910-906 Panel (Appendix 1) suggests that the height of caving for 910 and 908 Panels is ~80m, and a 30-40m caving height above 906 Panel.

Two 1-2m faults with major washout are located at the mining horizon and correlate with the location of the Pagoda Swamp. It is likely that the faults form the lineament that the surface drainage and Pagoda Swamp are located on.

There are two shallow piezometers in the Pagoda Swamp that show no obvious change in the swamp groundwater level that could be reasonable attributed to mining below the swamp. The piezometer hydrographs for the Pagoda Swamp standpipe piezometers, PG1 and PG2, are presented in Figure 28. The piezometers show that the groundwater level in the swamp varies about 50-100mm at its maximum variation. The trend in these variations appear to correlate with the CRD trend and therefore the swamp water level changes appear to be responding to changes in rainfall, with no discernible change from mining.

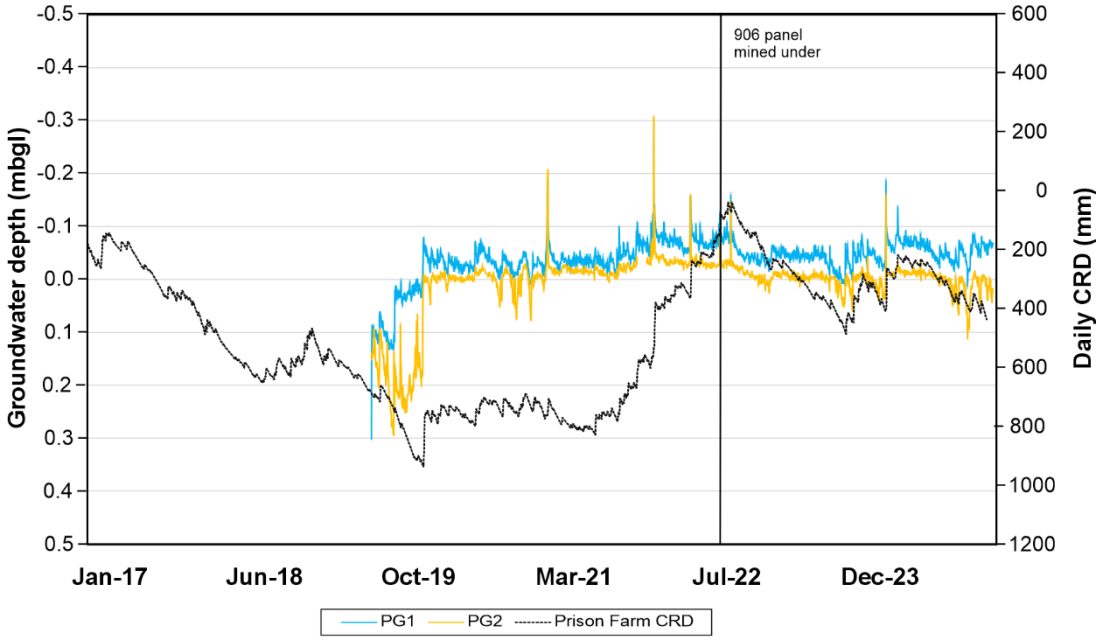

Figure 28: Hydrographs for Pagoda Swamp piezometers.

The modelling of 910-906 Panels suggests valley closure in the realm of 110mm in the vicinity of pagoda swamp. Model checks of panel closure for Airly MW13-16 are in the realm of measured horizontal movements.

The CLRP22 piezometer data, located above 910 Panel, is presented in Figures 22 and 23. CLRP22 experienced cumulative subsidence of approximately 160mm and shows a reduction in pore pressure in the Burra Moko Head Sandstone, but not in the Banks Wall Sandstone, which indicates that the mining induced pore pressure changes to not reach the upper water table above the Mt York Claystone.

9. SURFACE SUBSIDENCE

9.1 Literature Review and Site Experience

Clarence has yet to introduce panel-and-pillar partial extraction using the shortwall mining method, so there is no direct experience for comparison. There is however, experience of secondary extraction methods (longwall and pillar extraction) with geometries that are similar to and bracket the proposed geometry of 75m panels separated by a minimum spine pillar system with of 84m. The subsidence associated with mining these geometries is discussed in this section.

9.1.1 Subsidence over 906-910 Panels

Subsidence monitoring above 906-910 Panel indicates that the variable 40-55m barrier pillars between 82.5m wide panels and spine pillars of 60m combined pillar width are not large enough to control subsidence to less than 100mm for either a two or three panel mining geometry.

For 910 Panel, the first panel mined, the first survey in July 2020 shows a maximum subsidence of 98mm. However, this survey date includes additional subsidence influence from 908 Panel, with a subsidence trough shifted towards the pillar between 910 and 908 Panels. The exact subsidence for 910 Panel extraction only was not surveyed, however from this data we can assume that it was less than 98mm.

In October 2021 when both 910 and 908 Panels had been mined, subsidence survey data from 900D line indicates maximum subsidence of 147mm of subsidence over the central 40m barrier pillar. The 910-908 Panel geometry has not been able to maintain maximum subsidence over the panel at less than the limit of 100mm. Numerical modelling of this mining geometry suggests that the strata above the pillars is remaining intact, and that the panels are acting in an isolated manner. The subsidence appears to be due to compression of the strata above and below the pillars.

This subsidence is estimated to comprise 10-20mm of sag subsidence (the term used to describe subsidence that occurs as a result of the overburden strata sagging into each extracted panel if that panel were the only panel mined) and the remainder pillar compression.

The subsidence observed is consistent with a roof and floor stress bulb equal to 1.5 x pillar height average elastic modulus of 16GPa in the roof, 3GPa in the coal, and 10GPa in the floor. The theoretical load on the 910-908 40m pillar is estimated to be 16MPa at 250m depth, assuming a caving angle of 21°.

By July 2022, a further subsidence survey of 900D line conducted showed subsidence had increased from 147mm to 158mm. Given the bias of this subsidence to the 906 side of the subsidence trough, it is likely that this subsidence was caused by development of 906 Panel.

The secondary extraction of 906 Panel after 910 and 908 Panels has increased the maximum subsidence along D Line from 147mm to 193mm. The maximum subsidence is now located above the centre of all three panels above the central spine pillar system of 908 Panel. The panel geometry of 906 Panel is similar to 910 and 908 Panels, with similar 80m void widths and a 40-55m solid coal pillar between 908 and 906 Panels. The difference in geometry for 906 Panel is that the spine pillars have a smaller combined width of 55m compared with 60m, and the 906 Panel has a lower ratio of partial extraction from single sided lifting.

9.1.2 Longwalls 1-3

Longwalls 1, 2 and 3 have panel void widths of 180m, 206m and 206m, respectively. The chain pillars between panels are 39m wide. An extraction height of 3.7m is used for this assessment. SCT (1995) presents subsidence survey data for Longwalls 1 and 2 and SCT (1996) for Longwall 3. C Line, a cross line above Longwalls 1 and 2, shows sag subsidence over Longwall 1 is 124mm. When Longwall 2 is mined, total subsidence increases to 440mm centred over the chain pillar between the panels. Along C Line, the depth to the mining horizon ranges 250-270m (260m average) above Longwalls 1 and 2.

Pillar compression subsidence is estimated to be in the range 300-400mm. Estimates of elastic pillar compression range 90-190mm depending on assumptions around the size of the stress bulb. The experience from 908-910 Panel suggests a stress bulb of 1.5 x pillar width. Gale (2004) suggested a stress bulb of 3.5 x pillar width. Estimated elastic pillar compression of 90-190mm is significantly less than the 300-400mm observed, suggesting some non-elastic strata compression above the chain pillar.

The pillar between Longwalls 2 and 3 shows a similar trend where the sag subsidence is estimated at approximately 140mm for the empirical width/heights, and the total subsidence is approximately 650mm. Estimated elastic compression of the pillar is in the range 100-200mm using a 1.5-3.5 x pillar width stress bulb. This observation again suggests some strata softening above the pillars. The average theoretical pillar load on the pillars between Longwalls 1 and 2 and Longwalls 2 and 3 is approximately 22MPa.

D Line is a survey line along the centreline of Longwall 2. D Line shows maximum subsidence of 1.75m. The overburden depth along D Line is 170m, creating a supercritical panel geometry. This magnitude of subsidence is consistent with general Western Coalfield subsidence behaviour.

9.1.3 Longwalls 4 and 5

Subsidence data above Longwalls 4 and 5 indicate strata above the chain pillars has softened slightly and appears to be on the cusp of softening further.

Longwalls 4 and 5 at Clarence Colliery are 150m and 205m wide respectively. The chain pillar between them is 38.5m wide. Mills and O'Grady (1998) report that the centre of Longwalls 4 and 5 subsided 185mm and 280mm, respectively, after two extracted panels. The depth to the mining horizon is approximately 250m.

Sag subsidence from Longwall 4 was 73mm, implying 220mm of subsidence is attributed to pillar compression above the Longwall 4-5 chain pillar. The 220mm is twice the 112mm difference between subsidence in the centre of the panel measured and sag subsidence because sag subsidence is measured in the centre of the panel and pillar compression subsidence is measured over the chain pillar. A similar calculation for Longwall 5 indicates sag subsidence of 120mm and pillar compression subsidence of 200mm.

Estimates using an empirical approach indicate elastic strata compression of 85mm based on a stress bulb calibration from 908-910 Panels of 1.5 x pillar width. The pillar load is estimated to be 17MPa.

Only a small change in strata stiffness is required to increase the pillar compression to that measured. This pillar appears to be on the cusp of experiencing strata softening.

9.1.4 809 Panel

Panel 809 was double lifted leaving voids of 75m wide with a 56m pillar between. Maximum subsidence of 19mm was measured above this panel. Depth to the mining horizon at this location is 240m. A pillar width of 56m appears to provide an effective barrier between 75m panels. The average theoretical pillar load for this panel geometry is approximately 12MPa.

9.1.5 220 and 300 Series Panels

GHA (1993) presents the subsidence measured over the 220 and 300 series Panels. This data suggests non-elastic pillar compression.

Panels 222 to 225 have panel widths of 110m, 122m, 122m and 117m respectively. Extraction heights range 3.3-3.4m. Single rows of 22m wide pillars separate each panel. The extraction ratio within each panel is estimated to be 82%. Depth of cover ranges 175-200m.

C-D Cross Line surveyed the sag and pillar subsidence behaviour across the four panels. The panel width to depth ratios for Panels 222 to 225 are 0.55, 0.61, 0.68 and 0.67. These panels are subcritical in width. Sag subsidence is estimated from the Clarence datasets to be in the range 1.5-3% of extraction height or 50-100mm. Maximum subsidence for the first extracted panel was 40-45mm, consistent with the lower end of the expected range.

The addition of the second panel increased maximum subsidence to 500mm, with the maximum subsidence located over the pillar. The addition of the third adjacent panel increased maximum subsidence to approximately 800mm, with the location of the maximum subsidence towards the centre of the three panels. Theoretical elastic pillar compression subsidence is estimated in the range of 60-110mm depending on stress bulb height assumption of 1.5-3.5 x pillar width. The observed surface subsidence is significantly greater than the combined sag subsidence and estimated elastic pillar compression subsidence. Non-elastic pillar compression is inferred to have occurred.

The theoretical load on the two pillars between the first three extracted panels is approximately 19.5MPa. Estimated pillar strength is 18MPa, using Bieniawski's pillar design formula:

$$S_P = S_C(0.64 + 0.36\ W/H)$$

where S_C is coal strength estimated to be 6MPa, W is pillar width and H is the pillar height.

Pillar loading close to nominal pillar strength suggests that non-elastic strata compression may be a combination of pillar failure and strata softening above the pillar.

Pillar subsidence reduces between 224 and 225 Panels. This change is likely to be a combination of the average pillar load reducing to 16.5MPa and a block of solid coal located near the subsidence line.

Panels 308, 309 and 310 are 120m, 122m and 122m wide respectively. Extraction heights range 3.3-3.4m. The chain pillar widths separating the panels are 24m wide. Panel width to depth ratios of 0.58-0.63 indicate subcritical panel geometries. Individual panel sag subsidence is estimated to be in the range of 70-100mm.

P Line runs across the first three panels, where subsidence is approximately 600mm after two panels were extracted. Maximum subsidence occurs over the pillar. Maximum subsidence after three extracted panels increases to approximately 900mm centred over the central panel. These subsidence magnitudes and panel and pillar geometries are similar to the 220 series Panels and suggest non-elastic pillar compression subsidence.

9.1.6 609B Panel Stress Monitoring

The results of this monitoring are interpretive but suggest the pillars remain elastic.

Panel 609B is a partial pillar extraction panel, of 84m wide panels separated by a 60m wide combined spine pillar. An extraction ratio of 70% is estimated in the panels either side of the spine pillars. There is a 36m solid barrier pillar between 609B and 609C Panel. SCT (2004) reports the results of stress monitoring over the 609B spine and remnant pillars. Depth to the mining horizon is approximately 305m at this location.

The stress monitoring indicated that the remnant pillars were overloaded and shedding some load onto the spine pillars. The spine pillars indicated elastic loading at a measured load of 15-17MPa and subsidence of only 22mm. At the time of this monitoring, secondary extraction of adjacent 609A and 609 Panels had not yet started. The report estimated that a maximum of 150mm may be experienced once all panels were extracted.

This analysis suggests that strata above the 36m wide barrier pillars remained elastic.

9.1.7 Airly Mine

The panel-and-pillar geometry planned at Clarence is likely to cause less subsidence than the > 700mm of subsidence that developed at Airly Mine because the 1.6-2.2m seam height at Clarence is less and the overlying strata has a higher elastic modulus. Subsidence observed at Airly Mine highlights the potential for non-elastic strata softening above the pillars to increase surface subsidence. The experience also confirms the importance of conducting numerical modelling where rock failure above chain or barrier pillars can contribute to strata compression and subsidence.

A series of miniwall panels at Airly Mine caused over 700mm of surface subsidence that detailed numerical modelling attributed to non-elastic pillar compression of the 30m wide chain pillars located between 60m wide miniwall panels at a depth to the mining horizon of 280m (Heritage et al, 2022). This depth is similar to the depth of mining at Clarence.

A modelling assessment indicated that rock failure of the strata above the pillars was the cause of the increased subsidence. The modelling assessment also found that 70m pillars are wide enough to isolate adjacent panels and limit softening of the strata above the pillars for 61m wide panels. The 70m wide pillars and 61m void widths were successfully implemented in Mt Genowlan at Airly Mine, maintaining the subsidence below the 125mm limit for 4 adjacent miniwall panels. Table 5 shows the modelled and surveyed maximum subsidence for 4 adjacent miniwall panels MW13-16.

9.1.8 Summary of Observed Chain/Barrier/Spine Strata Behaviour

Table 6 summarises the panel geometries discussed in this section and their influence on elastic and non-elastic strata behaviour. Non-elastic strata behaviour is referred here as strata softening, whereby fracturing of the strata above the pillars reduces the stiffness of the strata and causes greater compression. The average pillar load in Table 6 is the theoretical pillar load, except for Panel 609B where the pillar load was measured. The magnitudes of measured subsidence are also tabulated to show the low levels of subsidence associated with elastic pillar behaviour for subcritical panel geometries.

Table 5: Comparison of Modelled and Surveyed Cumulative Maximum Subsidence for MW13-16

Panel	Modelled Maximum	Surveyed Maximum	Difference
MW13 (outlier outside panel)	28mm	30mm (38mm)	+2mm (+10mm)
MW14	63mm	78mm	+15mm
MW15	94mm	95mm	+1mm
MW16	114mm	109mm	-6mm

Table 6: Summary of Barrier/Chain/Spine Pillar Behaviour

Panel	Panel Geometry (m)*	Pillar Width (m)	Depth (m)	Average Pillar Load	Pillar Loading Characteristics	Subsidence
Airly – Mt Genowlan	60-70-60-70-60-70-60	70	280	12MPa	Elastic	78mm (2 x panels) 95mm (3 x panels) 109mm (4 x panels
809	75-56-75	56	240	12MPa	Elastic	19mm (2 x panels)
918	***75-84-75***	***84***	***265***	***16MPa***	***Expected Elastic***	***76mm (2 x panels) predicted***
609B	84-60-84	60	305	15-17MPa	Elastic	(no data)
910-908	82-60.5-82-40/55-82-60.5-82	40-55, 60.5	250	16MPa	Elastic	<98mm (2 x panels) 147mm (4 x panels)
LW4-5	150-39-205	39	250	17MPa	Cusp of Strata Softening	280mm (2 x panels)
LW1-3	180-39-206-39-206	39	260	22MPa	Softening	440mm (2 x panels) 650mm (3 x panels)
Airly – Mt Airly	61-30-61-30-61-30-61	30	270	18MPa	Softening	93mm (2 x panels) 196mm (3 x panels) 403mm (4 x panels) 550mm (5 x panels) 610mm (6 x panels) 700mm (10 x panels)
222-224	117-22-122-22-122	22	190	19.5MPa	Softening	500mm (2 x panels) 800mm (3 x panels)
308-310	120-24-122-24-122	24	200	20MPa	Softening	600mm (2 x panels) 900mm (3 x panels)

** Panel Geometry is identified as: Panel Width – Pillar Width – Panel Width… and so on*

The onset of fracturing of the strata overlying the pillars includes factors such as pillar load, strata strength, bedding strength and pillar width. These factors influence the ability of the strata to generate confinement and increase strength. At Clarence Colliery, overburden strata is assumed to be relatively consistent across the site. Pillar load and pillar width are therefore the most important factors for comparing subsidence behaviour across the mine site.

Table 6 shows that elastic behaviour is observed when the total spine/barrier/chain pillar widths are in the range 56-60m, and pillar loads are less than 15-17MPa for 60m pillars and less than 12MPa for 56m pillars. Non-elastic strata compression is observed when pillar loads are greater than 16MPa and the widths of spine/barrier/chain pillars is 40m or less.

These outcomes are not subsidence estimates, they show inferences on strata behaviour above pillars, that influence increases in subsidence due to non-elastic pillar compression. Strata softening above pillars leads to subsidence greater than estimated using elastic subsidence assumptions and panels that are no longer isolated from each other. The loss of this isolation causes an increase in caving height and greater overburden connectivity.

9.1.9 Implications for 918 Panels

The 918 Panel spine pillar system with a minimum width of 84m is anticipated, both empirically and numerically, to not experience strata failure above the pillars. The risk of surface subsidence increasing beyond estimated elastic compression is considered low.

The average load on the 84m barrier pillar is estimated to be 16MPa, assuming a caving angle of 21° and 285m depth of cover. The proposed 918 Panel mining geometry is included in Table 6. The average pillar loads for 918 Panel are consistent with pillar loading that has shown elastic strata compression behaviour and low levels of subsidence at Clarence Colliery and Airly Mine notwithstanding that 809 and 609B Panels were isolated panels where some load may have been distributed to surrounding coal. The spine pillar system width for 918 Panel is greater than the previous panels.

The impact of multiple adjacent panels needs to be considered in the design of proposed extraction panels. Additional panels have potential to increase elastic strata compression and cause non-elastic strata compression. For instance, extracting 908 Panel adjacent to 910 Panel increased the subsidence over 908 and 910 Panels to greater than 100mm by transferring some of the abutment load.

Airly Mine experience for 70m pillar widths and 60m panel widths observed >100mm of subsidence with four adjacent void widths. Although Airly Mine has comparatively weaker overlying strata and an extraction height of 2.8m, and so is not a direct comparison with Clarence , the experience highlights subsidence loading mechanisms and characteristics that may need to be considered with additional adjacent panels.

Based on the additional adjacent panel experience, this review highlights that if additional panels are mined adjacent to the proposed 918 Panel, further assessment is required. Assessment of subsidence from additional panels is not immediately required for 918 Panel but is likely to become a requirement in other mining areas where secondary extraction is planned.

It is recommended that surface subsidence monitoring is used to ensure subsidence is below 100mm for 918 Panel.

Further assessment may be required for subsequent panels elsewhere in the colliery holdings including the 900 Panel currently functioning as first workings mains development but planned for secondary extraction in the future. This further extraction can be assessed as needed after mining 918 Panel and does not directly impact the initial extraction of the 918 Panel.

9.2 Modelling Assessment

Centennial engaged SCT to conduct a geotechnical characterisation and numerical modelling subsidence assessment in the 900 area of Clarence to estimate surface subsidence for the 918 shortwall panel (SCT report CLR5844, 2026). The full report is included in Appendix 1, with a summary included in this section.

The objectives of the numerical modelling subsidence assessment were to:

- Validate the SCT numerical model approach of estimating subsidence by modelling the already mined and surveyed 910 to 906 Panels.
- Use the validated model to estimate the subsidence for 918 Panel with a 180m and 280m depth of cover model and two mining scenarios for each depth:
    - Shortwall extraction of 918B Panel and first workings in 918A Panel.
    - Shortwall extraction of 918A and 918B Panel.

9.2.1 910-906 Validation Model Outcomes

The numerical model outputs for the 910-906 validation model are presented in Figure 29, showing vertical stress, shear strain and modes of rock failure. The vertical stress presented in Figure 29a shows the stress reduction above the extracted panels and abutment stress above the pillars. The increased abutment stress compresses the pillar and causes subsidence above the chain pillar.

The shear strain and mode of failure plots in Figure 29b and 29c show the caving profiles of the 910 and 908 Panels extending ~80m above the seam, below the Burra Moko Sandstone. Horizontal shear is occurring along a claystone at this horizon. Double sided lifting was used for pillar extraction in 910 and 908. The singled sided lifting in 906 has produced caving profiles substantially smaller than the 910, 908 panels. Caving above the 906 Panel extends 30m to 40m above the seam.

No significant failure is observed above the spine and barrier pillars for 910 and 908 Panels. Shear fracture and reactivation is observed above 906 Panel and remnant pillars where single sided lifting has been modelled.

Subsidence derived from numerical modelling of 910 to 906 Panels closely aligns with surveyed subsidence over D Line. Double sided lifting was modelled for 910 and 908 Panels where the extraction height is 3.2m. Single sided lifting was modelled for 906 Panel with an average extraction height of 2.6m. Results are presented in Table 7.

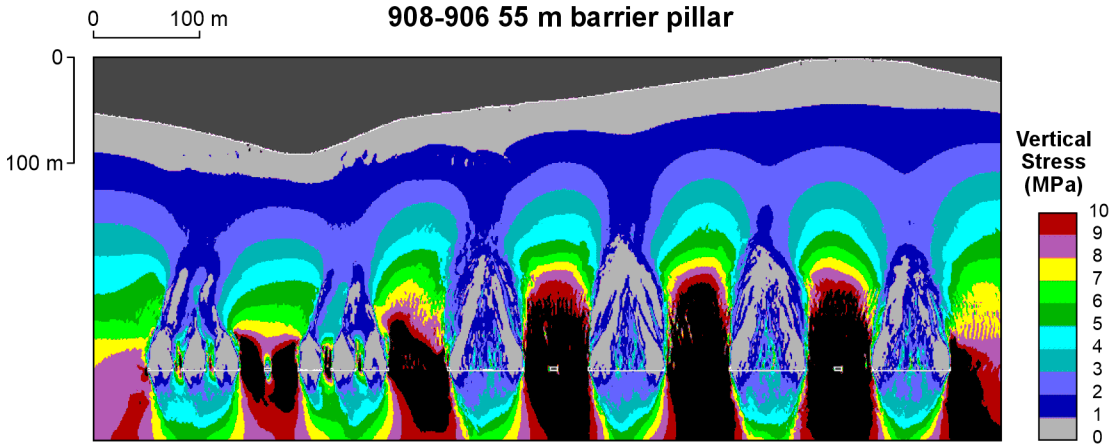

a) Vertical Stress.

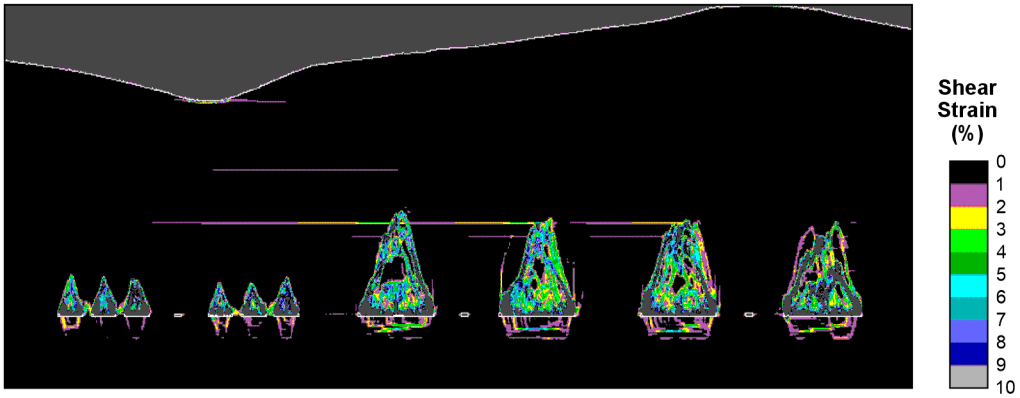

b) Shear Strain.

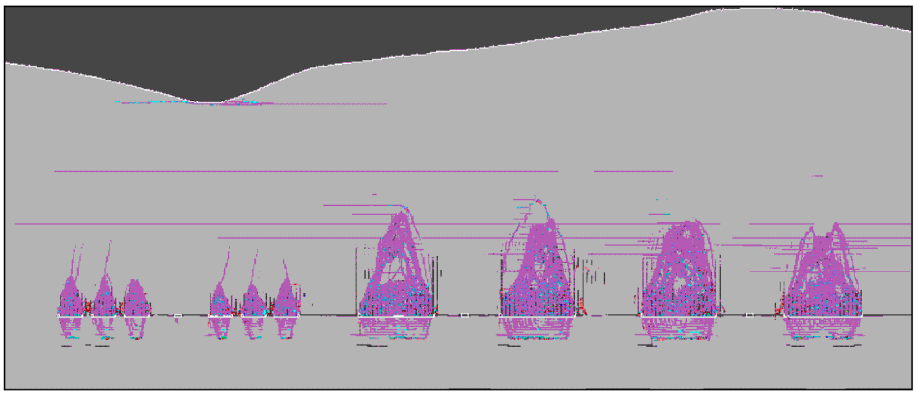

c) Rock Failure.

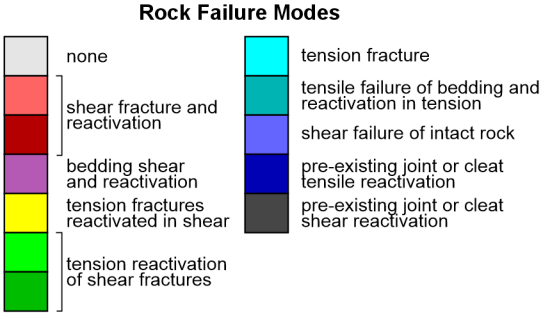

Figure 29: Panel 910, 908 and 906 caving models.

Table 7: Comparison of modelled and D Line surveyed subsidence for 910 to 906 Panel

	Cumulative Subsidence (mm)		Incremental Subsidence (mm)	
Panel	**Surveyed**	**Modelled****	**Surveyed**	**Modelled****
910	<98*	91	<98*	91
908	147	156	>63#	113
906	193	166	74	75

*Includes partial extraction of 908
#Reduced due to 910 survey including part of 908 extraction
**+-20mm survey tolerance should be applied to modelled results

9.2.2 918 Model Outcomes

The numerical model stratigraphic and lithological profile, including the geotechnical rock properties and strata properties, were used to model both the 910-906 validation model and the 918 Panel.

918 Panel modelling was conducted at 180m and 280m depth of cover. 918 modelling included:

- Shortwall extraction of 918Band first workings in 918A
- Shortwall extraction of 918A and 918B.

The extraction height was consistently 2.2m. For 918A and 918B2 shortwall panels, the modelled panel void widths were 75m and the total width of the spine pillar system was 84m including pillars and roadways. For 918B1 shortwall panel, the model panel width was 83m and the adjacent first workings in 918A have a combined width of 83m, with a spine pillar system width of 84m.

The vertical stress, shear strain and mode of rock failure are presented in Figure 30 for the 180m and Figure 31 for the 280m depth of cover models. Abutment stress is observed over the spine pillars and adjacent to the extracted shortwall panels. Vertical stress is increased through the spine pillars in the 280m depth model, as the abutment load is increased by the increased overburden.

Shear strain and mode of failure is presented in Figure 30 for the 180m and Figure 31 for the 280m depth of cover models. There are no signs of failure of the strata above the spine pillar in either depth model. The mine geometry does not appear to be at risk of significant subsidence increases due to strata softening. Caving fractures extend to a maximum of roughly 90m above the panel as shown by the shear strain in Figures 30 and 31. Caving fractures extend approximately 60-90m in the 280m depth model and 70-90m in the 180m depth model.

Subsidence estimates for shortwall extraction of 918 Panel are presented in Figure 32 and tabled in Table 8. The maximum subsidence estimates for 918 Panel with two adjacent shortwalls in 918a and 918b is 76mm. The maximum subsidence for the 280m depth model is located over the spine pillar. Maximum surface subsidence estimates for 918 Panel with two adjacent shortwalls in 918a and 918b is 71mm for 180m depth. The maximum subsidence for the 180m depth model is located over the panel centres.

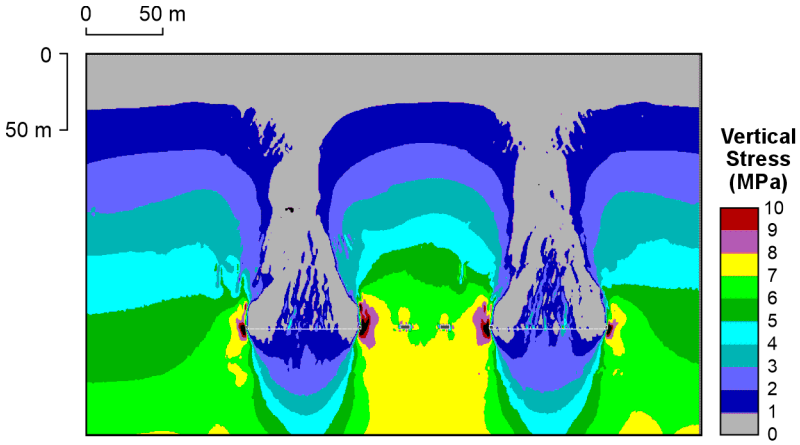

Vertical Stress.

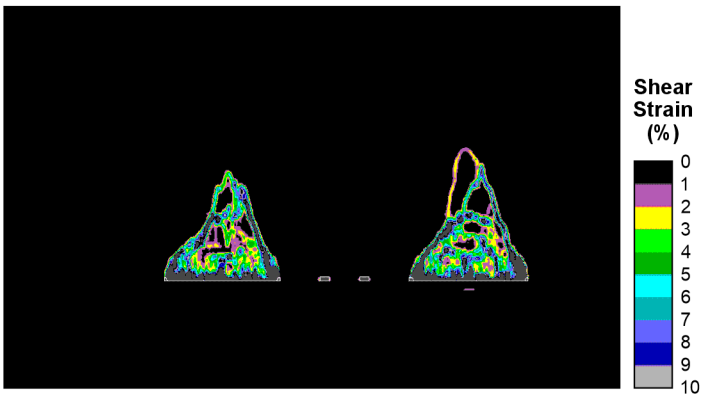

Shear Strain.

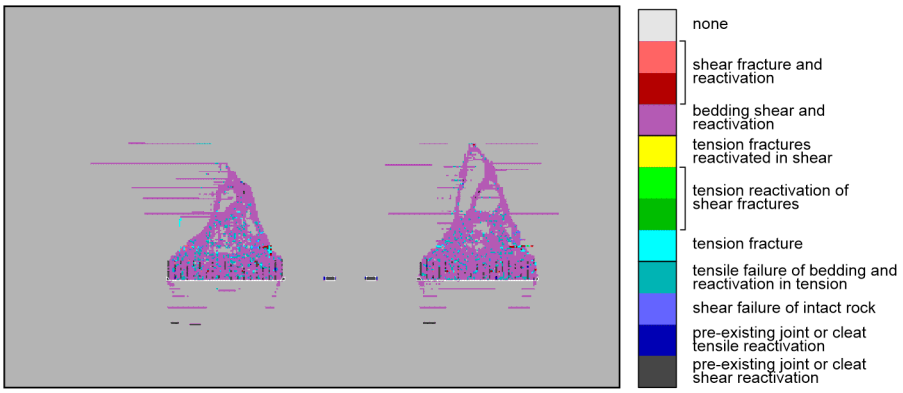

Rock Failure.

Figure 30: Panel 918 caving model 180m depth of cover.

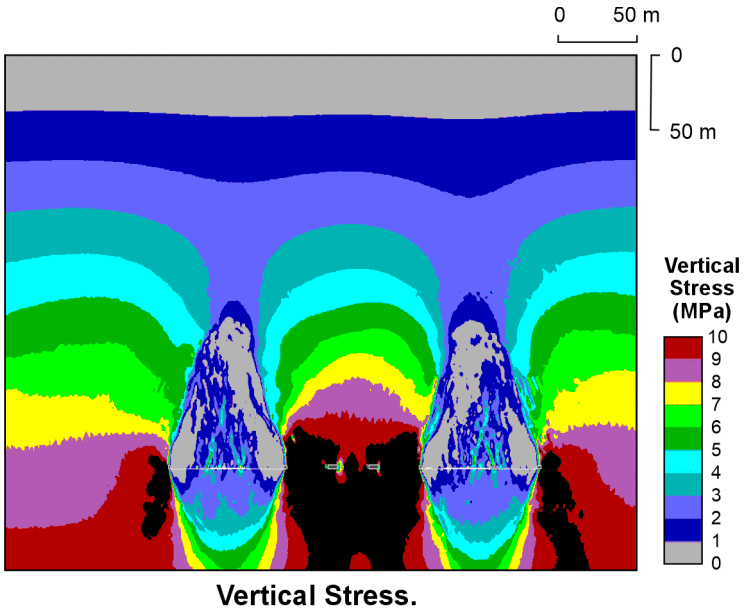

Vertical Stress.

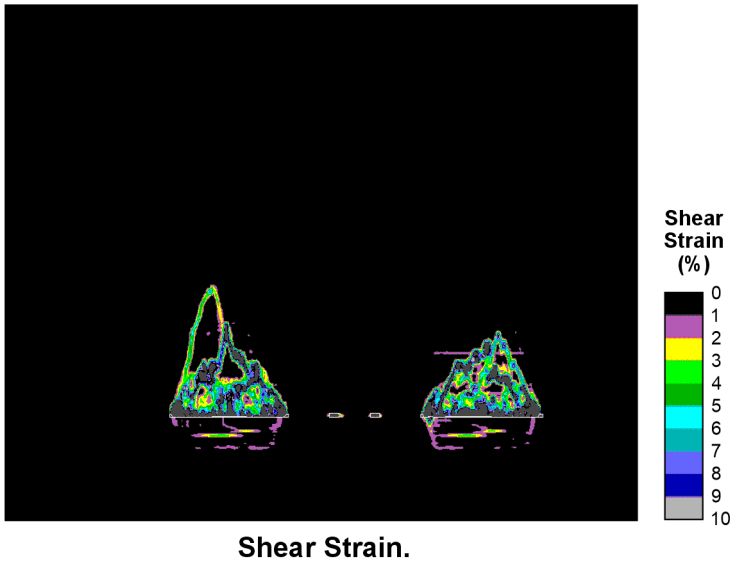

Shear Strain.

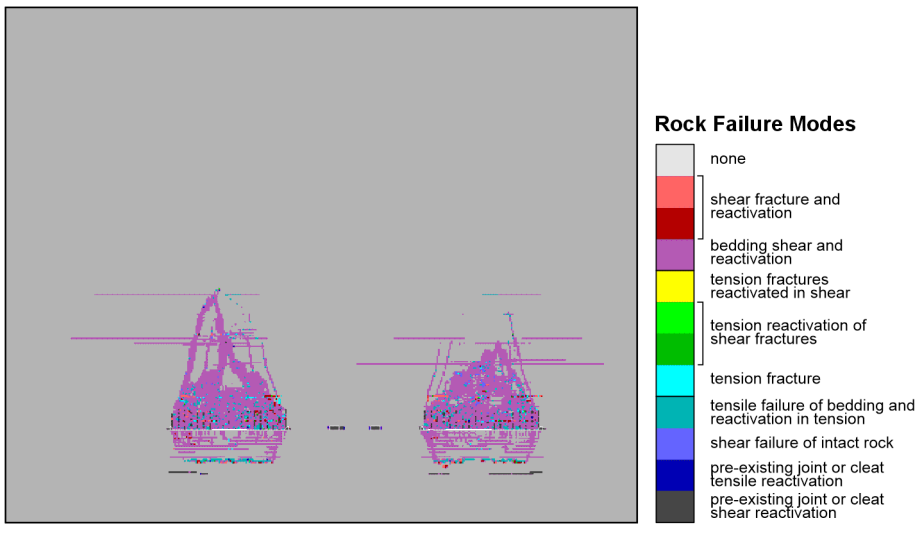

Rock Failure.

Figure 31: Panel 918 caving model 280m depth of cover.

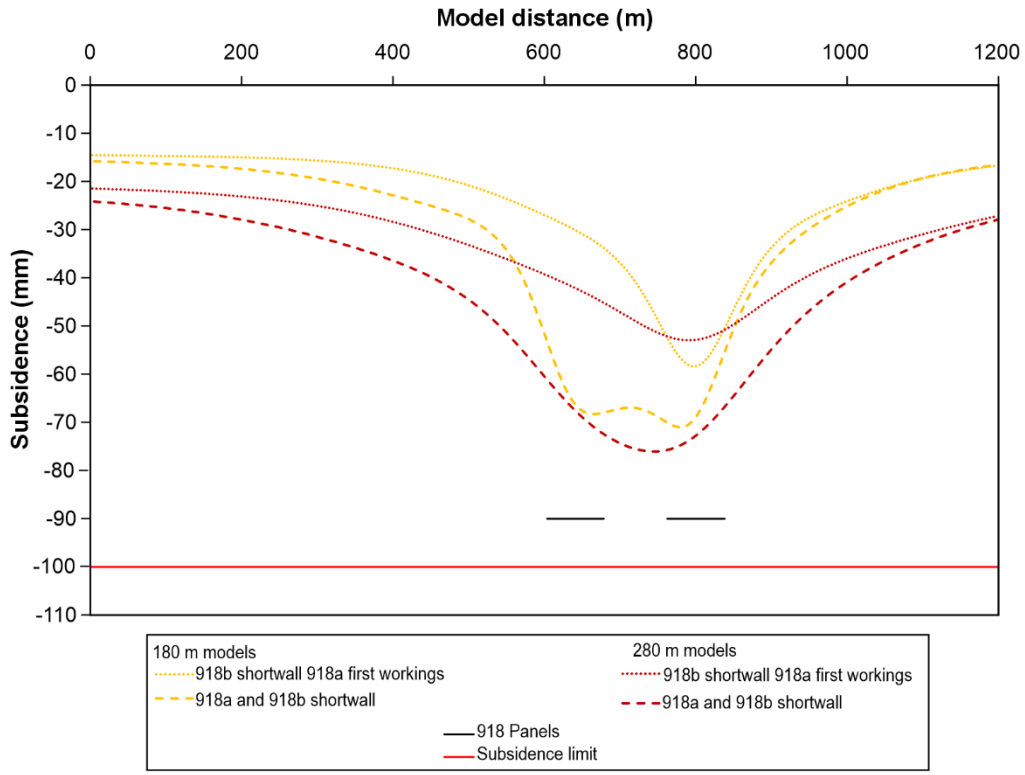

Figure 32: 918 Panel model surface subsidence.

Table 8: 918 Panel modelled subsidence estimates

Depth (m)	Panel width/depth	Modelled subsidence* (mm)	
		Shortwalls[1] (918A & 918B2)	Shortwall[2] (918B1) first workings (918A)
180	0.46	71	58
280	0.27	76	53

*±20mm survey tolerance should be applied to modelled results
[1] Panel void width 75m
[2] Panel void width 83

The proposed mining geometry includes a wider central spine pillar for panels inbye of 21 cut-through. The central pillar increases from 20m to 26m rib to rib. The increase in pillar width is anticipated to reduce the average load on the central spine pillar and is likely to correspond with a small reduction in the maximum surface subsidence for the deeper areas.

Model horizontal movements suggest panel closure of approximately 70-75mm. Although the model horizontal movements have not been exhaustively validated, experience at Airly MW13-16 shows model horizontal movements in the realm of measured horizontal movements.

9.2.3 Subsidence Modelling Addendum

Recommendations from the IEAPM review prompted an update to the modelling to address the following areas:

- The subsidence profile not extending to zero subsidence at the boundaries.
- The geotechnical assumption of massive sandstone strata (represented by the removal of pre-existing joints and bedding) in the Burra Moko Head and Banks Wall Sandstones.
- A sensitivity analysis to address the potential uncertainty or error margin.

These updates are presented in the SCT report CLR5844 Rev 1 (2026) also included in Appendix 1. To address the IEAPM recommendations and to update the modelling to include the widening of the spine pillar, SCT ran the following changes to the original models (base models) at the 180m and 280m depth scenarios:

- Increase in central spine pillar width to 26m – as per the mine design.
- Longer model equilibration run time pre-extraction.
- Increased model distance to boundaries to 1400m.
- Reduction in coal modulus of spine pillars from 3GPa to 2.5GPa to account for 3D pillar geometry loading in consideration of cut-throughs.

The above changes to the original model reduced the maximum subsidence of the subsidence profile for 918A and 918B2 panels by approximately 20mm.

To address the geotechnical assumption concerns and uncertainty analysis, SCT conducted the following parametric assessment to the updated model:

1. Removal of the massive sandstone assumption in the Burra Moko Head Sandstone and the Banks Wall Sandstone. The revised model includes a pre-existing joint and bedding network throughout the entire model. The effect of this change is less bridging at the top of the caved zone, resulting in an increase in sag subsidence, with an overall 2-5mm increase in maximum subsidence.
2. An uncertainty model assessing the impact of reduced strata stiffness. The assessment was achieved by reducing the average stiffness (Young's Modulus) of individual rock types by 1 standard deviation of the rock property dataset. This creates a lower bound of possible overburden stiffness. The uncertainty analysis model was conducted in conjunction with the non-massive sandstone model assumption.

The outcome of the uncertainty analysis provided subsidence profiles with a maximum subsidence of 65mm. The subsidence profiles for the three model scenarios are presented together with the original model outputs for the 180m and 280m depth models in Figure 33. The upwards shift in base model profile is evident, as well as the small increases in subsidence from the sensitivity assessments.

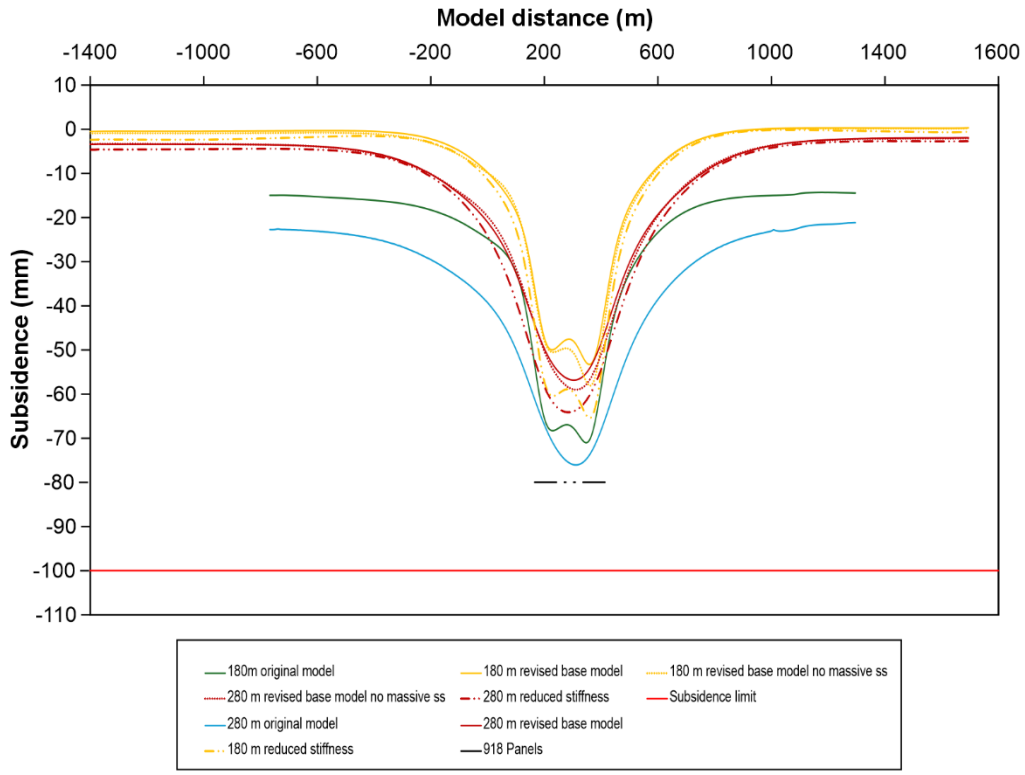

Figure 33: Subsidence profiles of 3 revised model scenarios compared with original model presented in report.

The revised modelling produced a maximum subsidence less than the original subsidence presented in Section 5.3.1 of this report. This reduction in subsidence is a result of the combined effects of model boundary and equilibration updates, increase in central pillar width, and uncertainty assessment with reduced stiffness of strata.

It is recommended that the original subsidence outcomes in this report be used for ongoing assessment as the more conservative outcome of the modelling assessments.

9.2.4 Discussion on Thickness of Caley Formation

The rock failure model in this report is based on the lithology of borehole CLRP27, located in 918B1 panel, where the thickness of the Caley Formation is 14m. The only other borehole in the vicinity of 918 panel is CLRP41, with the thickness of Caley Formation of 12m. The resulting height of caving in the models ranges 60-90m above the mining horizon, with a consistent Caley Formation thickness. The height of caving in the SCT model is not restricted to the Caley Formation and therefore not controlled by the thickness of the Caley Formation.

Given the subcritical nature of the panels, the maximum subsidence is primarily controlled by compression of the strata in the pillar system, with the sag subsidence from caving a lessor component. The compression of strata is related to all lithologies within the stress bulb above and below the mining horizon, not just the Caley Formation. SCT's experience is that using 1m detail in lithology through the overburden profile based on a representative borehole, provides reasonable subsidence predictions.

The Caley Formation thickness is not the control of caving height in the SCT model. Interbedded siltstone and sandstone exist within both the Caley Formation and the Burra Moko Head Sandstone, and so the thickness of the Caley Formation is not considered a key factor in determining subsidence.

The 20mm tolerance in subsidence predictions accounts for natural variability in lithology and geotechnical parameters, mining induced fracturing and survey error.

9.2.5 Discussion on Potential for Additional Subsidence

In additional to the uncertainty analysis discussed in Section 9.2.3, this section provides commentary on the potential for additional geotechnical changes that could provide for additional subsidence.

9.2.5.1 Roof and Floor Strength

The roof strata in the 918 panel consists of strong (approximately 80MPa Sandstone or siltstone).

The floor strata in the 918 panel consists of 2m of competent interbedded sandstone, mudstone and claystone with a high gamma signature in the geophysics. Below this immediate 2m floor is the Middle River Seam.

Slake durability testing has not been conducted for the 918 Panel boreholes, however there is a reasonable dataset in the 700s Panels, presented in Table 9. The slake durability in the roof and floor strata for the 700s Panels consists of claystone, mudstone and sandstone lithologies with a similar strength and high gamma response to the roof and floor of the 918 panel. The laboratory testing shows high slake durability >98%.

Table 9: Slake Durability for boreholes in the 700s area

Borehole	Height above Seam Floor (m)	Lithology	Slake durability Testing	
			ID1	ID2
CLRP23	2.21	Sandstone	99.1	98.4
CLRP23	-0.78	Sandstone	99.5	99.2
CLRP23	-1.82	Claystone	99	98.2
CLRP25	2.69	Mudstone	99.5	99
CLRP25	-0.16	Claystone	99.6	99.3
CLRP25	-0.73	Claystone	99.5	99.2
CLRP26	2.50	Claystone	99.4	98.9
CLRP26	2.04	Claystone	99.4	99
CLRP26	-0.23	Claystone	99.5	99.2
CLRP46	-0.13	Claystone	99.6	99.5
CLRP46	-0.43	Claystone	99.6	99.5

Immersion Testing was also conducted on boreholes in the 700s area for the same range in lithologies and roof and floor horizons tested for slake durability. The immersion testing results for the near roof and floor of the Katoomba Seam are presented in Table 10. The immersion test results show 67% of the samples were not sensitive to immersion, with the remaining 43% of samples at the lower end of slightly sensitive with an index of 2. Mark and Molinda (2007) present a relationship between immersion testing and slake durability as presented in Table 11.

The slake durability results and immersion test results are consistent with the immersion test results. These results indicate competent near roof and floor lithologies, even with the high gamma trace observed in the geophysical logs.

The roof and floor lithology is not anticipated to negatively impact the long-term stability of the pillars.

The floor strata below the immediate floor consists of the Middle River Seam, which inherently has a low strength and modulus due to the primary lithology of coal. Therefore, it is unlikely that the floor could have a lower average strength than what is modelled in the rock failure model. Any change in floor lithology is likely to be a stronger and/or stiffer lithology that would help to reduce subsidence due to strata compression.

Table 10: Immersion test results for boreholes in 700s area

Borehole	Height above Seam Floor (m)	Lithology	Immersion Index
CLRP26	-0.87	SA CS	1
CLRP26	-0.44	ST	0
CLRP26	2.09	CS/ST	2
CLRP26	1.72	ST	2
CLRP25	2.85	XT	0
CLRP25	3.35	ST	2
CLRP25	-0.23	CS	2
CLRP25	-1.02	CS	2
CLRP24	-0.54	ST	1
CLRP24	-0.08	ST	0
CLRP24	3.04	CS	1
CLRP24	2.14	ST	2
CLRP23	-0.31	ST	1
CLRP23	-1.28	CS	1
CLRP23	3.00	CS	0
CLRP23	2.34	CS	0
CLRP10	0.49	SS	2
CLRP10	0.91	ST	0
CLRP10	1.95	MS	2
CLRP10	-3.24	ST	2
CLRP10	-4.11	SH	1

Table 11: Moisture sensitivity classes and ratings from slake durability and immersion tests (from Mark and Molinda, 2007)

Moisture Sensitivity Class	Immersion Index	Slake Durability Index
Not Sensitive	0-1	100-98
Slightly Sensitive	2-4	98-92
Moderately Sensitive	5-9	92-80
Severely Sensitive	>9	<80

9.2.5.2 Flooding

The SCT model is not a time dependent model, and so the equilibrium state includes residual subsidence.

Our investigation into surveyed subsidence at Clarence Mine indicates that after steady state subsidence is achieved post extraction, acceleration may occur some years afterwards. It has been suggested that flooding is the cause of the subsidence increase. Although the post steady state acceleration of subsidence has been observed to approximately correlate with panel flooding, post steady state acceleration is also observed to occur without flooding.

We suggest that the post steady state acceleration of subsidence is due to ongoing remnant pillar failure, that could be accelerated by the introduction of water due to flooding. Therefore, the primary cause of the long term subsidence is related to the failure of remnant pillars or stooks, rather than the flooding itself.

Some examples of post steady state subsidence acceleration at Clarence are described below:

- 600s Panels - I and H Lines – The 600s Panels have single sided lifting, leaving remnant pillars of 12m width. The load on the spine and barrier pillars controls the subsidence. Failing of remnant pillars increases the abutment load on the spine and barrier pillars. The location of the increased subsidence due to flooding is where the depth of cover is the deepest, it is therefore likely that the flooding has weakened a portion of the remnant pillars to failure at the location of greatest pillar load – likely accelerating the long term remnant pillar failure.
- 908-910 Panels - B and D Lines – 908-910 Panels were double sided lifted. The additional subsidence along D Line could be attributed to both the failure of small remnant pillars or stooks, accelerated from flooding, and/or the first workings development of 906 Panel. The skewed nature of the additional subsidence to 906 panel suggests that 906 panel has a substantial influence in this additional subsidence. The small remnant pillars or stooks in double sided lifting are significantly smaller than in single sided lifting and many are likely to have already failed. Any remaining remnant pillars are susceptible to failure over time, and failure could be accelerated from flooding. B Line is located in the greatest depth of cover over 908 and 910 panels. The area around B Line has a portion of larger remnant pillars to the north, at the greatest depth of cover, which would be susceptible to weakening and failure from flooding. It is likely that the flooding accelerates the typically slow process of remnant pillar failure over time.

- Panel 714 single sided lifting – B Line – 714 Panel is an example of post steady state subsidence acceleration without panel flooding. The subsidence survey data shows an increase in subsidence 6 years after steady state subsidence. This panel was not flooded.

The SCT numerical modelling of 908-910 panel was based on full extraction, assuming all the remnant pillars have failed. The numerical model is validated on the final flooded subsidence with failed remnant pillars.

The nature of extraction of 918 panel is such that there are no remnant pillars. Therefore, flooding in 918 panel is not anticipated to materially increase the subsidence due to the mine approach having no remnant pillars or stooks and the spine and barrier pillars have a substantial FOS.

9.2.5.3 Faulting

The presence of faults may have the potential to increase subsidence in particular mining geometries. For the 918 Panel at Clarence, where the panel geometry is significantly sub-critical and subsidence is primarily driven by pillar compression, faults are not anticipated to increase the subsidence for this subsidence mechanism. Also see commentary in Section 7 regarding faults and pillar stability.

9.3 Cumulative Subsidence

The edge of 918B2 Panel is 300m from the edge of 906 panel. Central between these two panels is the first workings 900 Panel of 155m panel width, leaving a 70m wide barrier pillar next to 906 Panel and a 75m wide barrier pillar to 918B2 Panel. 918B1 Panel has a 66m wide barrier to the 900 Panel, however this is less of a concern as 918B1 Panel is an isolated panel with a small magnitude of sag subsidence only.

The experience of developing the first workings of 906 panel, suggests an observed increase the subsidence of 910-908 Panels of 11mm. The barrier pillar between 906 Panel and 908 Panel was 40m wide.

900 Panel is anticipated to produce subsidence of less than 20mm after first workings development. Current GNSS unit 900_05 is currently being mined directly under and shows <10mm of subsidence, with more to come once the panel development progresses further inbye.
Given the >70m barrier pillar widths between the 900 Panel and 906 and 918B2 panels, together with the small magnitude of subsidence anticipated for 900s panel, it is anticipated that the cumulative subsidence effects between the three panels result in minor subsidence increases over the 900s panel and the barriers, and not impact the 918 panel maximum subsidence.

The spine pillar system between 918A and 918B panels and the adjacent barrier pillar to the 900 Panel are large enough in width to maintain separation between the caved zones of each extracted panel. i.e. fracturing of the strata above the pillars was not modelled to occur, maintaining isolated caved zones in adjacent panels. As such, there is not anticipated to be an increase in caving height due to extraction of adjacent panels.

9.4 Subsidence Predictions, Effects and Impacts Assessment

The subsidence estimates in this report are for mine design purposes to apply with consent conditions and to inform the subsidence predictions. The subsidence predictions and impacts assessment is not included in this work scope and are understood to be conducted by Mine Subsidence Engineering Consultants (MSEC).

10. REFERENCES

ACARP 2005. Gale and Hebblewhite, "Systems Approach to Pillar Design – Module 1: Pillar Design Procedures" ACARP Project No. C9018. Final Report – Volume 1 (of 3). January 2005.

AMIRA 1994. Gale and Mills, Coal Pillar Design Guidelines – P351, Report No. AMI10157, January 2004.

Bieniawski, 1992. A method revisited: coal pillar strength formula based on field investigations In Proceedings of the Workshop on Coal Pillar Mechanics and Design. Pittsburgh, PA, IC9315 pp158-165.

Corbett, P, 2025. Personal communications by email 4 July 2025.

Ditton, S and Merrick, N, 2014. A new subsurface fracture height prediction model for longwall mines in the NSW coalfields. Geological Society of Australia, 2014 Australian Earth Sciences Convention (AESC), Sustainable Australia. Abstract No 03EGE-03 of the 22nd Australian Geological Convention, Newcastle City Hall and Civic Theatre, Newcastle, New South Wales. July 7 - 10. Page 136.

DGS, 2015. Geotechnical Data for Aquifer Disturbance Study in B and C-Zones above LWs 415 and 416, Springvale Colliery, DGS Report No. SPV-003/7c, unpublished.

EMM, 2022. Annual Environmental Monitoring Report (AEMR) 1 January 2021 to 31 December 2021, Report No. E210603 RP#3, Version 2 FINAL, March 2022.

Gale, W, and Hebblewhite, B, 2005. ACARP Project No. C9018 - SYSTEMS APPROACH TO PILLAR DESIGN Module 1: Pillar Design Procedures January 2005.

Gale, W, 2009. Aquifer Inflow Prediction above Longwall Panels, ACARP Project C13013, published 2009.

Heritage, Y, Boyling, A and Corbett, P, 2022. "Determination of the subsidence mechanism for subcritical miniwall panels, Airly Coal Mine." In Proceedings of the Eleventh Triennial Conference on Coal Mine Subsidence: Subsidence Engineering – From Art to Science, Kirkton Park, Pokolbin, NSW, 1–3 May 2022, pp 111–120.

Heritage, Y, 2025. ACARP Project C33024: Improved Model Upscaling of Overburden Hydraulic Conductivity for Input into Groundwater Models. Summary in May 2025 ACARP Current Projects Report , pp 12-13.

Mark and Chase, 1997. Analysis of Retreat Mining Pillar Stability (ARMPS) in Proceedings: New Technology for Ground Control in Retreat Mining, IC9446 pp17-34.

Mark and Molinda, 2007. "Development and Application of the Coal Mine Roof Rating (CMRR)", 2007, URL : https://stacks.cdc.gov/view/cdc/226764

Mills, KW, 2012. Observations of ground movements within the overburden strata above longwall panels and implications for groundwater impacts. Proceedings of 38th Symposium on the Advances in the study of the Sydney Basin, Hunter Valley, NSW. 14 Coalfields Geology Council of NSW.

Mills, KW, 2022. A perspective on the Mechanics of Mine Subsidence Above Longwall Panels in Proceedings of 11th Triennial Mine Subsidence Technological Society Conference, Pokolbin, NSW, 1-3 May 2022, pp 1-38.

SCT, 2026. Numerical Modelling Subsidence Assessment for the 900 Area at Clarence Colliery, SCT Report CLR5844 Final Rev1, dated 19 February 2026.

Strata2, 2021. Panel Design and Associated Subsidence Estimates, Report No. CLA-040-RevA 9Draft), February 2021.

Strata2, 2022. Review of Subsidence Data from Partial Extraction Areas (2021), Report No. CLA-064-Rev0, February 2022.

Tammetta, P, 2012. "Estimation of the Height of Complete Groundwater Drainage Above Mining Longwall Panels" Groundwater, National Groundwater Association doi:10.1111/gwat.12003, NGWA.org pp1-12.

UNSW, 2022. Numerical modelling study of mine subsidence related to shortwall extractions, Report No. 2022CL01, May 2022.

APPENDIX 1 – SCT REPORT CLR5844 REV1

SCT OPERATIONS PTY LIMITED

Strata Control Technology

CENTENNIAL COAL COMPANY PTY LTD

Numerical Modelling Subsidence Assessment for the 900 Area at Clarence Colliery

CLR5844

SCT Operations Pty Ltd PO Box 824 Wollongong NSW 2520 Australia
Phone: +61 2 4222 2777 Email: sctnsw@sct.gs Website: www.sct.gs
ABN: 23 078 328 953

REPORT TO Peter Corbett
General Manager Technical Operations
Centennial Coal Company Pty Ltd
1384 Castlereagh Highway
Lidsdale NSW 2790

TITLE Numerical Modelling Subsidence Assessment for the 900 Area at Clarence Colliery

REPORT NO CLR5844

PREPARED BY Rhys Pitchers
Yvette Heritage

DATE 19 February 2026

Rhys Pitchers
Senior Geotechnical Engineer

Yvette Heritage
Managing Director/
Principal Geotechnical Engineer

Report No	Version	Date	Revisions
CLR5844	Draft	5 March 2025	
CLR5844	Draft V2	13 March 2025	
CLR5844	Draft V3	11 April 2025	
CLR5844	Draft V4	17 April 2025	
CLR5844	Draft V5	19 May 2025	
CLR5844	Final	24 June 2025	
CLR5844	Draft Rev1	16 February 2026	
CLR5844	Final Rev1	19 February 2026	

EXECUTIVE SUMMARY

Centennial Coal Company Pty Ltd (Centennial) own and operate Clarence Colliery (Clarence) an underground coal mine located near Lithgow in New South Wales, Australia. Clarence targets the Katoomba Seam using first workings, partial extraction (single and double sided lifting) and plans to use shortwalls to extract panels in the 900 area. Centennial engaged SCT Operations Pty Ltd (SCT) to conduct a geotechnical characterisation and numerical modelling subsidence assessment in the 900 area of Clarence to estimate surface subsidence for the 918 shortwall panels.

Clarence has a 100 mm subsidence limit in its DA-504-00 development consent area, which includes the 918 shortwall panel. The partial extraction of panels 910, 908 and 906 resulted in 195 mm maximum surface subsidence surveyed along 900 D Line and was conducted in the IRM.GE.76 development consent area, which has a subsidence limit of 500 mm.

The objectives of the numerical modelling subsidence assessment were to:

- Validate the SCT numerical model approach of estimating subsidence by modelling the already mined and surveyed 910 to 906 panels.
- Use the validated model to estimate the subsidence for 918 panel with a 180 m and 280 m depth of cover model and two mining scenarios for each depth:
    - Shortwall extraction of 918B1 panel and first workings in 918A panel.
    - Shortwall extraction of 918A and 918B2 panel.

Subsidence estimates for shortwall extraction of 918 panel are presented in Table S1. 918B1 Panel void width is planned to be 83 m. 918A and 918B2 Panel void widths are planned to be 75 m. The total spine pillar width including roadways was modelled as 84 m. The proposed spine pillar width is 84 m from cut-through 1 to 20 increasing to 90 m from cut-through 21 to 52. The increase in spine pillar width (21-52 CT) is anticipated to reduce the maximum subsidence marginally, in the deeper areas, from the estimates presented below.

The maximum subsidence estimates for 918 panel with two adjacent shortwalls in 918A and 918B2 is 76 mm for 280 m depth. The maximum subsidence for the 280 m model is located over the spine pillar. Maximum surface subsidence estimates for 918 panel with two adjacent shortwalls in 918A and 918B2 is 71 mm for 180 m depth. The maximum subsidence for the 180 m depth model is located over the panel centres.

This report includes an addendum chapter in response to an IEAPM review which presents the additional numerical modelling and outcomes. Additional numerical modelling includes an update to base models, a sensitivity analysis and an uncertainty model. The details are outlined in Chapter 6. The addendum modelling did not exceed the original maximum surface subsidence estimates of 76 mm. Given that the original model is a more conservative estimate, it is recommended that the maximum subsidence from the original subsidence outcomes in this report be used for ongoing assessment.

Table S1: 918 Panel modelled subsidence estimates

Depth (m)	Panel width/depth	Modelled subsidence* (mm)	
		Shortwalls[1] (918A & 918B2)	Shortwall[2] (918B1) first workings (918A)
180	0.46	71	58
280	0.27	76	53

*±20 mm survey tolerance should be applied to modelled results
[1] Panel void width 75 m
[2] Panel void width 83 m

TABLE OF CONTENTS

PAGE NO

1. INTRODUCTION

Centennial Coal Company Pty Ltd (Centennial) own and operate Clarence Colliery (Clarence) an underground coal mine located near Lithgow in New South Wales, Australia. Clarence targets the Katoomba Seam using first workings, partial extraction (single- and double-sided lifting) and plans to use shortwalls to extract panels in the 900 area. Centennial engaged SCT Operations Pty Ltd (SCT) to conduct a geotechnical characterisation and numerical modelling subsidence assessment in the 900 area of Clarence shown in Figure 1.

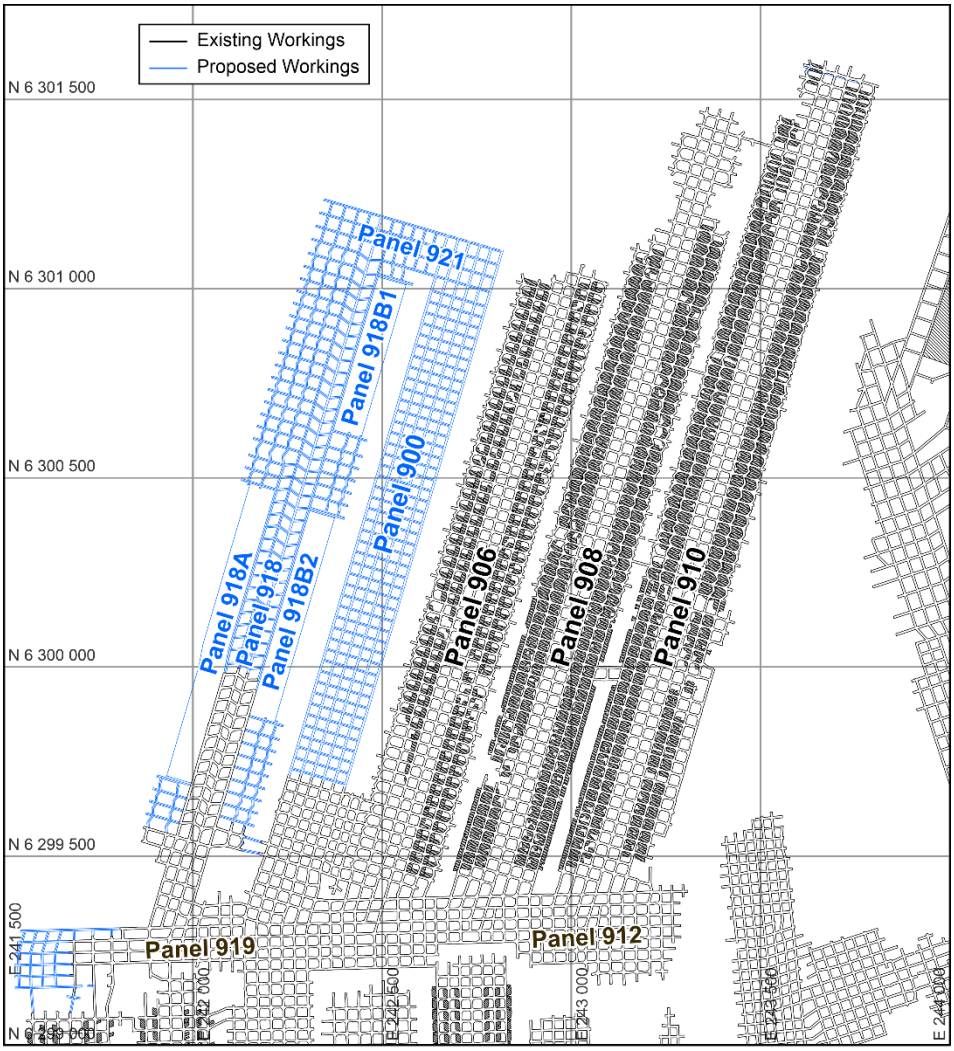

Figure 1: Mine plan showing existing 906, 908 and 910 panels and proposed 900s and 918 panels.

Clarence has a 100 mm subsidence limit as part of its mining approval for 918 Panel. Due to the undulating topography the depth of cover ranges from 160 m to 320 m in this area. The partial extraction of panels 910, 908 and 906 resulted in 195 mm of maximum surface subsidence surveyed along 900 D Line.

The objectives of the numerical modelling subsidence assessment were to:

- Validate the SCT numerical model approach of estimating subsidence by modelling the already mined and surveyed 910 to 906 panels.
- Use the validated model to estimate the subsidence for 918 panel with a 180 m and 280 m depth of cover model and two mining scenarios for each depth:
    - Shortwall extraction of 918B panel and first workings in 918A panel.
    - Shortwall extraction of 918A and 918B panel.

The modelled subsidence of 910 to 906 panel was compared with the surveyed subsidence to validate model results and to understand any variations between modelled and measured results. Modelling assumptions and parameters were refined with geotechnical basis in the validation assessment and are considered in the rock failure model for the first workings and shortwall extraction of 918 panel. 918 918B1 shortwall panel void width is planned to be 83 m. 918A and 918B2 shortwall panel void widths are planned to be 75 m. The total spine pillar width including roadways was modelled as 84 m.

Model subsidence results are presented for several scenarios. Tilts and strains are understood to be assessed by MSEC and are beyond the scope of this assessment.

SCT uses FLAC2D (ITASCA) software for numerical modelling assessments. The FLAC2D rock failure model uses site-specific rock properties derived from geotechnical testing of rock core and a model strength profile inferred from geophysics. SCT's in-house code is based on the Mohr-Coulomb Failure Criterion and represents multiple failure modes. These modes include shear and tensile failure of intact rock, shear and tensile failure of bedding and shear and tensile reactivation of failed elements, joints and bedding. Strain softening of the strata is also incorporated into the model based on geotechnical rock testing.

This report includes an addendum chapter in response to an IEAPM review which presents additional numerical modelling and outcomes. Additional numerical modelling includes:

- An update to base models where model boundary distance was increased, equilibrium pre-extraction steps were increased, spine pillar coal modulus was reduced from 3 GPa to 2.5 GPa and the central spine pillar width was increased from 20 m to 26 m.
- A sensitivity analysis model where massive sandstone strata was removed from the Burra Moko Head and Banks Wall Sandstones by reintroducing joints and bed partings
- An uncertainty model which includes non-massive sandstone strata and a reduction in strata stiffness of the rockmass inferred from geotechnical testing of key lithologies.

1.1 Scope

The following scope for this assessment is as outlined in email correspondence on 11 November 2024.

The work program consists of:

- *Geotechnical characterisation to determine geotechnical parameters for each rock type based on site specific rock test data. The stratigraphic rock property profile is based on inferred UCS from borehole geophysics. This allows for comparison of rock properties between the 910-906 panels and 918 panel.*
- *Modelling of 910-908-906 pillar extraction panels to conduct a validation/calibration assessment to gain confidence that the model is representing the correct failure mechanisms, and to refine rock properties, where appropriate and within reason, if required.*
- *Modelling of 918 shortwall panel based on 918 lithology and strength profile with learnings from 910-906 panel calibration assessment. A deeper and shallower profile are to be modelled.*

Additional scope items for 918 subsidence estimates was agreed in email correspondence on 25-26 February 2025:

- *subsidence predictions for additional 918 Panel development in areas where second shortwall void is not present.*

A revised mine plan was provided on 3 April 2025 to be included in the report and comment made on application of model subsidence estimates to revised mine plan.

1.2 Background on Subsidence Theory

The extraction of a coal seam underground results in the redistribution of stress, which strains the rockmass and may result in rock failure. Extraction methods such as pillar extraction, shortwall and longwall mining extract the coal seam in a predetermined panel and allow the overburden to cave as the extraction panel retreats. The subsidence that occurs above the extraction panel is referred to as sag subsidence (Mills, 2017).

Coal pillars are designed to be left between panels and are subject to abutment loading from adjacent panels and tributary loading from roadway development. The loading onto the chain, barrier or spine pillars creates compression of the coal pillar and compression of the strata above and below the pillar. The subsidence that occurs at the surface above a pillar between two extracted panels (goafs) is referred to as pillar compression.

When subsidence is subcritical (i.e. panel width / overburden depth < 1), and with increasing overburden depth, the pillar compression between two extracted panels can be substantially greater than the sag subsidence. The geometry of the pillars between two panels then becomes important in controlling the subsidence magnitude.

The Young's modulus (stiffness) of the strata is a key parameter in determining the pillar compression. Small changes in modulus can create substantial changes in pillar compression.

The panel width is an important factor in pillar compression as it influences the total abutment load. The pillar width is also an important factor as it impacts the average abutment load.

Additionally, when the abutment load exceeds the strength of the strata above the pillar, strata failure above the pillar occurs. Strata failure above the pillar acts to soften the strata (reduce stiffness) and increase pillar compression subsidence magnitudes (Heritage, 2022). In this scenario, post failure stiffness is a key parameter.

In subcritical, multiple panel scenarios, the chain pillar subsidence can cumulatively increase the overall subsidence magnitude. Likewise, the failure of the strata above the pillars may only onset when the cumulative abutment load exceeds the strata strength after multiple panels are extracted.

To limit subsidence in mine design, the mining geometry and strata geotechnical properties (intact and post failure) are equally important.

2. CONCLUSIONS AND RECOMMENDATIONS

2.1 Conclusions

Subsidence derived from numerical modelling of 910 to 906 panels closely aligns with surveyed subsidence over D Line. Double sided lifting was modelled for 910 and 908 panel where the extraction height is 3.2 m. Single sided lifting was modelled for 906 panel with an average extraction height of 2.6 m. Results are presented in Table 1.

Table 1: Comparison of modelled and D Line surveyed subsidence for 910 to 906 Panel

	Cumulative Subsidence (mm)		Incremental Subsidence (mm)	
Panel	**Surveyed**	**Modelled****	**Surveyed**	**Modelled****
910	<98*	91	<98*	91
908	147	156	>63#	113
906	193	166	74	75

*Includes partial extraction of 908
#Reduced due to 910 survey including part of 908 extraction
**+-20 mm survey tolerance should be applied to modelled results

The validation of 910 to 906 subsidence outcome provides confidence that the numerical model is producing representative surface subsidence. The numerical model stratigraphic and lithological profile, including the geotechnical rock properties and strata properties, were used to model both the 910-906 validation model and the 918 panel. For the 918 panel two depth of covers where modelled including a 180 m and a 280 m model. Mining methods modelled include:

- Shortwall extraction of 918B and first workings in 918A.
- Shortwall extraction of 918A and 918B.

The modelled extraction height is 2.2 m. 918B1 modelled panel void width is 83 m. 918A and 918B2 model panel void widths are 75 m. The total spine pillar width including roadways was modelled as 84 m. Following the revised mine plane the proposed spine pillar width is 84 m from cut-through 1 to 20 increasing to 90 m from cut-through 21 to 52. Noting the proposed mining geometry has been revised to include a wider central spine pillar for panels inbye of 21 cut-through. The central pillar increases from 20 m to 26 m rib to rib. The increase in pillar width is anticipated to reduce the average load on the central spine pillar and is likely to correspond with a small reduction in the maximum surface subsidence for the deeper areas.

Subsidence estimates for shortwall extraction of 918 panel are presented in Table 2. The maximum subsidence estimates for 918 panel with two adjacent shortwalls in 918A and 918B2 is 76 mm. The maximum subsidence for the 280 m depth model is located over the spine pillar. Maximum surface subsidence estimates for 918 panel with two adjacent shortwalls in 918A and 918B2 is 71 mm for 180 m depth. The maximum subsidence for the 180 m depth model is located over the panel centres.

2.2 Recommendations

A subsidence survey program is recommended to monitor subsidence during 918 panel shortwall extraction to compare measured subsidence with the modelled subsidence estimates and to provide monitoring for TARP response.

For 2D survey lines, it is recommended that the survey control is located outside the angle of draw. A survey control at least 150 m beyond the 918 panel footprint should be sufficient.

Table 2: 918 Panel modelled subsidence estimates

Depth (m)	Panel width/depth	Modelled subsidence* (mm)	
		Shortwalls[1] (918A & 918B2)	Shortwall[2] (918B1) first workings (918A)
180	0.46	71	58
280	0.27	76	53

*±20 mm survey tolerance should be applied to modelled results
[1] Panel void width 75 m
[2] Panel void width 83 m

To provide comparison of the surveyed subsidence with the model results, and to monitor the dynamic and progressive maximum subsidence trough, at a minimum GNSS units would ideally be located:

- in the centre of the first panel 918A
- above the centre of spine pillars between 918A and 918B2
- above the centre of 918B2
- above the centre of 918B1
- GNSS units located outside the panel edges to map the trough profile.

3. GEOTECHNICAL CHARACTERISATION

3.1 Topography

The topography above the Clarence underground workings is undulating with gully eroded creek systems and steep gradients leading to localised hilltops. Surface reduced levels over area 900 are presented in Figure 2 which show an incised creek system extending northwest from the start of 910 panel and west over 910, 908 and 906 panel. The topography grades up to the north and south of this incision through the 910, 908 and 906 panels.

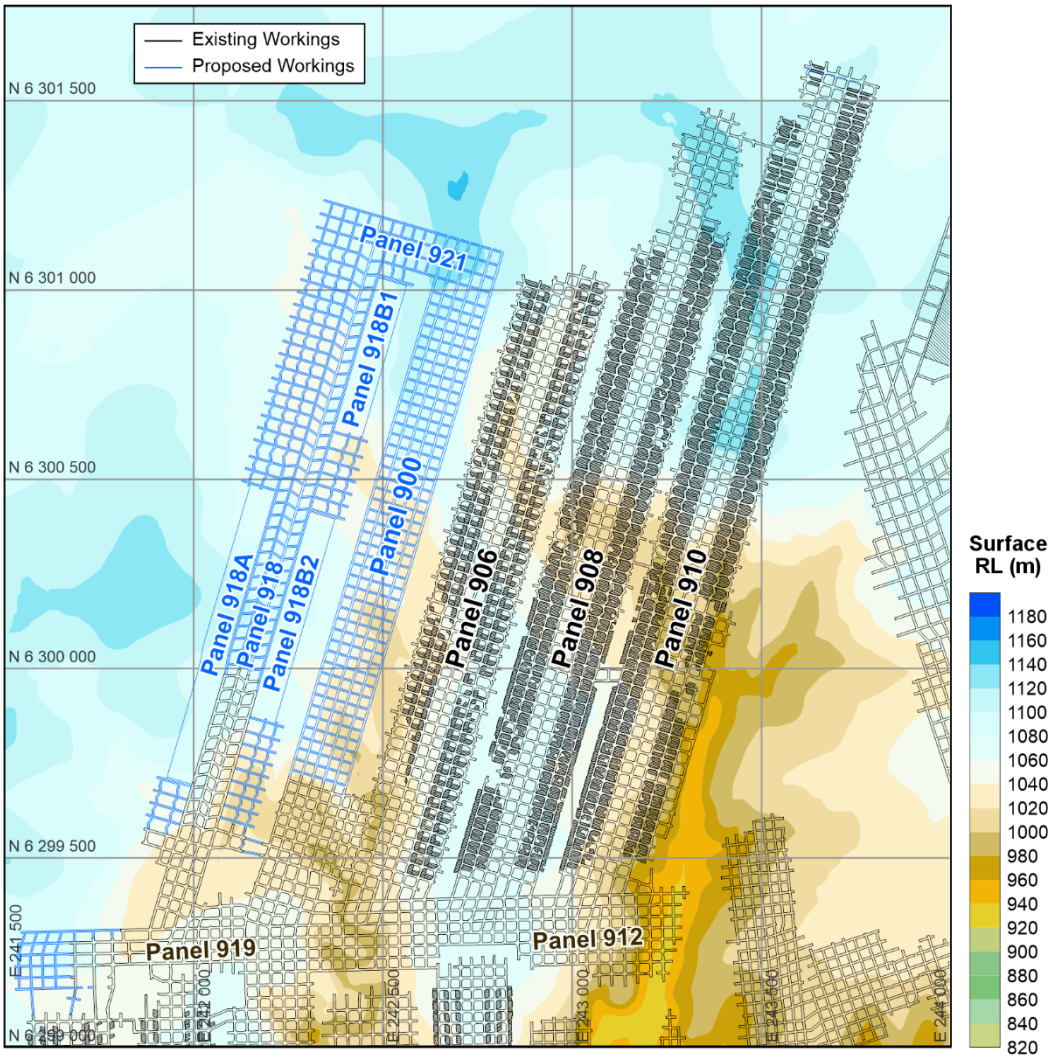

Figure 2: Clarence surface topography over 900 area.

There are relative topographic high points over the northeast of 918 panel and over the midpoint of shortwall 918A. There is a gully eroded creek trending northwest through the roadways between 918B1 and 918B2 and roadways north of 918A. The surface topography dips towards a localised low over the southeast corner of 918 panel.

The Katoomba Seam RL is presented in Figure 3a and an east-west cross-section profile is presented in Figure 3b. Figure 3a also shows the slight dip of the Katoomba Seam to the southwest. Figure 3b shows the change in topography across the 910-906 panels and 918 Panel. Noting the profile extends through the incised creek gully. Figure 3b shows the general increase in surface RL to the west as the surface transitions out of the gully towards higher ground.

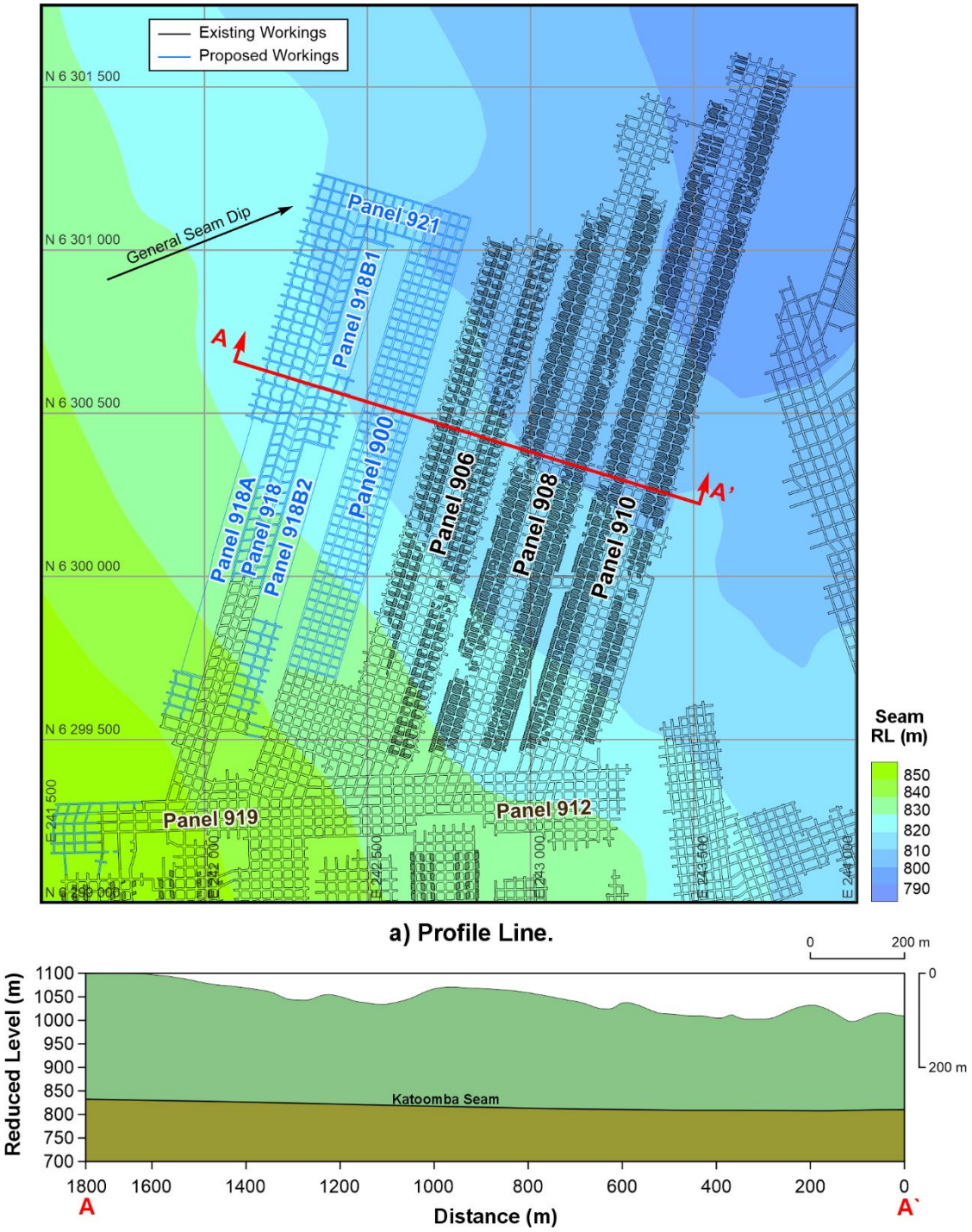

Figure 3: EW cross section showing profile of surface compared to gently dipping Katoomba Seam.

3.2 Depth of Cover

The Katoomba Seam depth of cover over the 900 area panels is presented in Figure 4. All boreholes supplied for this assessment are also presented in Figure 4. Due to the change in topography over the area the depth of cover varies from 160 m to 320 m. The depth of cover variation is principally driven by the undulating topography and incised creek gullies which overlies all the 900 area panels to varying degrees.

Over 918 Panel the greatest depth of cover is in the northeast and over the midpoint of shortwall 918A. In these areas the depth of cover reaches ~290 m. The shallowest area is in the southeast corner where depth of cover is ~180 m. A range of maximum and minimum depth of cover for each relevant panel is presented in Table 3.

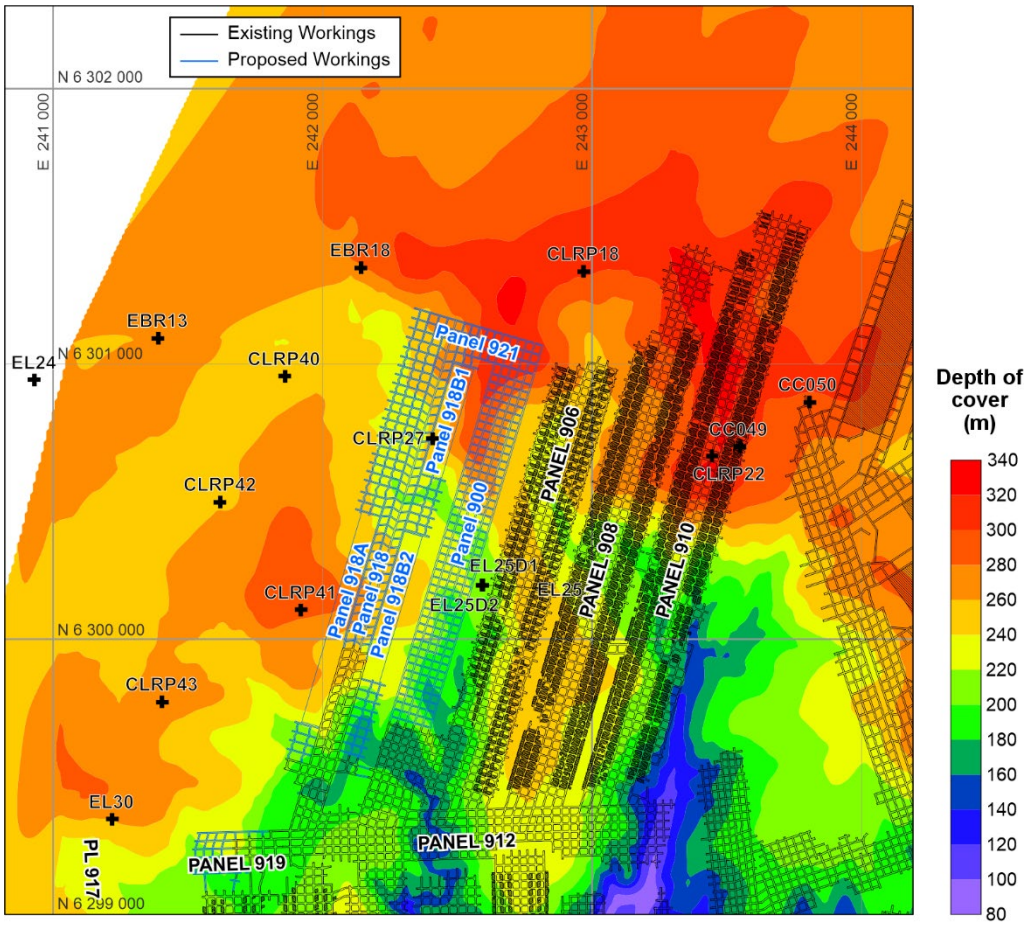

Figure 4: Katoomba Seam depth of cover for 900 panels.

Table 3: Depth of cover range over key 900 panels

Panel (m)	Min depth of cover (m)	Max depth of cover (m)
918	180	290
910	150	325
908	240	320
906	160	295

3.3 Seam Thickness

The Katoomba Seam thickness is presented in Figure 5. The Katoomba Seam is thickest in the east of the 900 area, reaching 3.4 m over 910 panel. The thickness of the seam reduces to the west over 918 Panel where the minimum is ~1.9 m. Maximum seam thickness in 918 Panel is over the east reaching ~2.3 m. A range of maximum and minimum seam thicknesses for each relevant panel is presented in Table 4.

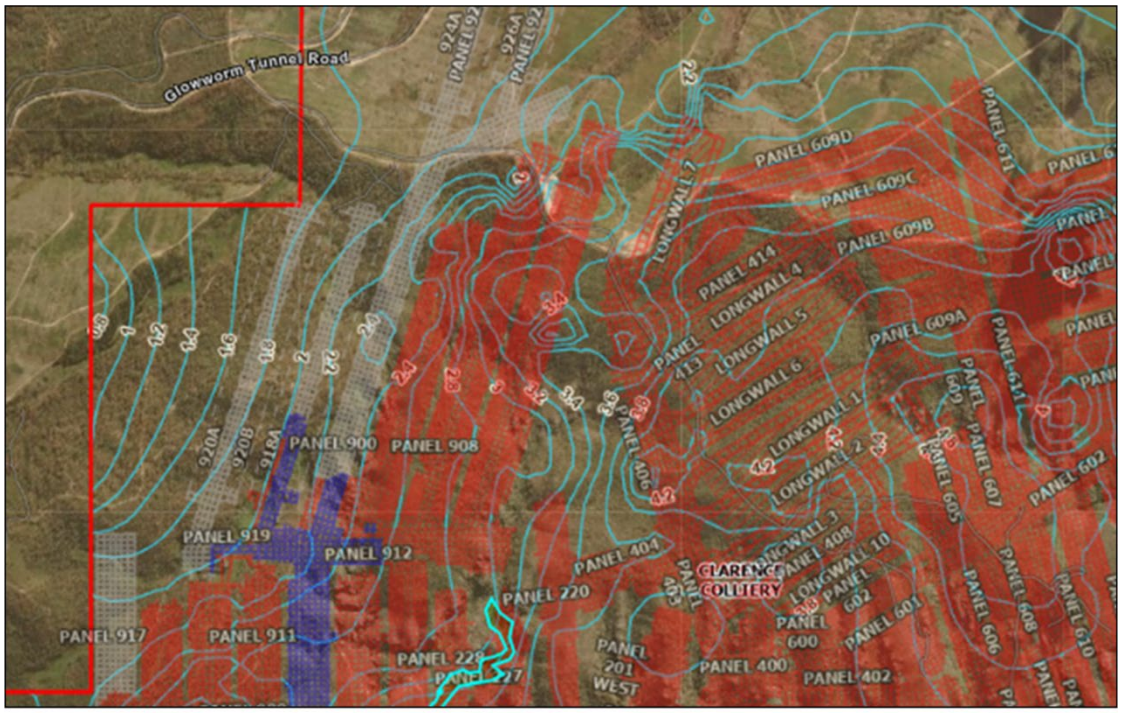

Figure 5: Katoomba Seam Thickness.

Table 4: Katoomba Seam thickness range over key 900 panels

Panel (m)	Min. Seam Thickness (m)	Max. Seam Thickness (m)
918	1.9	2.3
910	2.6	3.4
908	2	3.4
906	2.3	3

3.4 Stratigraphy

The stratigraphy at Clarence includes Triassic sedimentary strata ranging from 160 m to over 320 m, where thickness is impacted by the eroded creek systems through the surface. A generalised stratigraphic representation is shown in Figure 6. The Triassic strata includes the Burralow Formation, the predominately massive Banks Wall Sandstone and the Burra Moko Sandstone which form the cliffs and pagodas of the Newnes Plateau. An example of an eroded gully is shown in Figure 6 which cuts through the Burralow Formation. The Mount York Claystone separates the Burra Moko and Banks Wall Sandstones and is a key stratigraphic unit hydrologically and geotechnically. The Caley Formation is an interbedded siltstone, sandstone and claystone unit that underlies the Burra Moko Sandstone.

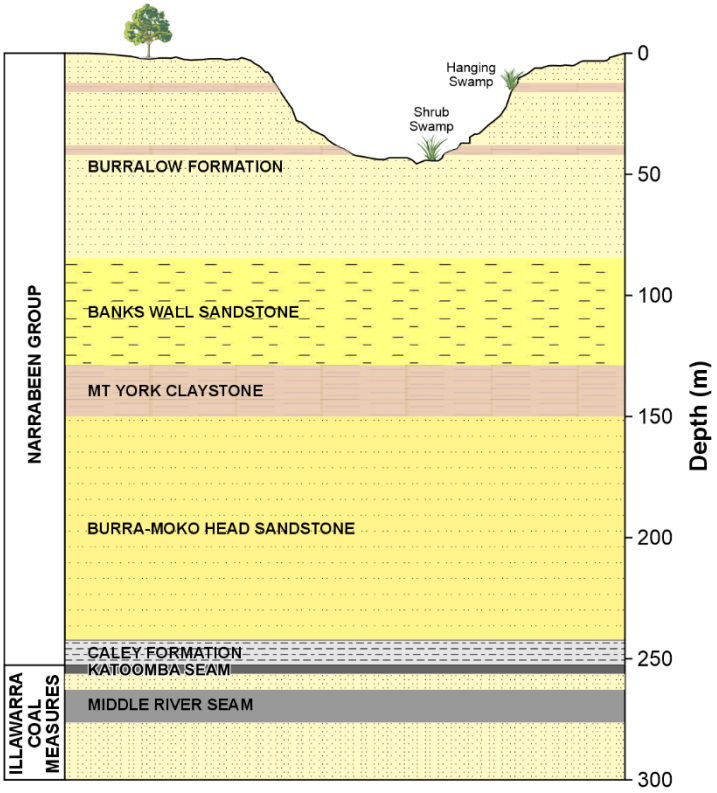

Figure 6: Stratigraphy at Clarence Colliery.

The Permian sedimentary strata underlies the Triassic strata, of which the Katoomba Seam is the first economic seam in the Illawarra Coal Measures of the Western Coalfield. Beneath the Katoomba Seam is a clay rich interbedded lithology followed by the thick Middle River Coal Seam (MDR). Multiple coal seams exist beneath the MDR with varying interburdens of siltstone/sandstone/claystone. Boreholes supplied for this study extend down to the Lithgow Seam. Borehole CLRP42 stratigraphy is presented in Figure 7.

3.5 Geotechnical Cross-Section

A geotechnical fence across multiple boreholes is presented in Figure 8. A borehole map can be found in Figure 4. The geotechnical fence includes geophysical logs lithological logs and stratigraphic logs – where available. The geophysical logs are comprised of density (g/cm^3), gamma (API) and sonic inferred UCS (MPa).

Several key geotechnical characteristics are presented in the geotechnical fence and include:

- Immediate roof (initial 2 m)
    - Strength: Greater than 75 MPa
    - Gamma: ~180 API
    - Lithology: interbedded siltstone/sandstone.

- Above initial roof: Caley Formation
    - Strength: 25 MPa to 100 MPa
    - Gamma: 60 API to 180 API
    - Lithology: interbedded siltstone/sandstone/claystone (some shales and conglomerates may be present).
- Overburden:
    - Burra Moko Sandstone
        - Strength: 25 MPa to 100 MPa
        - Gamma: 45 API to 180 API
        - Lithology: predominantly sandstone.
    - Mount York Claystone
        - Strength: not sufficient sonic logs
        - Gamma: 20 API to >200 API
        - Lithology: predominantly claystone and sandstone.
    - Banks Wall Sandstone
        - Strength: not sufficient sonic logs
        - Gamma: 10 API to 45 API
        - Lithology: predominantly sandstone and conglomerate.
    - Burralow Formation
        - Strength: not sufficient sonic logs
        - Gamma: 10 API to 140 API
        - Lithology: predominantly sandstone. Minor amounts of claystone (YS5 and YS6) and conglomerate.
- Seam: The Katoomba Seam is thickest in the east and gradually thins to the west.
- Floor: The interburden between the Katomba Seam and MDR is generally ~4 m and where the interburden increases, additional coal plies are observed.
    - A localised reduction in interburden thickness is observed in borehole CLRP27 to less than 2 m.

The MDR is typically 16 m thick over the 900 panels.

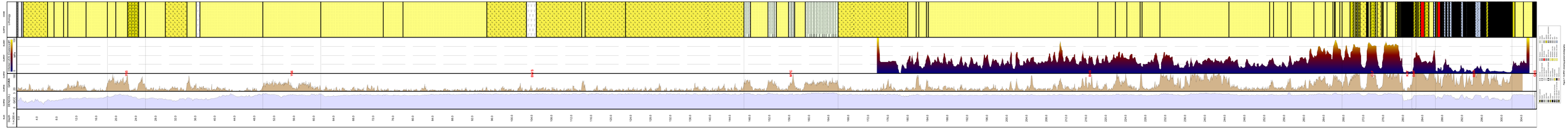
Lithology
Gamma Ray
Density
Neutron
Resistivity
Sonic
Caliper
Bit Size
Depth (m)

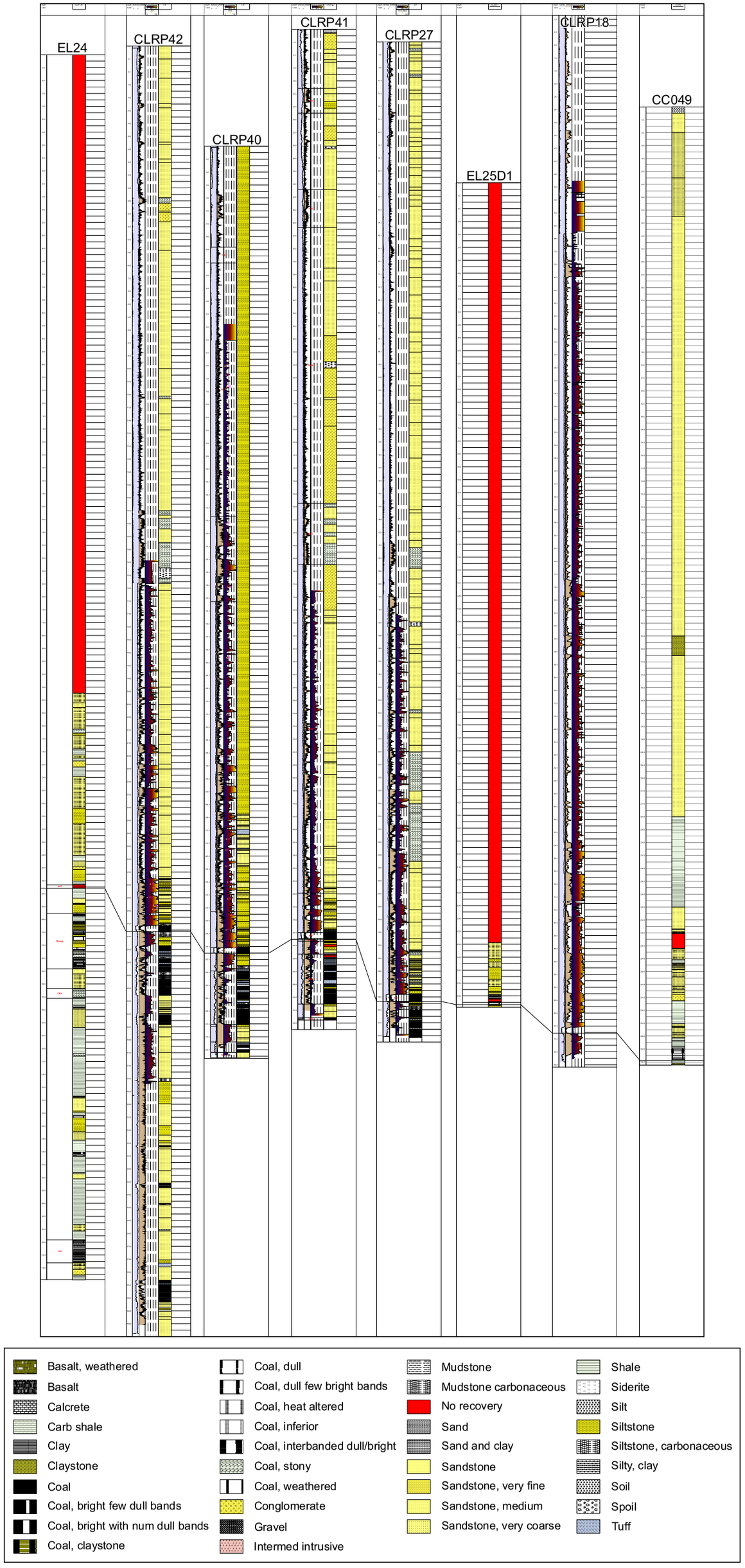

Figure 8: Geotechnical fence across 900 panels.

The geotechnical fence suggests there is a general consistency in strength and stratigraphy across the 900 area panels. Noting the localised change in interburden between the Katoomba and MDR seams.

3.6 Stressfield

Stress measurements from Clarence, Springvale and Angus Place mines have been compiled to supplement the limited Clarence Colliery database. Stress measurement results are presented as a Tectonic Stress Factor (TSF) which is a useful method of allowing stress measurements taken in different rock types and geotechnical properties to be compared. The stress measurements taken at Clarence, Springvale and Angus Place mines were compared with SCT's database of stress measurements in underground coal mines.

The TSF is a means of normalising the stress irrespective of the material stiffness and can be calculated using Equation 1 below:

$$\sigma'_H = v/(1-v) \times \sigma'_V + TSF \times E$$ [Equation 1] (Nemcik et al, 2006)

σ'_H = Horizontal stress (MPa)
v = Poisson's Ratio
σ'_V = Horizontal stress (MPa)
E = Youngs Modulus (GPa)

SCT overcore stress measurements have previously been conducted at Clarence Colliery. The results from a stress measurement campaign in the roof of 408 panel (SCT, 1992) are presented in Figure 9. Depth of cover was in the order of 200 m. Noting the measurements were conducted at two sites (408 6CT and 7CT). Principal horizontal stress orientation was 29° to 76°, consistent with the regional northeast principal horizontal stress orientation. Stress measurements from Springvale (SCT, 1993) and Angus Place (SCT, 1996a and SCT 1996b) are included to supplement measurements at greater depth. The red Angus place data points represent SCT 1996a and the blue Angus place data points represent SCT 1996b.

The stress measurements typically show a medium to low principal horizontal stress environment when compared with the SCT database for stress measurements in Australian underground coal mines. Noting some outliers at both Clarence and Angus Place which indicate the potential for elevated stress, however within the Australian experience. Further stress measurements in the Clarence 900 area would assist in refining the characterisation of the stressfield at depth.

3.7 Geotechnical Testing

Geotechnical testing has been conducted for several boreholes at Clarence. The geotechnical testing database supplied for this assessment consists of Unconfined Compressive Strength (UCS) testing. Triaxial strength geotechnical testing at Springvale has been used to supplement this assessment.

3.7.1 Unconfined Compressive Strength

All UCS test data from Clarence provided for this assessment is presented in Figure 10 relative to Young's modulus. The rock types tested have been divided into predominant lithology. The general range of rock strength is 5 MPa to 100 MPa as indicated by geotechnical laboratory testing. The general range of rock stiffness is 3 GPa to 35 GPa based on the tangent Young's modulus.

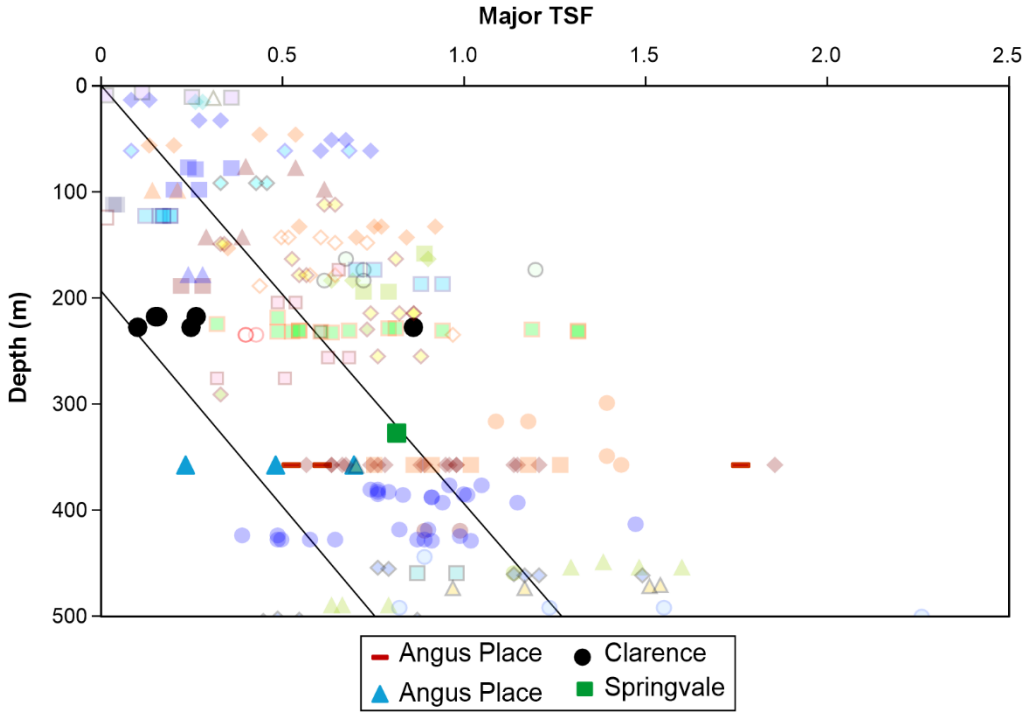

Figure 9: Stress measurements at Clarence, Springvale and Angus Place compared with SCT database for stress measurements in underground coal mines.

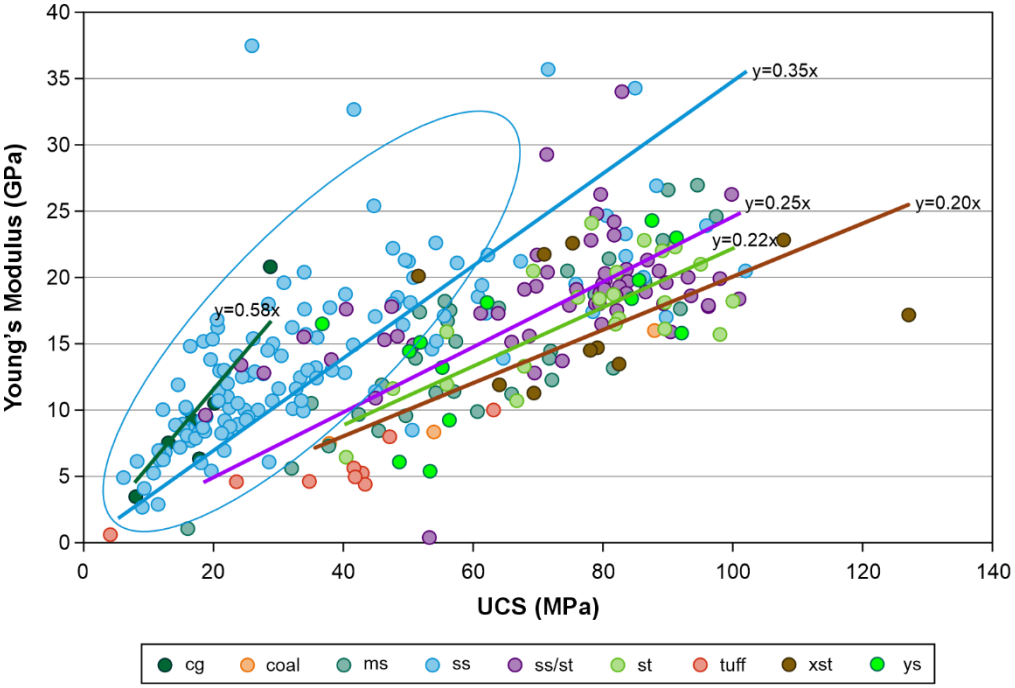

Figure 10: UCS relative to Young's Modulus for key lithologies at Clarence.

Figure 10 shows the relationships between rock type and stiffness. Rock types with larger grain size such as conglomerates and sandstones typically show a stiffer relationship to rock strength. The finer grained materials such as the siltstone and carbonaceous siltstones show a softer relationship to rock strength as illustrated by the relative strength to stiffness ratios in Figure 10.

The area highlighted in Figure 10, with the blue oval, shows the majority of sandstone samples from the Caley Formation, Burra Moko Sandstone and Banks Wall Sandstone. The sandstones from these formations indicate a stiffer relationship to rock strength. This finding informed the model rock properties for the sandstone in these units where stiffness was increased from the average 0.35 to 0.38, which is representative of the sandstone samples from these formations.

UCS data relative to key stratigraphic formations is presented in Figure 11. The box and whisker plot assists in understanding the general range of UCS for each of these formations – noting that the amount of testing in the Burra Moko and Banks Wall sandstones is substantially less than the Caley and Farmers Creek formations as coring is generally focussed around the mining horizon.

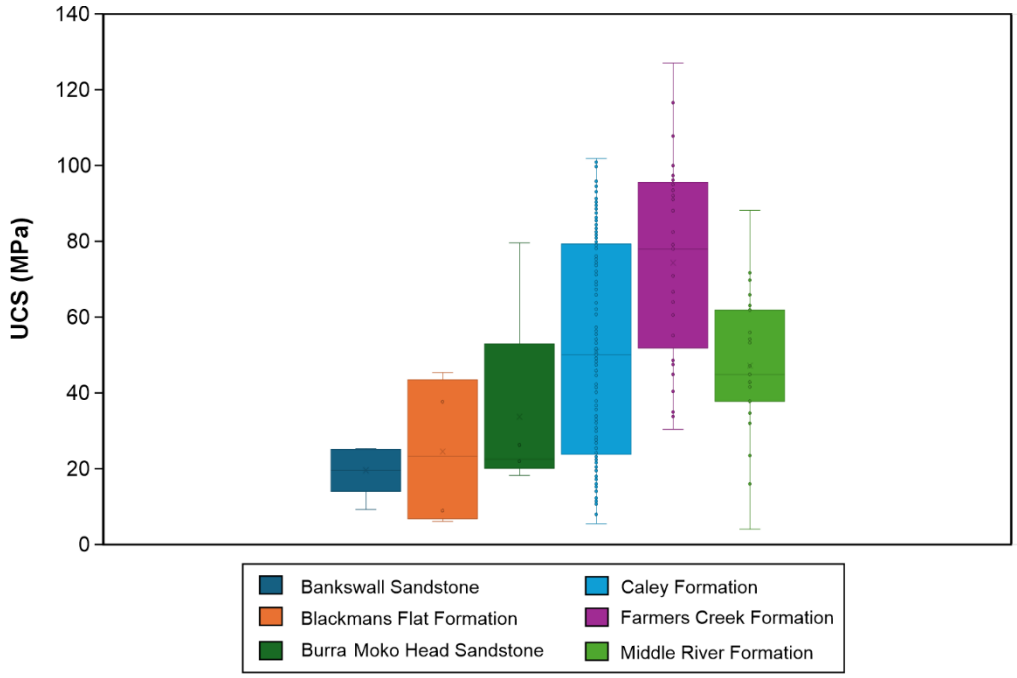

Figure 11: UCS range for rock samples in key stratigraphic units.

3.7.2 Inferred UCS

Downhole geophysical sonic velocity is commonly used to estimate the unconfined compressive strength (UCS) of clastic rocks (McNally, 1987). An empirical relationship can be derived between a rock sample tested for UCS in a geotechnical laboratory and the correlated downhole sonic velocity from borehole geophysics. Samples that fit the criteria of shear failure with a consistent corresponding sonic velocity are used for the relationship.

The relationship used to infer the UCS is presented in Equation 2 from Seedsman et. al. (2009). It is understood that Equation 2 is commonly used to derive strength from sonic velocity at Clarence. The relationship was supplied to SCT by Clarence Mine for this assessment.

$$Inferred\ UCS\ (MPa) = 5785 * Exp\ (-\frac{17374}{velocity}) \quad \text{[Equation 2] (Seedsman et. al., 2009)}$$

$$\text{Velocity – sonic velocity (m/s)}$$

4. MINING GEOMETRY AND SURVEYED SUBSIDENCE

In respect to this assessment, the sequence of panel extraction was, 910 panel extracted first, followed by 908 panel and then 906 panel. 910 and 908 panels were double side lifted to effectively fully extract the seam, while 906 panel was single side lifted achieving partial pillar extraction of approximately 80% recovery.

910 and 908 panels each consist of two extraction panels of ~80 m width separated by a combined spine pillar width of 60 m wide. The barrier pillar width between the panels is variable due to lifting of the barrier pillar. The barrier pillar width ranges approximately 40 m to 55 m wide.

906 panel consists of two partial extraction panels of ~80 m width and spine pillars of combined width of 55 m. The barrier pillar between 908 and 906 panel is also variable from lifting of the pillar width an approximate width range of 40 m to 55 m.

Subsidence over pillar extraction panels 910, 908 and 906 was monitored with subsidence lines B, D and E. Subsidence line D is the most complete across the three panels. The B Line, D Line and E Line survey locations are presented in Figure 12. The cumulative subsidence profiles for D Line are presented in Figure 13. Subsidence surveyed along D line were taken at different intervals over the years and include different stages of 910 to 906 production and subsequent subsidence. The survey dates and stages of production are presented in Table 5. Additional surveys were taken in 2024 after 906 panel completion in March 2023.

The proposed mine plan – presented in Figure 1 – shows 918A and 918B2 panels separated by a four-heading and three pillar spine pillar system. Centennial has chosen a conservative approach to not mine below the surface swamps. As such, panel 918A is shortened in the North, and 918B is split into B1 and B2 panels. 918B1 panel has a panel void width of 83 m, while 918A and 918B2 have 75 m void widths.

The mining geometry for 918 panel is presented in Figure 14. Figure 14a presents the double shortwall geometry, representing the greatest abutment loading scenario. The shortwall panels are separated by spine pillars with two pillar width scenarios separated by 5.5 m wide roadways:

- Cut-through 1-20: 26.5 m, 20 m and 26.5 m
- Cut-throughs 21-52: 26.5 m, 26 m and 26.5 m.

The mining geometry over the northern 918 panel is presented in Figure 13b. Where 918B1 shortwall panel void width is 83 m. First workings are proposed in 918A panel only. Roadways of 5.5 m are proposed, pillar widths are 27 m, 30.5 m and 31 m from east to west.

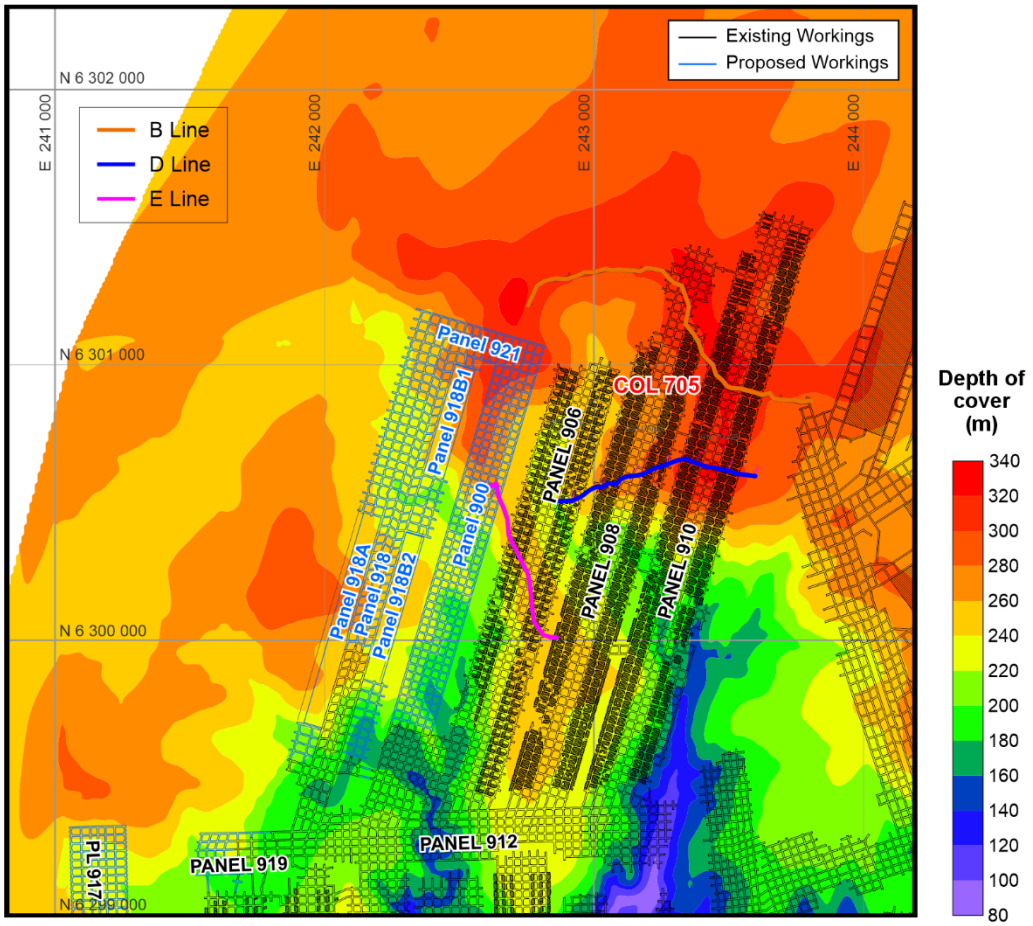

Figure 12: Location of subsidence lines relative to 900 Area.

Table 5: Survey dates relative to production

Dates	Survey completed	910	908	906
March 2020	No survey	Secondary extraction (near D Line)	Developed	-
April 2020	No survey	Secondary extraction ongoing	Developed	-
30/07/2020	**D Line**	Production complete	**Secondary extraction approaching D Line**	**-**
14/10/2020	D Line		Production complete	-
18/10/2021	**D Line**			**Developing (at E Line)**
18/07/2022	D Line			Developed past D Line
23/03/2023	D Line			Secondary extraction
13/05/2024	D Line			**Production Complete**
16/08/2024	D Line			
12/11/2024	**D Line**			

Note: Bold surveys to be used for model comparison.

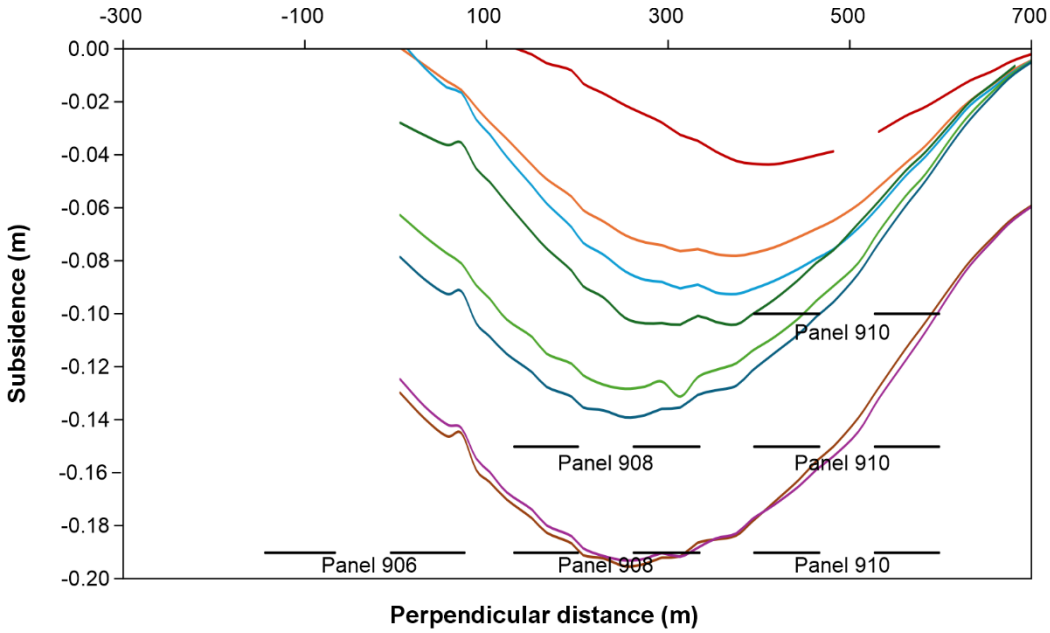

Figure 13a: Original subsidence surveys.

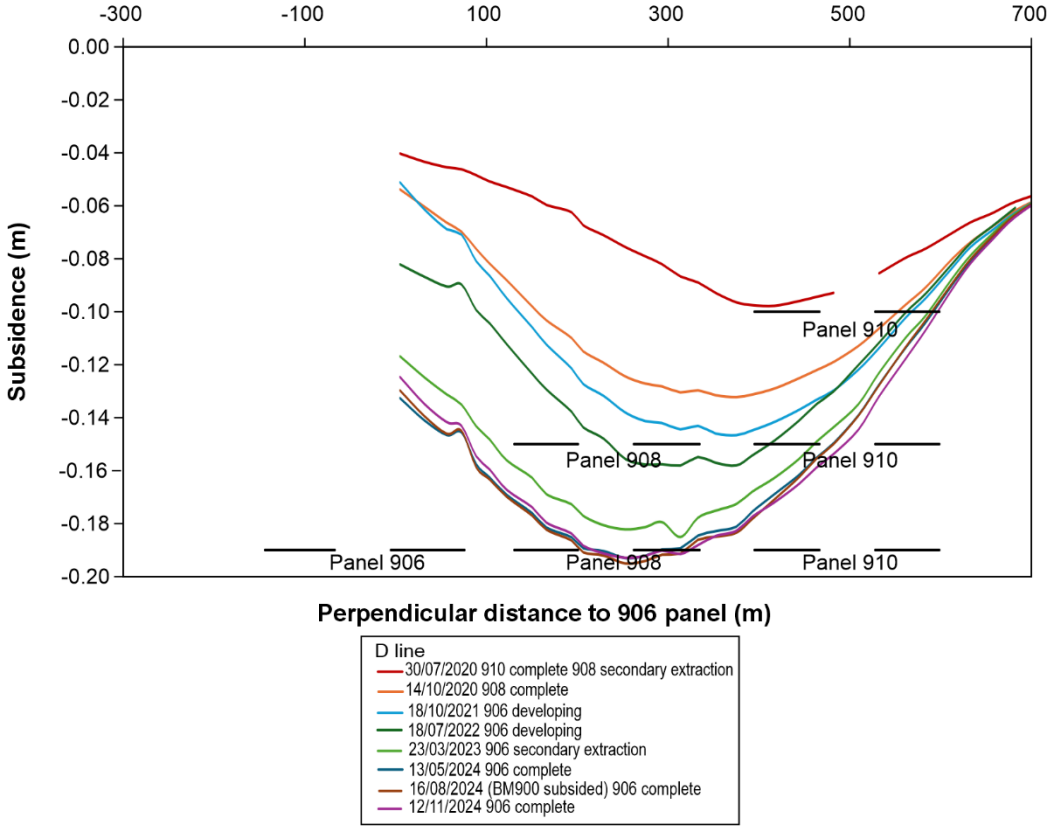

Figure 13b: Subsidence surveys with 54mm of subsidence applied to D line survey from 30/07/2020 to 13/05/2024.

Figure 13: Subsidence surveys conducted for D line over 910 to 906 panels.

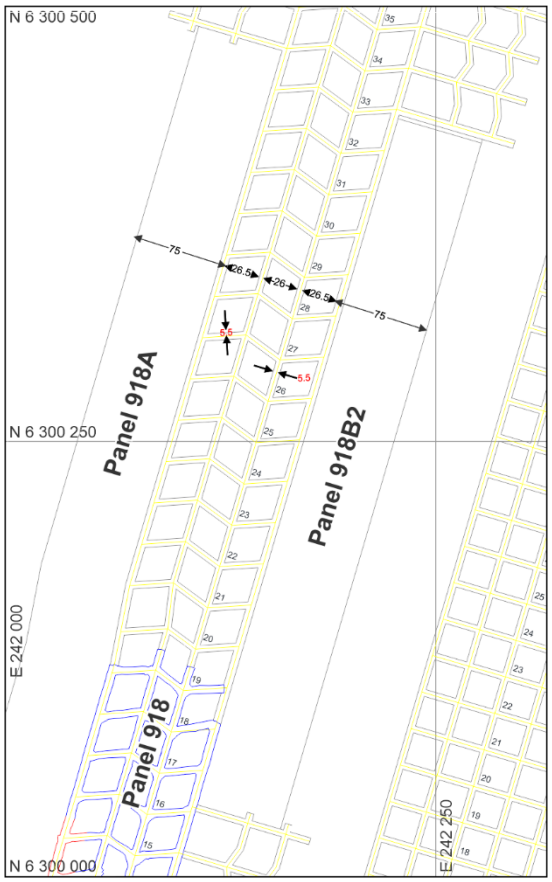

a) 918 Panel geometry.

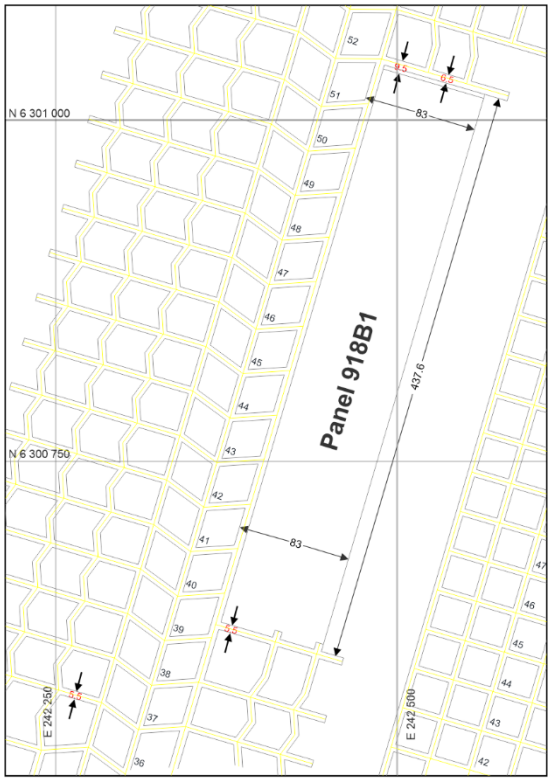

b) 918B1 Panel geometry.

Figure 14: 918 Panel geometry.

The D Line surveys were all surveyed without resurveying the control peg, D1, until August 2024. After extraction of all three panels was completed, the control peg was resurveyed and was found to have subsided 54 mm. Figure 12a presents the subsidence surveys for D Line. Figure 12b presents the subsidence surveys for D Line with an offset of 54 mm for all survey dates up to and including the 13/05/2024. D1 subsidence peg is within the angle of draw of the first extracted panel, 910. It may be that not all the 54 mm should be allocated to the first survey of 910 and partial 908, and this should be considered in the interpretation of results. However, it is likely that approximately 40 mm of the 54 mm would have been attributed to the first survey. In this case, perhaps the first survey line could have 15 mm less subsidence.

A summary of key observations of the surveyed subsidence profiles in Figure 12 is included below:

- The first survey line on 30/7/2020 includes 910 panel extraction and is influenced by 908 panel extraction approaching D Line. This is why the subsidence trough is skewed to the left of the two 910 extraction panels. The maximum subsidence for this survey line is 98 mm.

- The 908 panel extraction includes 3 survey lines (14/10/202, 18/10/2021 and 18/7/2022). The first two survey lines have a trough roughly located over the central barrier pillar. The third survey line begins to skew to the west of the previous survey lines and coincides with the completion of the development of 906 panel. It is likely that the 906 panel development has contributed to the third 908 survey on 18/7/2022. For this reason, the second 908 survey line (18/10/21) is used for the model comparison. The maximum cumulative subsidence after 908 extraction is 147 mm.

- 906 panel cumulative subsidence is represented by the D Line subsidence with a trough approximately over the central pillar of the three panels. The maximum subsidence after all three panels is 193 mm.

A summary of the D line surveyed subsidence is included in Table 6.

Table 6: Maximum Subsidence from D Line surveyed subsidence

Panel	Surveyed Subsidence (mm)
910	98*
908 cumulative	147
906 cumulative	193

*Includes partial extraction of 908

5. NUMERICAL MODELLING ASSESSMENT

Underground mining causes an opening around which the *in situ* stressfield is redistributed. The magnitude and direction of the redistributed stress is modified and depending on the geotechnical properties of the strata it is either able to accommodate the redistributed stress or the strength of the strata is exceeded. When the strength of the strata is exceeded, rock failure and the associated strain softening occurs, and the stress is redistributed further until equilibrium is achieved. Caving and subsequent subsidence from partial and full secondary extraction can be simulated using a numerical modelling approach.

SCT uses FLAC2D (ITASCA) software for numerical modelling assessments. The FLAC2D rock failure model uses site-specific rock properties derived from stress measurements, geotechnical testing of rock core and a model strength profile inferred from geophysics. SCT's in-house code is based on the Mohr-Coulomb Failure Criterion and represents multiple failure modes. These modes include shear and tensile failure of intact rock, shear and tensile failure of bedding and shear and tensile reactivation of failed elements, joints and bedding. Strain softening of the strata is also incorporated into the model based on geotechnical testing. Further explanation of the SCT modelling approach is presented in Appendix 1 and model modes of rock failure are presented in Appendix 2.

5.1 Methodology

This numerical modelling subsidence assessment includes three model scenarios:

- 'As mined' pillar extraction of 910 to 906 panel.
- 918 panel with a 180 m and 280 m depth of cover model, both models included the following mining geometry variations:
    - Shortwall extraction of 918B1 and first workings in 918A
    - Shortwall extraction of 918A and 918B2.

The model geotechnical rock properties and stressfield are presented in this section of the report. Model lithology and inferred strength is derived from Borehole CLRP27. The characterisation showed that Borehole CLRP27 was representative of the strata at the locations of both models, considering the sparse borehole locations. A composite log of CLRP27 is presented in Appendix 3. The CLRP27 borehole location is presented in Figure 4, alongside all borehole supplied for this assessment.

The 910 to 906 panel model includes a surface topography that is based on the 900 D subsidence line. The model surface topography uses the D line surface RL relative to the perpendicular distance across the panels. As such, the model represents smaller peg distances and steeper slopes than in the D line, in order to represent the depth of cover in the perpendicular representation of D Line.

Modelling the pillar extraction of 910 to 906 panel was done from east (910) to west (906). In each of the three areas, the eastern panel was extracted prior to the western panel, a roadway of 6 m width was included through the centre of the 60 m spine pillar. Double sided lifting was modelled for 910 and 908 panel where the extraction height is 3.2 m. Single sided lifting was modelled for 906 panel where the extraction height is 2.6 m.

Modelling of 910 and 908 panels included full extraction of the full panel width. 906 partial extraction panel required a different modelling approach to replicate the 3D nature of single sided lifting in a 2D model. An effective pillar width was calculated based on the width and length of the pillar which converts the 3D pillar geometry into 2D. This results in a smaller pillar and wider roadway being extracted to represent the pillar stability and abutment load in single sided lifting.

The 918 panel models include two depth variations, a 180 m and a 280 m depth of cover model. These depths represent the near maximum and minimum depths of the Katoomba Seam over 918 panel and were chosen to model the end members of the predicted subsidence. Both models include a flat surface topography. Modelling the shortwall extraction of 918 panel was done from east (918B) to west (918A) following the expected mining sequence. 918A and 918B2 panel geometry included 2 x 75 m panels and an 84 m spine pillar, consisting of three pillars of 27 m, 21 m and 27 m width with 2 x 6 m wide roadways. 918B1 panel width is 83 m. Spine pillar width is 84 m. First workings in panel 918A has a width of 83 m, consistent with the proposed mining geometry for 918A in the north, adjacent to shortwall 918B1. The extraction height is 2.2 m from the base of the Katoomba Seam. Noting that the maximum Katoomba seam thickness is 2.3 m which only encompasses a small area of 918.

The revised mine plan has an increase in the central spine pillar width inbye of 21 cut-through, from 20 m to 26 m. Increasing the spine pillar system width to 90 m. The model geometry is based on the original mine plan supplied for this study where the spine pillar width system is 84 m. The increase in pillar width is anticipated to reduce the average load on the central spine pillar and is likely to correspond with a small reduction in the maximum surface subsidence for the deeper areas.

5.1.1 Rock Properties

The model geotechnical rock properties are derived from the geotechnical laboratory test results presented in this study. Triaxial strength test results from Springvale Mine have been used to supplement the cohesion and internal friction angle of the strata and are presented in Appendix 4. The model geotechnical rock properties are presented in Table 7.

Subsidence results from the 910 to 906 modelling assessment were validated against subsidence surveys. The validation process informed key changes around geotechnical properties which included a stiffer UCS to Young's modulus sandstone relationship for relevant overburden units as discussed in Section 3.7. Additionally, massive sandstone was modelled in the Burro Moko Sandstone and fresh (unweathered) Banks Wall Sandstone by removing joints and bedding in these units – allowing these sandstones to behave in a massive manner.

The SCT in-house code applies a randomisation of the inputted UCS following a normal distribution function that varies the UCS to represent the natural variability in rock. UCS may vary by approximately 40% within a normal distribution about the mean UCS value of the unit whilst maintaining the nominated value of Young's Modulus (stiffness). Figure 15 presents the strata UCS from which model input cohesion values are derived for 910 to 906 panel and 918 panel models.

Table 7: Clarence model geotechnical rock properties

Lithology	UCS (MPa)	Young's Modulus (GPa)	Joint Friction Angle (deg)	Bedding Cohesion (MPa)	Bedding Tension Strength (MPa)	Poisson's Ratio
Coal	20.5	3	36	2.5	0.3	0.3
Coal Contact	20.5	3	30	1.5	0.1	0.3
Carbonaceous Claystone	20.5	3	30	2.5	0.1	0.3
Carbonaceous Tuff	20.5	3	20	0.5	0.05	0.3
Claystone	10 to 60	2.5 to 15	20	1	0.1	0.3
Tuff	5 to 30	1.25 to 7.5	15	1	0.01	0.3
Siltstone	5 to 110	1.2 to 27.5	33	3	0.2	0.25
Sandstone Bedded	5 to 140	2 to 53.2	35	2.5 to 4	0.2	0.25
Conglomerate	10 to 80	5 to 40	39	5	0.2	0.3

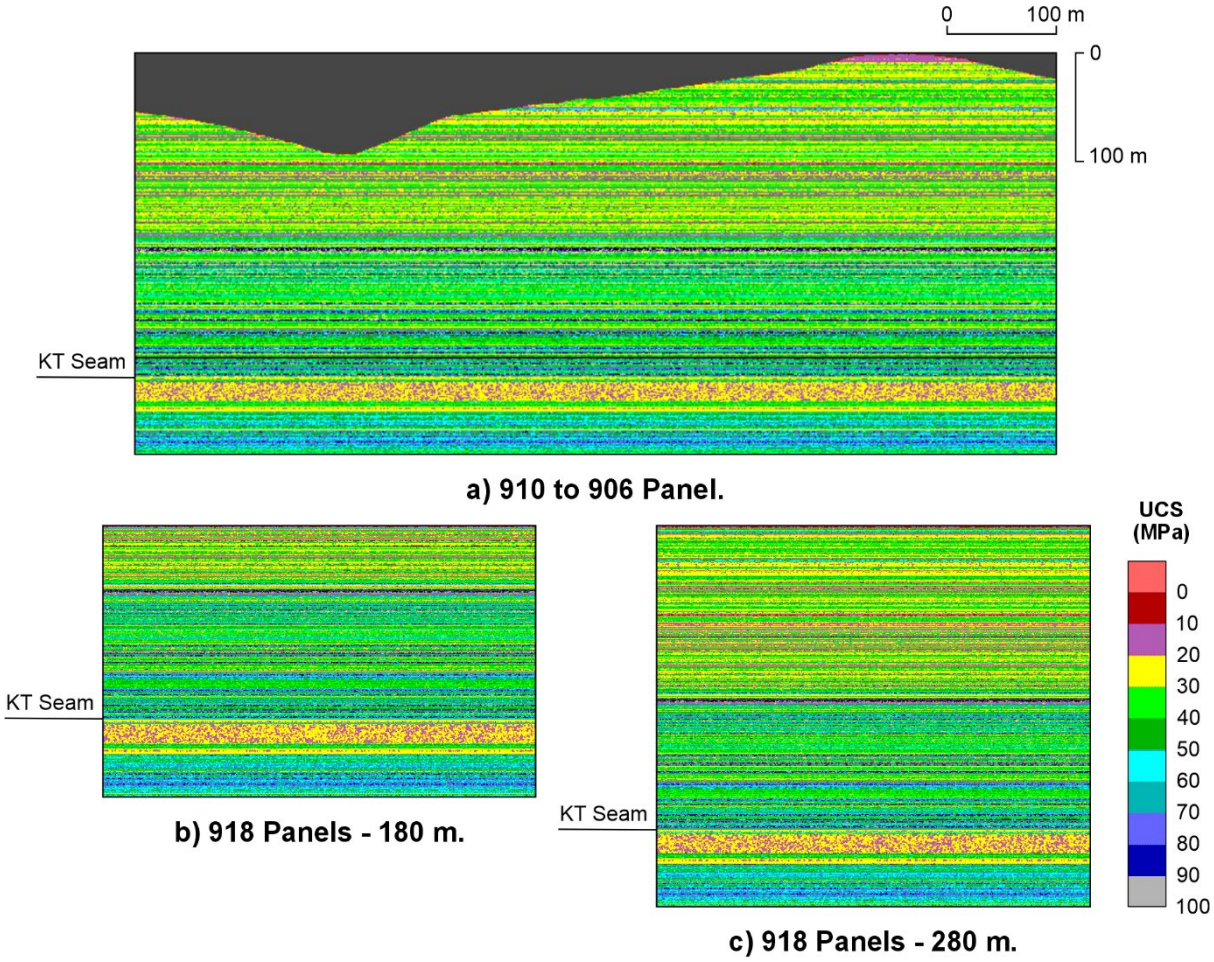

Figure 15: Model UCS of stratigraphy.

5.1.2 Model Stress

The numerical model incorporates both vertical and horizontal stress. Vertical stress is derived from the weight of the overburden where 100 m is generally equivalent to 2.5 MPa – derived from the unit weight of rock. Horizontal stress is incorporated into the strata based on the TSF, stiffness of the strata and depth, following Equation 1. The model TSFs are derived from the stress measurements presented in Section 3.6. Model input TSFs at the Katoomba Seam horizon are presented in Figure 16 and Table 8. The model horizontal stress reduces proportionally to zero at surface.

The model TSFs are representative of a medium to low stress environment in comparison with the SCT database. The model TSFs closely represent the measurements taken at Clarence at ~200 m and Angus Place and Springvale at ~350 m depth of cover.

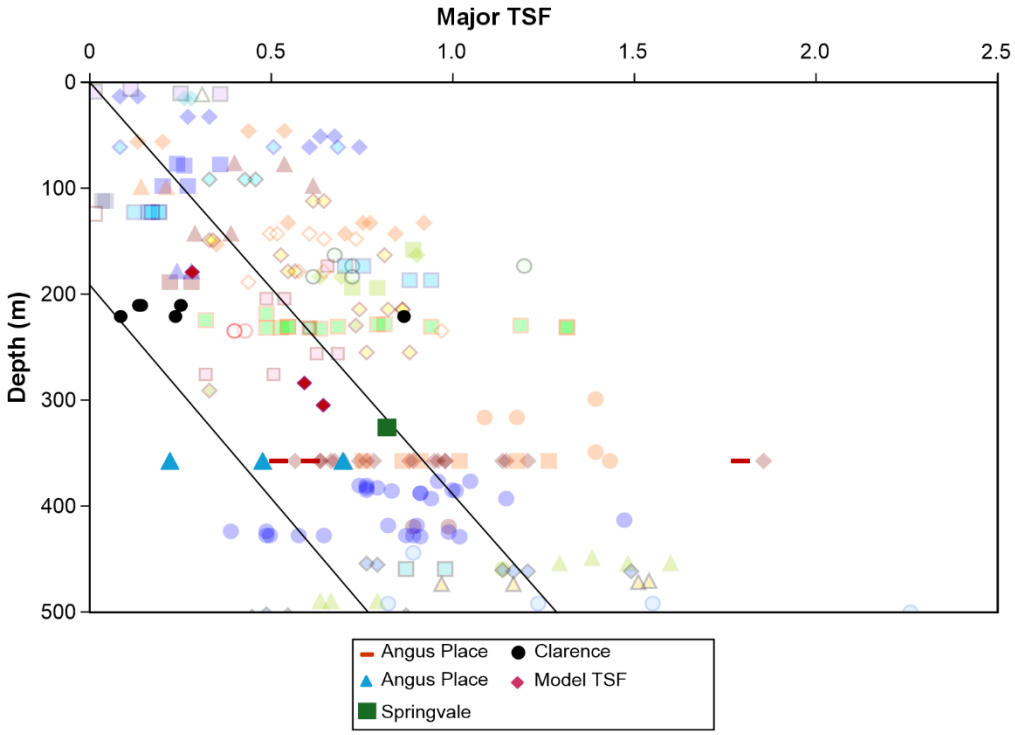

Figure 16: Model major TSF compared with Clarence, Springvale and Angus Place stress measurements and SCT database for stress measurements in underground coal mines.

Table 8: Clarence Model TSFs

Panel	Depth of Cover (m)	TSF major	TSF minor
910 to 906	320	0.65	0.32
918	180	0.3	0.15
918	280	0.6	0.3

5.2 910 to 906 Panel Modelling

The vertical stress, shear strain and mode of rock failure are presented in Figure 17. The vertical stress presented in Figure 17a shows the stress reduction above the extracted panels and abutment stress above the pillars. The increased abutment stress compresses the pillar and causes the chain pillar subsidence. The stress through the pillars exceeds 10 MPa as indicated by the black regions. Pre and post mining stresses are presented in Appendix 1.2.

Shear strain presented in Figure 17b shows the caving profiles of the 910 and 908 panels extending ~80 m above the seam, below the Burra Moko Sandstone. Horizontal shear is occurring along a claystone at this horizon. Double sided lifting was used for pillar extraction in 910 and 908. The singled sided lifting in 906 has produced caving profiles substantially smaller than the 910, 908 panels. Caving above the 906 panels extends 30 m to 40 m above the seam.

Modelling also shows high strain through the MDR Seam in the floor of the Katoomba Seam due to extraction of 910 and 908 panels. Some strain is seen in the MDR beneath 906 panels but it is not as extensive as 910 and 908 panel due to the reduction in pillar extraction.

The mode of rock failure is presented in Figure 17c which shows predominantly bedding shear, shear failure and reactivation of shear failure above the panels and bedding shear failure below the panels. No significant failure is seen above the spine and barrier pillars for 910 and 908 panels. Shear fracture and reactivation is seen above 906 panels and remnant pillars where single sided lifting has been modelled. Due to the relatively thin remnant pillars in 906 rock failure above the pillars is more extensive.

5.2.1 Assessment of 910 to 906 Model and Survey Subsidence

This section discusses the surface subsidence derived from the model post mining vertical displacements. The model post mining vertical displacements are presented in Appendix 1.2.

Cumulative Subsidence

900 D Line is the most complete set of subsidence surveys taken for 910 to 906 panel and is presented in Figure 18 alongside the model surface subsidence. D Line survey line was surveyed throughout panel 910 to 906 extraction without resurveying the survey line control peg (D1). An additional survey of the D1 control peg, post panel 906 extraction showed that the control peg had subsided 54 mm.

In this assessment, all previous surveys have been lowered 54 mm consistent with the survey of D1 taken 12/11/2024 which confirmed D1 had subsided 54 mm. The assumption to lower all surveys from the end of 910 extraction the full 54 mm is based on model results suggesting that the majority of subsidence at the location of the control peg would have occurred during the extraction of the adjacent 910 panel.

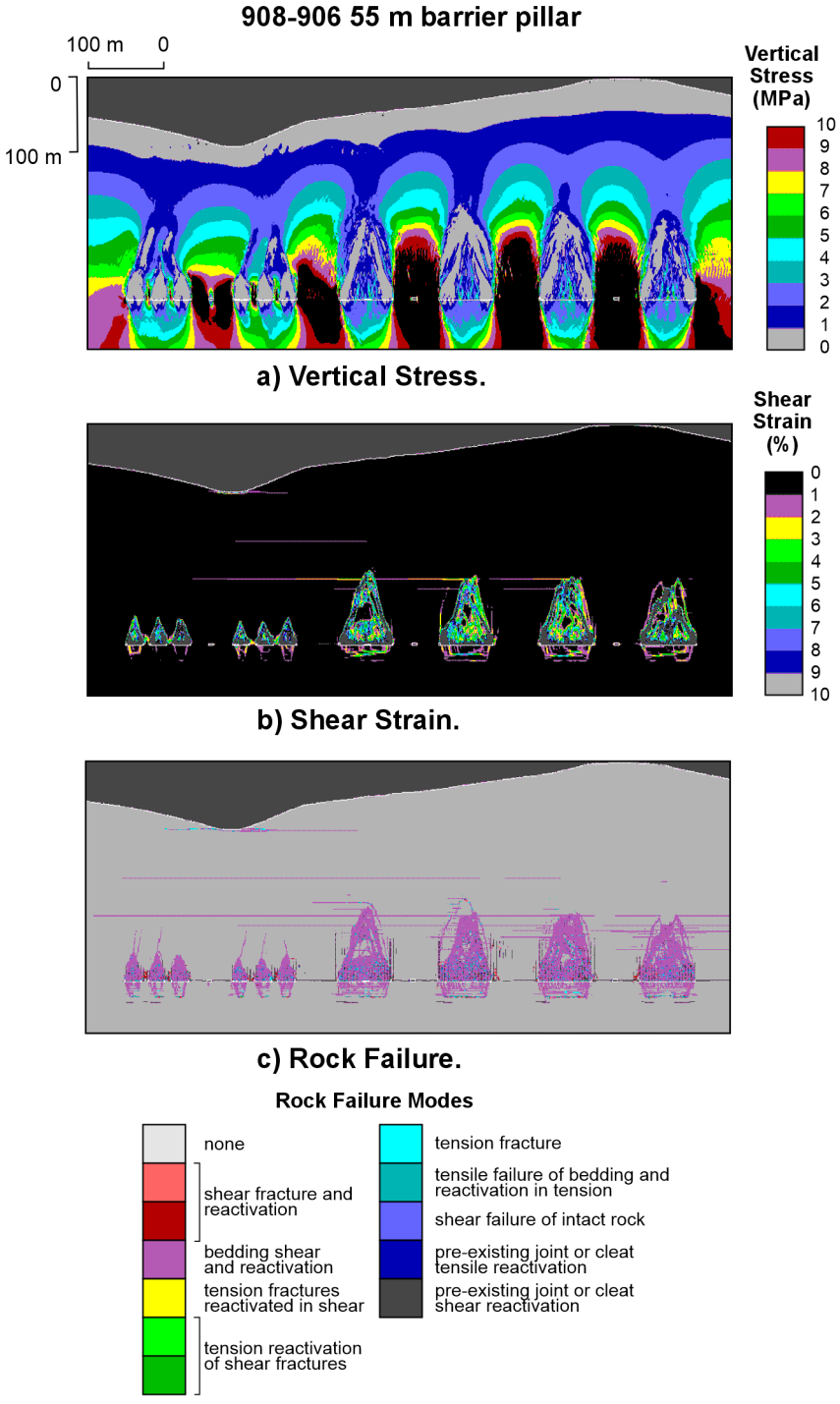

Figure 17: Panel 910, 908 and 906 caving models.

There is close alignment between the maximum subsidence for 910 and 908 in the survey and modelled data. The maximum surveyed subsidence for 910 panel is 98 mm, the maximum modelled subsidence is 91 mm. The 910 subsidence trough is skewed to the west with the subsidence trough located over the barrier pillar between 910 and 908. Partial extraction of 908 had already begun prior to the date of the first survey (30/07/2020) with the location of extraction likely influencing the D Line subsidence. The location of the subsidence trough for the modelled 910 panel is directly over the spine pillars of 910 panel as would be anticipated for two adjacent panels.

The maximum surveyed subsidence for 908 panel is 147 mm, the maximum modelled subsidence is 156 mm. The survey subsidence trough is located slightly to the west of the central barrier pillar between 910 and 908 panels. The modelled cumulative subsidence trough is located over the barrier pillar, however slightly to the east. The model trough location is consistent with the deeper depth of cover to the east.

The validation of the 910-908 model subsidence provides confidence that the model is producing representative surface subsidence for the fully extracted panels.

The maximum surveyed subsidence for 906 panel is 193 mm, the maximum modelled subsidence is 166 mm. The maximum cumulative subsidence for 910 to 906 panel is greater than the maximum model subsidence by 27 mm. The incremental subsidence analysis in the following section helps tease apart the mechanics contributing to the cumulative subsidence profiles for 906 extraction.

Incremental Subsidence

The incremental survey and model subsidence profiles are presented in Figure 19. The incremental profile for 910 panel remains unchanged from Figure 18.

The 908 incremental subsidence is not anticipated to be an accurate representation of 908 incremental subsidence as the 910 survey subsidence line was taken after pillar extraction of 908 had begun and therefore some of the 908 incremental subsidence is captured in the 910 survey line. For this reason, the 908 incremental survey subsidence maximum is 63 mm less than the model incremental maximum subsidence of 113 mm.

For 906 Panel, the maximum model incremental subsidence magnitude matches the surveyed maximum incremental subsidence. The maximum incremental subsidence magnitude for D Line is 74 mm. Maximum model incremental subsidence is 75 mm. 908-906 modelled barrier pillar width is 55 m.

The model results show the model subsidence trough in a similar location to the 906 incremental subsidence of D Line.

The consistency of the 906 panel incremental model subsidence with the survey incremental subsidence magnitude of D Line, together with the subsidence trough location, gives confidence to the modelled approach of partial pillar extraction in 2D.

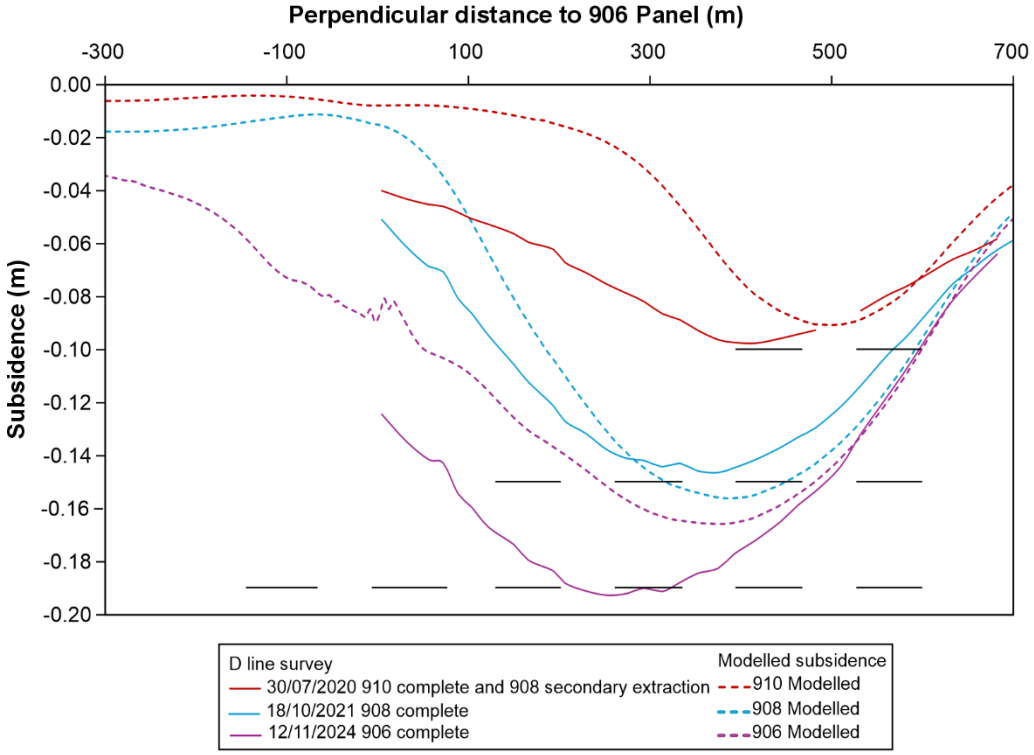

Figure 18: 900 D line subsidence surveys compared with model subsidence.

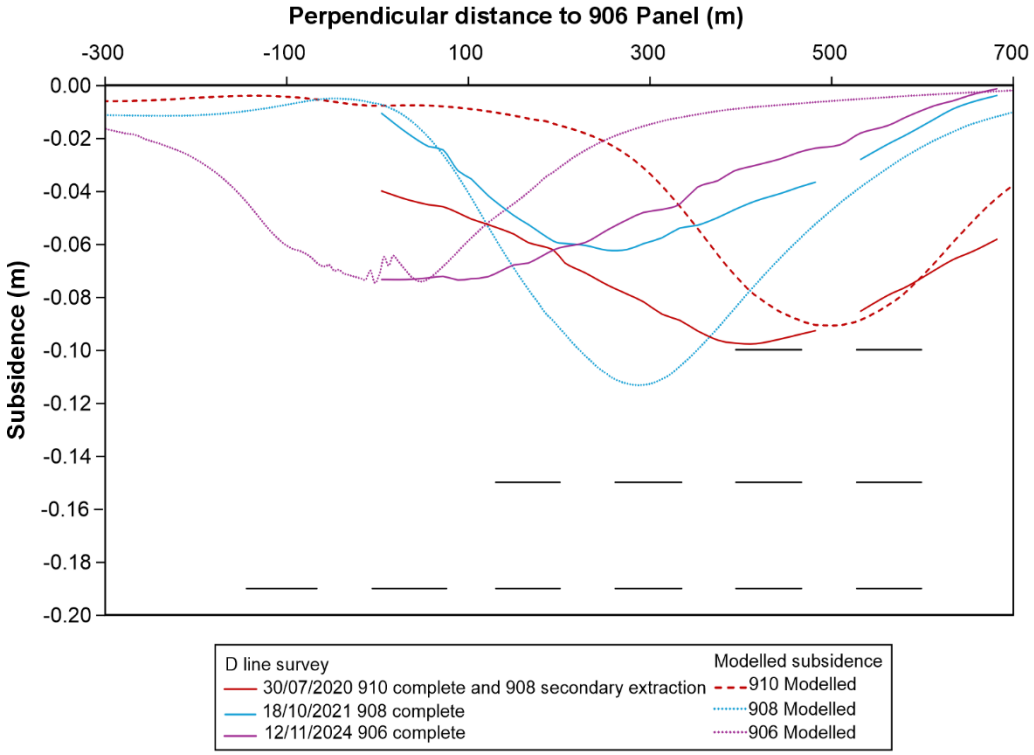

Figure 19: Incremental subsidence surveys compared with incremental model subsidence.

5.2.2 Discussion on subsidence results and impacts of barrier pillar width

The survey lines are taken at oblique angles over the panels, where D Line has a general southwest heading over 908 and 906 panel and traverses down the localised topographic high. With the variability in barrier pillar width from lifting off the barrier pillars, there is potential for variability in pillar compression behaviour along the panel.

Given the subcritical nature of the panels, the mechanism primarily contributing to the subsidence is chain pillar compression. The pillar width between the panels is therefore a key factor in the magnitude and location of the subsidence tough. The barrier pillars exhibit variability in their pillar width due to the nature of lifting from the barrier pillar. The surveyed mine plan indicates a range in barrier pillar width of 40 m to 55 m. It is possible that in some locations the barrier acts as a 55 m pillar, in others a 40 m pillar, or somewhere in between.

Survey and model incremental subsidence is summarised below:

D Line

- Maximum 906 incremental survey subsidence 74 mm.
- Subsidence trough over 906 eastern panel and 908-906 barrier pillar.
- Surface RL varies by ~100 m.
- Depth of cover 310 m to 220 m.

910-906 Model

- Maximum 906 incremental model subsidence 75 mm.
- Subsidence trough over 906 eastern panel.
- Surface RL varies by ~100 m. *Derived from D line.*
- Depth of cover 300 m to 220 m.

The similarity in D line survey and 906 model incremental subsidence suggests the modelled barrier pillar width of 55 m may be representative of the actual 908-906 barrier pillar over which D line surveys.

The maximum cumulative D line surveyed subsidence is matched for 910 and 908 panels by modelling but is underestimated in 906 panel by modelling.

The incremental D line survey subsidence is matched in 910 and 906 by modelling, noting a representative 908 incremental subsidence survey does not exist for comparison.

The reason for the difference in cumulative subsidence but not incremental subsidence of 906 between surveyed and modelled results could be explained by the oblique alignment of the survey lines and the potential variation in barrier pillar width along the survey line. The model presents a 2D perpendicular section of the 910-906 panels along D Line topography.

Due to the oblique angle of D line, it is possible that the 910-908 effective barrier pillar width perpendicular to the 906 portion of the survey line is less than the modelled 55 m barrier pillar width that matches the 908-910 survey line to the north. This may be contributing to the increased cumulative 906 D line maximum subsidence and may also be impacting the incremental subsidence trough which is drawn eastward over the 906 eastern panel and 908-906 barrier pillar.

Additional modelling was conducted which modelled a 40 m barrier pillar between 910 and 908 – not presented in this report. The additional model showed a maximum 908 cumulative subsidence of 213 mm. This result shows the potential impact a reduced barrier pillar width can have on maximum subsidence.

In summary, D line appears to exhibit a 55 m effective barrier pillar width for the 910-908 barrier pillar and hence the cumulative subsidence between the survey and measured results are aligned for 908. But where D line crosses 906 panel the perpendicular 910-908 barrier pillar may be in the order of 45-50 m and therefore the increased loading on the pillar may be increasing the cumulative subsidence over D line. D line crosses 906 panel more than 200 m outbye of where D line crosses 910 panel, a distance over which barrier pillar width variation is possible.

5.3 918 Panel Model

918 panel modelling was conducted at 180 m and 280 m depth of cover. 918 modelling included:

- Shortwall extraction of 918B1 and first workings in 918A
- Shortwall extraction of 918A and 918B2.

The results of the shortwall extraction of both panels at 180 m and 280 m depth of cover are presented here. The vertical stress, shear strain and mode of rock failure are presented in Figure 20a for the 180 m and Figure 20b 280 m depth of cover models. Vertical stress in the 180 m depth of cover model is comparatively low to the deeper model. Abutment stress in the order of 10 MPa is seen adjacent to the extracted shortwall panels. However, the stress is generally 7 MPa to 8 MPa through most of the pillars. Vertical stress is increased through the spine pillars and in the barrier pillars in the 280 m depth model, as the abutment load is increased by the increased overburden. The vertical stress in the pillars exceeds 10 MPa as indicated by the black regions. Pre and post mining stresses is presented in Appendix 1.2.

Shear strain is presented in Figure 20a for the 180 m and Figure 20b 280 m depth of cover models. There are no signs of failure of the strata above the spine pillar in either depth model. The mine geometry does not appear to be at risk of significant subsidence increases due to strata softening. Caving fractures extend to a maximum of roughly 90 m above the panel as shown by the shear strain in Figure 20b. Caving fractures extend approximately 60-90 m in the 280 m depth model and 70-90 m in the 180 m depth model. Floor fracturing below the panels in the deeper model exhibit greater strain than the shallower model due to the higher shear stress generated below the deeper panels.

The mode of rock failure in Figure 20a for the 180 m and Figure 20b 280 m depth of cover models. The mode of rock failure above the panel is predominantly bedding shear failure and reactivation. Some bedding shear appears to occur near the top of the caving fractures.

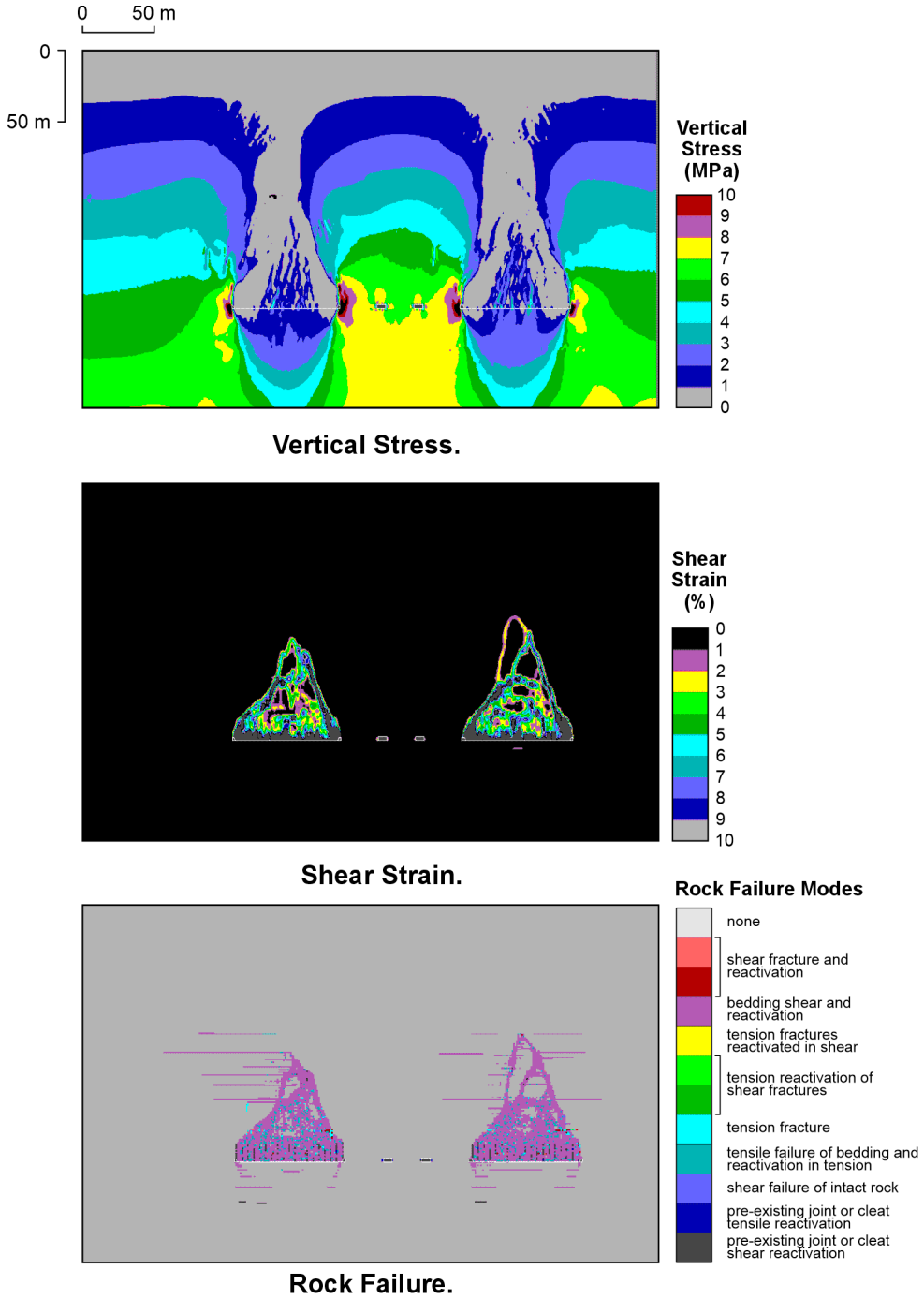

Figure 20a: Panel 918 caving model 180 m depth of cover.

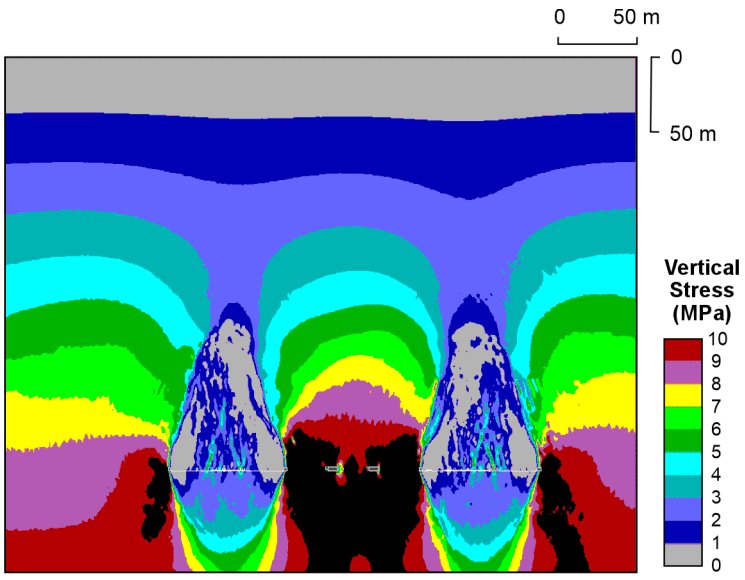

Vertical Stress.

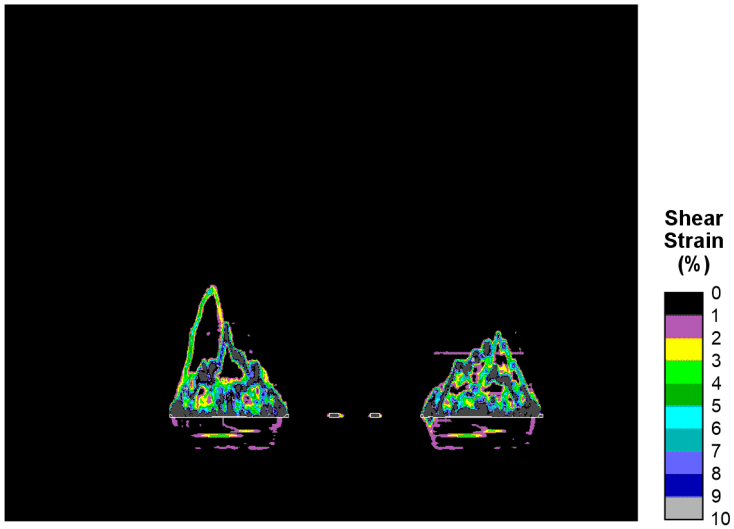

Shear Strain.

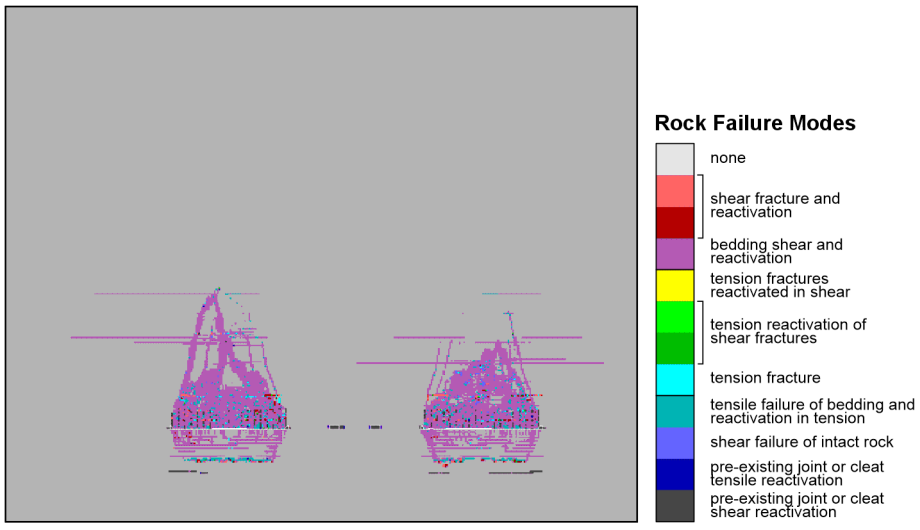

Rock Failure.

Figure 20b: Panel 918 caving model 280 m depth of cover.

5.3.1 918 Panel Model Subsidence

This section discusses the surface subsidence derived from the model post mining vertical displacements. The model post mining vertical displacements are presented in Appendix 1.2. The 918 panel model surface subsidence is presented in Figure 21 for the two depths and mining methodologies modelled. A summary of maximum model subsidence is presented in Table 9 and explained below.

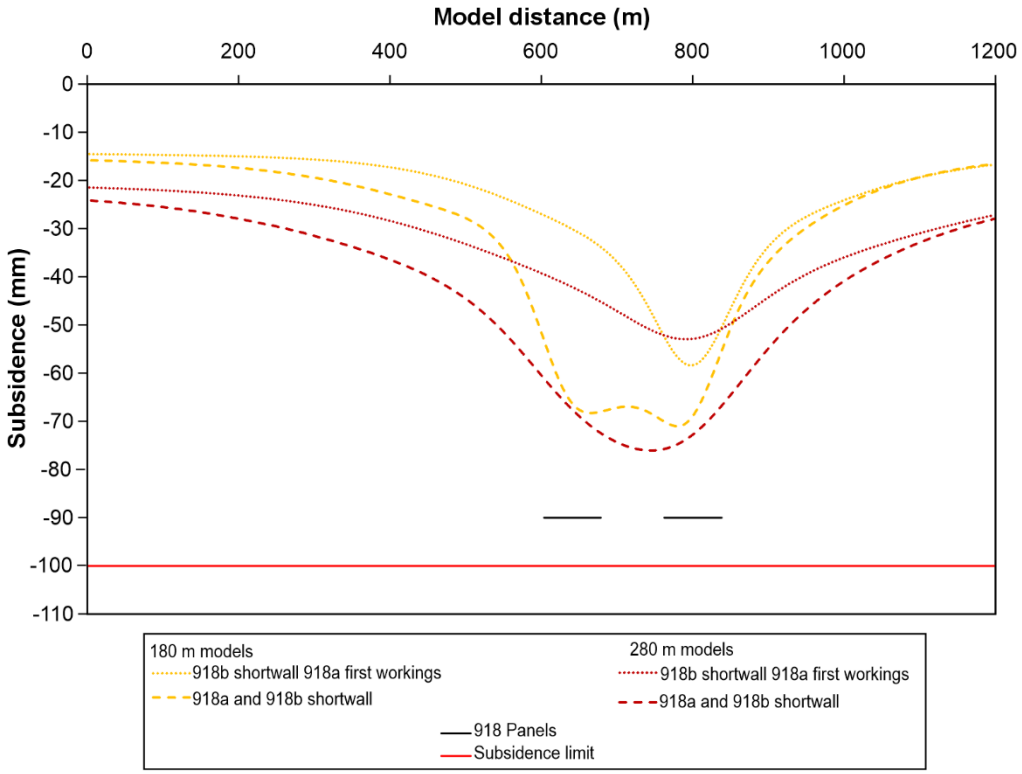

Figure 21: 918 Panel model surface subsidence.

Table 9: 918 Panel modelled subsidence estimates

Depth (m)	Panel width/depth	Modelled subsidence* (mm)	
		Shortwalls[1] (918A & 918B2)	Shortwall[2] (918B1) first workings (918A)
180	0.46	71	58
280	0.27	76	53

*±20 mm survey tolerance should be applied to modelled results
[1] Panel void width 75 m
[2] Panel void width 83 m

Shortwall extraction (918B1) and First Workings in 918A

The maximum model subsidence is 53 mm for the 280 m depth model. The maximum model subsidence is 58 mm for the 180 m depth model. A ±20 mm survey tolerance should be applied to these subsidence results.

The subsidence trough for both model depths is anticipated over the 918B1 panel due to shortwall extraction. The subsidence profile is relatively gentle where the strata above the spine pillars and barrier pillars is being compressed by the overburden. The maximum subsidence is greater in the 180 m depth model due to greater sag subsidence associated with a shallower environment and increased panel width to depth ratio.

Shortwall extraction (918A and 918B2)

The maximum model subsidence is 76 mm for the 280 m depth model. The maximum model subsidence is 71 mm for the 180 m depth model. A ±20 mm survey tolerance should be applied to these subsidence results. The difference in the subsidence profiles is due to the increase in depth.

The subsidence profile for the deeper 280 m depth model section is governed primarily by chain pillar compression. The panel width to depth ratio is 0.27, which would typically give a low level of sag subsidence. The subsidence profile for the shallower 180 m depth model section shows a combination of sag subsidence and chain pillar compression. The panel width to depth ratio of 0.42 suggests that the sag subsidence is going to be more prominent in the subsidence profile. The 180 m model chain pillar subsidence is less than the 280 m depth chain pillar subsidence due to the reduced abutment load on the pillar.

The maximum subsidence for 918 panel is predicted over the spine pillar between shortwall 918A and 918B2 with some bias to 918A where the greatest depth of cover is anticipated. There is not a significant difference between the maximum modelled subsidence across the depth range. However, given the maximum depth isn't consistent across both panels, the maximum subsidence may be less than the model 280 m depth.

A subsidence survey program is recommended to monitor subsidence during shortwall extraction to compare measured subsidence with the modelled subsidence estimates and to confirm the subsidence does not exceed the 100 mm subsidence limit. It is recommended that the survey control is located outside the angle of draw. A survey control at least 150 m beyond the 918 panel footprint should be sufficient.

Application of results to increased pillar size

The mine plan has an increase in the central spine pillar width inbye of 21 cut-through, from 20 m to 26 m. The model includes the more conservative pillar width scenario with the 20 m central spine pillar. The increase in the central spine pillar width is anticipated to reduce the average load on the pillar and as a result, provide a small reduction in the surface subsidence.

6. ADDENDUM

Recommendations from the IEAPM review prompted an update to the modelling to address the following areas:

- The subsidence profile not extending to zero subsidence at the boundaries.
- The geotechnical assumption of massive sandstone strata (represented by the removal of pre-existing joints and bedding) in the Burra Moko Head and Banks Wall Sandstones.
- A sensitivity analysis to address the potential uncertainty or error margin.

6.1 Summary

To address the IEAPM recommendations and to update the modelling to include the widening of the spine pillar, SCT ran the following changes to the original models (base models) at the 180 m and 280 m depth scenarios:

- Increase in central spine pillar width to 26 m – as per the mine design.
- Longer model equilibration run time pre-extraction.
- Increased model distance to boundaries to 1400 m.
- Reduction in coal modulus of spine pillars from 3 GPa to 2.5 GPa to account for 3D pillar geometry loading in consideration of cut-throughs.

The above changes to the original model reduced the maximum subsidence of the subsidence profile for 918A and 918B2 panels by approximately 20 mm.

To address the geotechnical assumption concerns and uncertainty analysis, SCT conducted the following parametric assessment to the updated model:

1. Removal of the massive sandstone assumption in the Burra Moko Head Sandstone and the Banks Wall Sandstone. The revised model includes a pre-existing joint and bedding network throughout the entire model. The effect of this change is less bridging at the top of the caved zone, resulting in an increase in sag subsidence, with an overall 2-5 mm increase in maximum subsidence.
2. An uncertainty model assessing the impact of reduced strata stiffness. The assessment was achieved by reducing the average stiffness (Young's Modulus) of individual rock types by 1 standard deviation of the rock property dataset. This creates a lower bound of possible overburden stiffness. The uncertainty analysis model was conducted in conjunction with the non-massive sandstone model assumption.

The outcome of the uncertainty analysis provided subsidence profiles with a maximum subsidence of 65 mm. The subsidence profiles for the three model scenarios are presented together with the original model outputs for the 180 m and 280 m depth models in Figure 22. The upwards shift in base model profile is evident, as well as the small increases in subsidence from the sensitivity assessments.

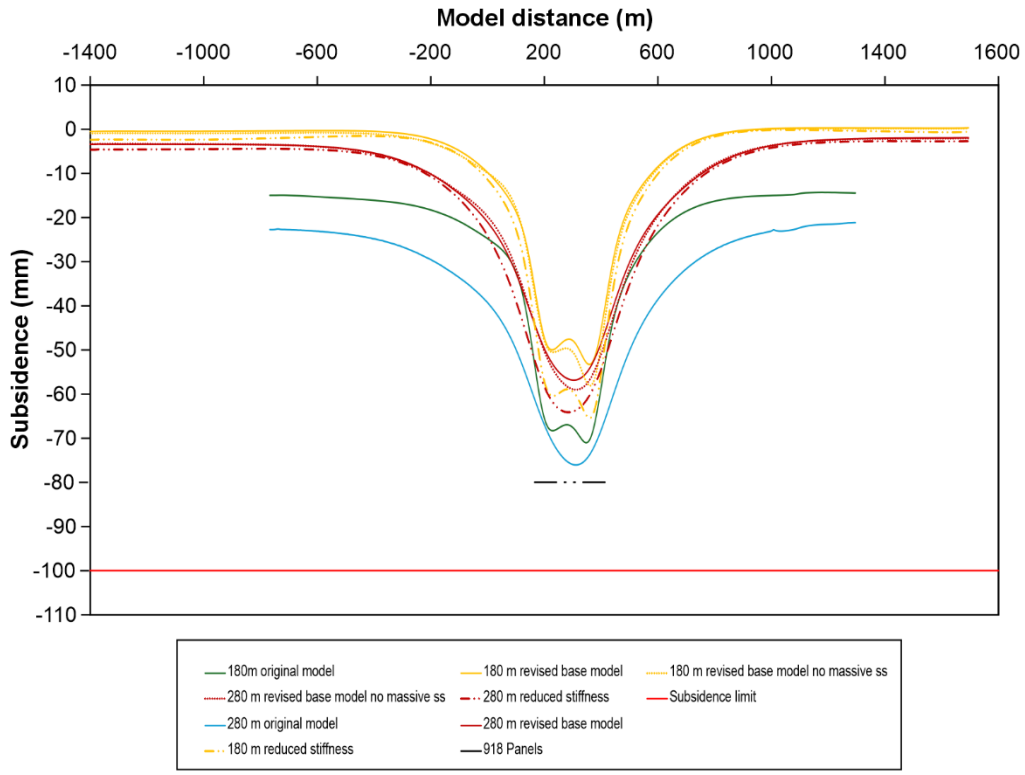

Figure 22: Subsidence profiles of 3 revised model scenarios compared with original model presented in report.

The revised modelling produced a maximum subsidence less than the original subsidence presented in Section 5.3.1 of this report. This reduction in subsidence is a result of the combined effects of model boundary and equilibration updates, increase in central pillar width, and uncertainty assessment with reduced stiffness of strata.

It is recommended that the original subsidence outcomes in this report be used for ongoing assessment as the more conservative outcome of the modelling assessments.

6.2 Further Detail on Updated Model Approach and Outcomes

6.2.1 Base model updates

The original model in this report showed the extents of the subsidence profile with an approximate 15-20 mm asymptote for the 180 m and 280 m depth models. It was found that this was due to a combination of inefficient model equilibration run time and boundary proximity prior to extraction. The updated models reduced the asymptote for the 180 m depth model to zero and the 280 m model to approximately 2-4 mm.

The updated models increased the proximity to the model boundary to ~1400 m. The equilibration run time was increased from 1000 steps to 50,000 steps, with model histories confirming model equilibration.

Two other key updates to the base model included:

1. Increase in pillar width to 26 m

The original models were based on an earlier mine plan where the central spine pillar was 20 m pillar wide. As an outcome of the geotechnical assessment, the central pillars were increased to 26 m. This updated pillar width is included in the updated model. The outcome of this increase in pillar width is expected to produce a lower average abutment load, and reduction in spine pillar compression subsidence.

2. Reduction in spine pillar coal modulus from 3 GPa to 2.5 GPa

   The model is a 2D representation of a 3D pillar geometry. A 2D model assumes an infinite pilar length, when in reality, the pillar has cut-throughs that reduce the pillar strength and increase the average tributary and abutment load.

   In this scenario, it is not considered appropriate to reduce the pillar width to account for this reduced pillar strength and increased vertical load, due to the impact a reduced pillar width has on the onset of strata softening above the pillar system. A key design component of the subsidence modelling assessment is to maintain elastic pillar compression by controlling fracturing and strata softening in the strata above the pillar. Therefore, maintaining the design pillar width is critical to this design criteria.

   A reduction in coal stiffness was applied to indirectly increase the strain in the coal pillar by a factor consistent with the cut-through ratio. i.e. cut-throughs create a 1.2 factor increase in load, and therefore a 1.2 factor increase in strain and compressive subsidence of the coal pillar for the ~2 m high coal seam.

   As the pillar stability assessment shows that the pillars have a long term stable FOS, the modulus reduction method is considered appropriate to allow for the 3D pillar geometry in the 2D model.

   The outcome of this change is anticipated to be in the order of 2 mm as the 2 m coal pillar hosts a small portion of the pillar compression subsidence that is largely comprised of the compression in the stress bulb.

6.2.2 Removal of Massive Sandstone Assumption

The massive sandstone strata assumption was included based on experience from Airly Mine modelling, the nature of cliff formation at Clarence and surrounds, and the observations and measurements of caving behaviour by others such as DgS in the Ditton height of fracturing model (Ditton, 2014).

The updated model scenario includes the removal of this massive sandstone assumption and continues the bedding and joint fracture network through the Burra Moko Head Sandstone and the Banks Wall Sandstone.

This model was not anticipated to substantially increase the subsidence due to the subcritical mining geometry and the location of these two units. The majority of the subsidence is pillar compression subsidence in the stress bulb. The massive sandstone units are not located in the horizon of greatest stress concentration of the stress bulb. The Burra Moko Head Sandstone is located at the top of the caved zone and has the potential to impact the transfer of sag subsidence to the surface through additional bridging capacity. This would be anticipated to be more evident in the shallower model than the deeper model.

The outcome of this model change, continuing the fracture network through the two sandstone units, produced a relatively small increase in subsidence. The maximum subsidence of the 180 m depth model is at the location of the individual panel troughs, while the 280 m depth model shows only one trough centred over the chain pillar. This is due to the pillar compression subsidence dominating the subsidence profile in the deeper model. The 180 m depth model showed a maximum subsidence increase of 5 mm, located in the individual panel troughs. The 280 m depth model showed a 2 mm increase in maximum subsidence, located in the single trough over the chain pillar.

6.2.3 Uncertainty Model

The primary mechanism producing the subsidence for the 918 model is the pillar compression over the spine pillar system. There are two geotechnical characteristics that have the greatest potential to increase subsidence from the base model. These geotechnical characteristics are listed and discussed below.

1. Reduction in system stiffness due to rock failure occurring in the strata above and below the mining horizon

   Reduction in system stiffness was a critical design component of the subsidence modelling assessment. Reduction in system stiffness occurs when there is fracturing of the strata above and below the pillar system due to the vertical load exceeding the confined strength of the strata. The narrower the pillar system width, the greater the risk of fracturing occurring in the strata above the pillars. The fracturing of the strata substantially reduces the stiffness of the strata from the intact strata stiffness.

   The mechanism of strata stiffness softening was observed at Airly Mine MW2-9, where subsidence magnitudes substantially greater than the allowable limit were observed. The SCT rock failure model was used to prove the mechanism of strata system softening from fracturing of the strata above the coal pillars, producing subsidence consistent with observations. Not only did the SCT model produce similar subsidence outputs, but it also produced the surface tensile fractures that were observed on the surface at Mt Airly. (Heritage et al, 2022)

   The SCT model was subsequently used to design Airly Mine's future panels under Mt Genowlan (MW13-16, MW17-18) with the key design consideration of managing the risk of strata softening to keep the subsidence within the 125 mm subsidence limit. These panels have since been mined and have provided validation of the design approach and model subsidence (Heritage et al, 2025).

   SCT brought this Airly knowledge to the Clarence shortwall numerical modelling subsidence design assessment. A key criteria was for the model to not show any onset of fracturing in the strata above the coal pillars and between the individual caved zones.

   Therefore, as system stiffness has been included as a design criteria for this assessment by assessing the rock failure in the model, it is not considered appropriate or realistic to artificially reduce the stiffness of the strata to below intact levels.

2. A lower modulus (intact stiffness) of the strata than used in the model

   Rock properties from the Clarence rock test database were compiled to characterise site specific rock properties and geotechnical relationships to inform the model input rock properties. Clarence provided a site derived sonic velocity to UCS relationship that was used to produce a UCS profile for the model lithology to the surface. Model lithology and rock properties are input in 1 m layers in the numerical model. Young's modulus for each 1 m rock layer is determined from a Young's Modulus to UCS relationship based on Clarence laboratory rock test data. There is a unique relationship for each lithology.

   SCT's experience and parametric modelling indicate that small variations in modulus for individual units or variations in lithology do not make material changes in the overall subsidence; a systemic or large offset in modulus is required to produce material changes in pillar compression.

   Figure 23 presents the Young's Modulus to UCS relationship for the induvial rock types of the Clarence rock test dataset. A reduction by one standard deviation in Young's Modulus is also presented for each rock type on Figure 23. This one standard deviation reduction in Youngs Modulus forms the lower bounds of the dataset and was applied to the model for the uncertainty analysis. The reduced modulus model was applied in conjunction with the removal of the massive sandstone assumption to provide a cumulative uncertainty result.

   The outcome of the uncertainty model analysis produced a further increase in subsidence of 7 mm for the 180 m depth model and 5 mm for the 280 m depth model.

The cumulative maximum subsidence for the updated models, including the uncertainty analysis was 65 mm for the 180 m depth model and 64 mm for the 280 m depth model. The maximum subsidence in the 180 m depth profile was located in the subsidence troughs located over the centre of each panel, while the maximum subsidence was located over the central pillar system in the single trough of the 280 m depth model.

The revised models produced a maximum subsidence less than the original model presented in the body of this report. Given that the original model is a more conservative estimate, it is recommended that the maximum subsidence from the original subsidence outcomes in this report be used for ongoing assessment.

6.2.4 Do these changes impact the 910-906 validation exercise?

The 906-910 Panel survey lines were not surveyed at the most optimal times in relation to the mining sequence. In the first subsidence survey after 910 panel completion, 908 Panel was already developed, and secondary extraction was approaching the survey line. Therefore, a confident 910 completion survey was not conducted.

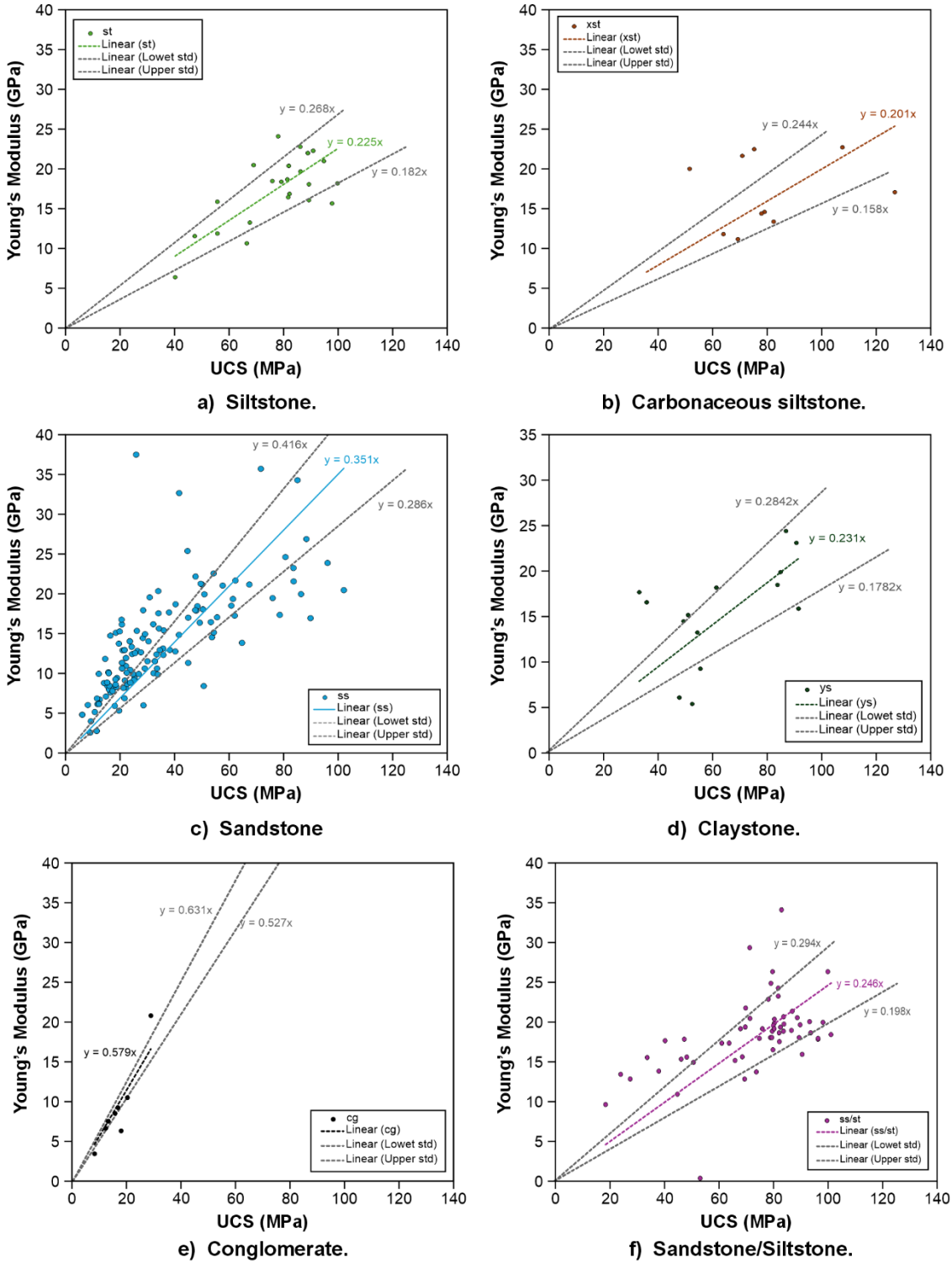

Figure 23: UCS versus Young's Modulus relationship for key rock types of the Clarence rock test dataset.

The 908 Panel survey line is the best example of a survey line for double sided lifting (close to full extraction) and prior to 906 panel development. The 908 Panel original model maximum is 113 mm greater than the 908 Panel cumulative subsidence survey maximum. Based on the revised 918 Panel modelling, a ~20 mm reduction in subsidence is considered possible, due to the improved model equilibration, model boundary proximity and reduced coal modulus. A reduction in subsidence of ~20 mm would produce subsidence within 10 mm of the survey data. This validation is within an acceptable level of tolerance.

Additionally, if the massive sandstone strata assumption was removed, the model subsidence would be anticipated to increase to be closer to the surveyed subsidence.

7. REFERENCES

Heritage, Y., Boyling, A. and Corbett, P., 2022. "Determination of the Subsidence Mechanism for Subcritical Miniwall Panels, Airly Coal Mine" In Proceedings of the Tenth Triennial Conference: Mine Subsidence Technological Society, Pokolbin, 2022: pp 111-119.

McNally, G.H., 1987. Estimation of coal measures rock strength using sonic and neutron logs. Geoexploration Amsterdam Volume 24. November 1987.

Mills, K., 2017. Subsidence Mechanisms about Longwall Panels - In Proceedings of the Ninth Triennial Conference: Mine Subsidence Technological Society, Pokolbin, 2017: pp 63-79.

Nemcik, J., Gale, W. and Fabjanczyk, M., 2006. Methods for Interpreting Ground Stress Based on Underground Stress Measurements and Numerical Modelling in Proceedings of Coal Operators Conference 2006.

SCT, 1992. Stress Measurements in the Immediate Roof 408 Panel – Clarence Colliery. CLR0329. 26 November 1992.

SCT, 1993. Lateral Stress Measurements in Roof Maingate 19 – 8 Cut-through. SPR0975. 12 October 1993.

SCT, 1996a. Virgin Stress Measurements – 401 Panel, 19 Cut-through, Springvale Colliery. ANP0222. 16 February 1996.

SCT, 1996b. Virgin Stress Measurements at the End of Maingate 21 Angus Place Colliery. ANP1032. 26 April 1996.

Seedsman R, Gordon, N and Aziz N, 2009. Analytical Tools for Managing Rock Fall Hazards in Australian Coal Mine Roadways, ACARP Project C14029. Published March 2009.

APPENDIX 1 – NUMERICAL MODELLING APPROACH

In this study a two-dimensional finite difference numerical model is used to assess the strata behaviour and mine subsidence resulting from secondary extraction. The development process of the model is outlined in Figure A1.1.

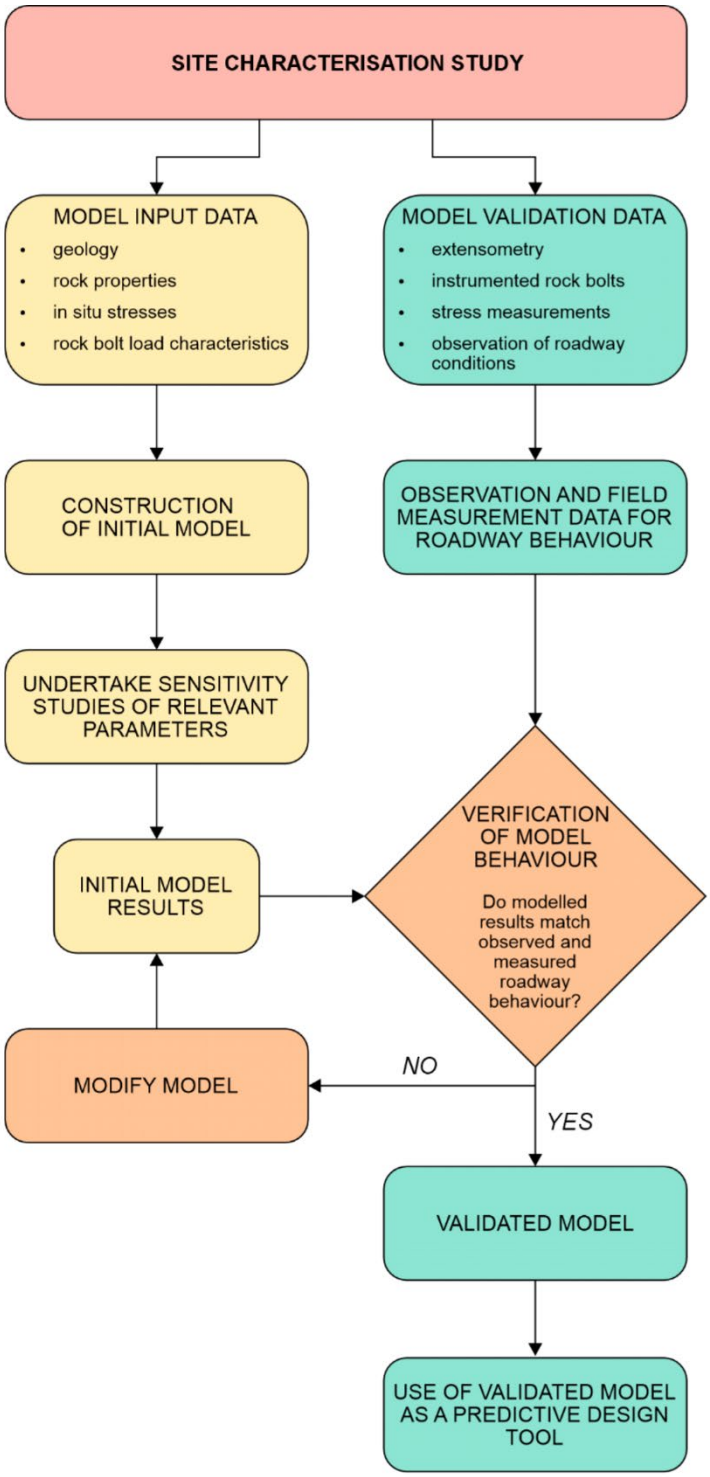

Figure A1.1: Computer model development process.

The two dimensional code used in the modelling process is FLAC2D. The rock failure routines used within FLAC have been developed by SCT. The mathematical framework for SCT's constitutive model is based on a Mohr-Coulomb approach where the Mohr-Coulomb failure envelope is defined using a bi-linear relationship defined by cohesion, internal friction angle and Mohr Circles. The constitutive model used by SCT is very similar to the bilinear strain-softening/hardening, ubiquitous joint model (SUBI) included in FLAC Version 8.1 (Itasca, 2024).

The model simulates new or re-activated rock fracture/s and stores the orientation of the fractures. Shear fracture, tension fracture of the rock, bedding plane shear and tension fracture of bedding is determined in the simulation using the SCT in-house rock failure routines. Shear banding is observed in model outputs where multiple zones (3 to 5 and greater) fail in shear together. The stability of pre-existing jointing, faults or cleat is also addressed in the simulations where appropriate.

Ground displacements, rock fracture and stress redistributions can be assessed within various rock units and geometries about the extraction panel. In the SCT constitutive model, as well as Itasca's SUBI model, the intact rock matrix exhibits strain-softening post-failure behaviour. A weakness plane of any orientation is also included in the model, and this weakness plane can also exhibit strain-softening behaviour.

It is well known that the nature and strength of strata is variable away from a sampled location and as such the rock units are best estimated as having a strength range rather than a single universal property. The strength within a unit may vary by approximately ±40 % within a normal distribution about the mean UCS value of the unit whilst maintaining the nominated value of Young's Modulus (stiffness). This approach allows for local variability in material properties to be accommodated within the modelling process.

Whilst UCS is varied, the internal friction angle of the material is consistent. The variation in UCS is used to redefine the cohesion of the material.

When the geotechnical strength parameters of the rock are overcome, which are assessed by the SCT rock failure routines, then the material properties of the strata are assigned residual geotechnical properties. The internal friction angle is maintained, and the cohesion is reduced to 0 as shown in Figure A1.2. The intact and residual strength properties are presented in Figure A1.2. The transition from intact to residual is controlled by FISH routine which drops intact cohesion to residual cohesion without the need to involve a strain excursion. This assumes brittle failure and is considered a conversative approach.

In the models the caved material forms the goaf. The goaf develops strength on the basis of:

i. An increasing stiffness with vertical strain.

ii. Confinement within the goaf material which has developed as a result of the overburden converging onto the goaf.

The goaf loading characteristics are based on field extensometer data, together with measured vertical abutment load balance and subsidence validation from previous studies. The general goaf loading characteristics are presented in Figure A1.2.

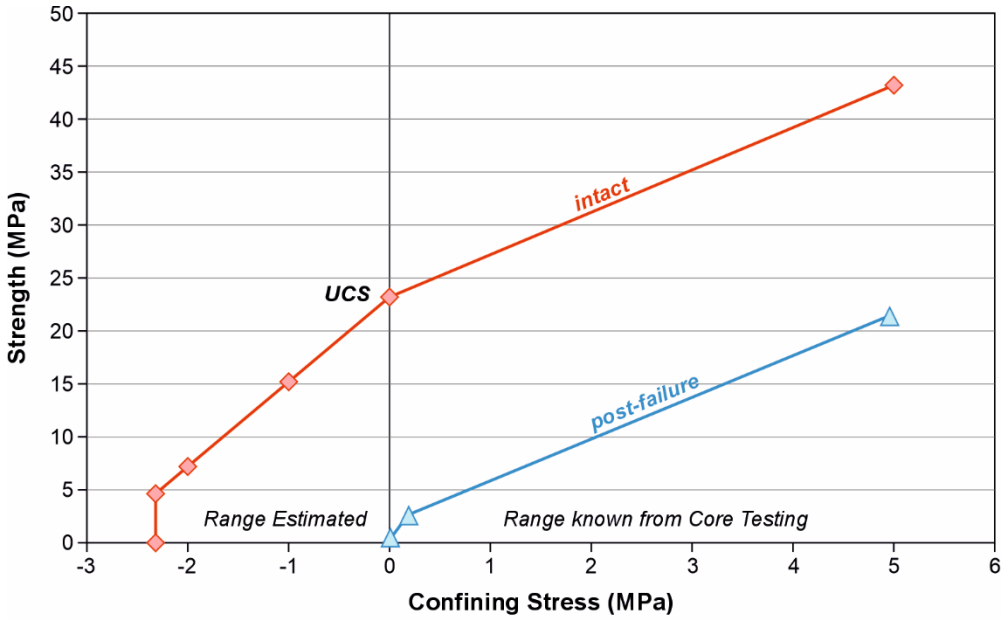

Figure A1.2: Generalised strength characteristics for rock units.

Jointing is incorporated within the model on a random manner with an average spacing of 4 m. Bedding plane partings are similarly included with an average vertical spacing of 3 m.

In the model, the rock properties utilised are:

i. UCS and tensile strength.
ii. Young's Modulus, Poisson's Ratio.
iii. Triaxial strength factor (relates to friction angle).
iv. Bedding plane cohesion, friction, and tensile strength.
v. Joint and bedding parting cohesion and friction angle.

Each rock unit defined in the model is characterised by these properties, however, for ease of visualisation, the UCS is used in the report to present the range in rock properties within the sections.

The coal seam is modelled on the basis of *in situ* strength rather than strength obtained from laboratory UCS testing of core. This is a standard approach due to the sampling problems with coal and the availability of large-scale measurements of coal.

The vertical stress is defined on the basis of lithostatic load and is equivalent to 2.5 MPa per 100 m depth based on a rock density of 2500 kg/m^3. The horizontal stress in each unit is a function of tectonic strain and "the Poisson effect" of the vertical stress. The horizontal stress in each rock unit is defined by the following relationship:

$$\sigma'_H = v/(1-v) \times \sigma'_V + TSF \times E$$ (Nemcik et al, 2006)

σ'_H = Horizontal stress (MPa)
v = Poisson's Ratio
σ'_V = Horizontal stress (MPa)
E = Youngs Modulus (GPa)
TSF = Tectonic Stress Factor

This relationship has been determined by stress measurements (Nemcik et. al. 2006) and indicates that the horizontal stress is related to the stiffness of the rock units (E) and the tectonic strain in the area. In general, horizontal stress is greatest in the stiffer units (high E) and is least in the coal.

The horizontal stress is input into the model for each layer or rock unit. The horizontal stress within a rock unit is composed of components relating to vertical stress (Poisson's Ratio effect) and from tectonic strain caused by crustal movements. The stresses relating to crustal movements are typically related to the stiffness of the unit and the higher the Young's Modulus of the unit the higher the stress within it.

However, adjustments are made to be consistent with the depth stress relationship of the area. In general, the horizontal stress is determined by the tectonic strain (formula used above) and stress modifications caused by faulting and slip along structures in the upper crust. These effects are incorporated in the stress field within the model.

1.1 Model Grid

Left hand side boundary conditions
Fixed pore pressure
Fixed in x-axis
Free in y-axis

Right hand side boundary conditions
Fixed in x-axis
Free in y-axis

Model base boundary conditions
Fixed pore pressure
Fixed in y-axis
Free in x-axis

Model surface (top) boundary conditions
Free in x-axis and y-axis

Model Grid Extents and Grading
The cross-section models are 1700 m wide. The depth of the model is dependent on the depth of the mining environment:

1. 910-906 models: 770 m total depth and is presented in Figure A1.3.
    a. 300 m depth of mining + 70 m below seam level + 400 m non-detailed grid.
2. 918 models (280 m mining depth): 750 m total depth and is presented in Figure A1.4.
    a. 280 m depth of mining + 70 m below seam level + 400 m non-detailed grid.
3. 918 models (180 m mining depth): 650 m total depth and is presented in Figure A1.5.
    a. 180 m depth of mining + 70 m below seam level + 400 m non-detailed grid.

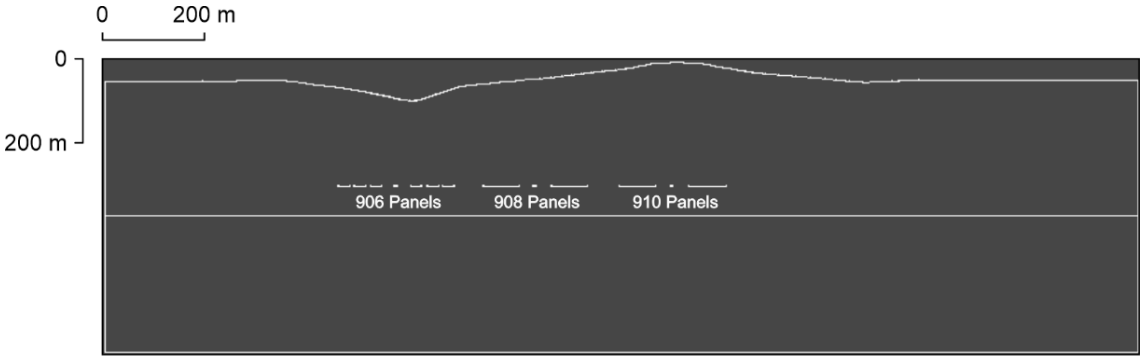

Figure A1.3: 910 to 906 Panel Model full extents.

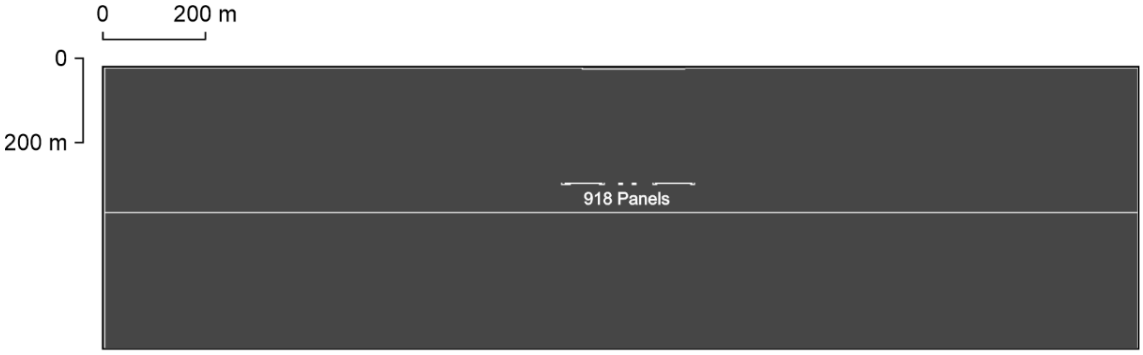

Figure A1.4: 918 280 m depth Model full extents.

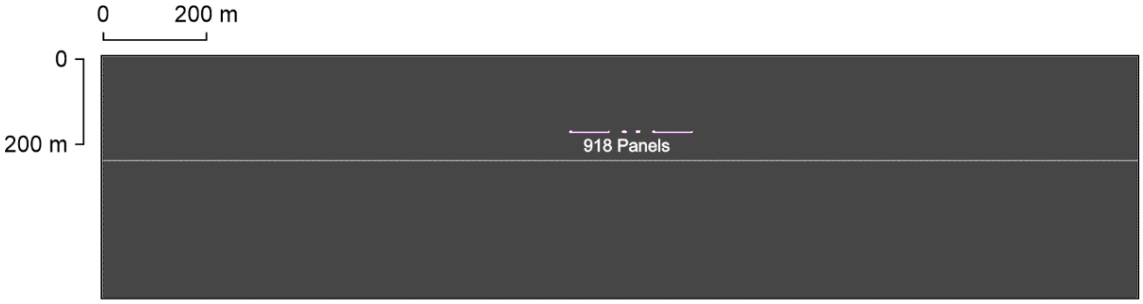

Figure A1.5: 918 180 m depth Model full extents.

The cross-section model environment – used in the Clarence assessment – has 1 m square element that exist around the area of mining and area of interest, extending to the surface. The grid height at the seam level has been adjusted to accommodate the variation in mining height for the different mining scenarios modelled.

The 1 m square element extend 70 m below the coal seam. Beneath this the grid begins to grade out over 400 m, there are 30 elements vertically with a ratio of 0.9. The 'detailed' model extends from 0 m to 1500 m. The grid grades laterally from the right hand side boundary over 200 m at a ratio of 1.1.

1.2 Pre mining and Post mining stress states

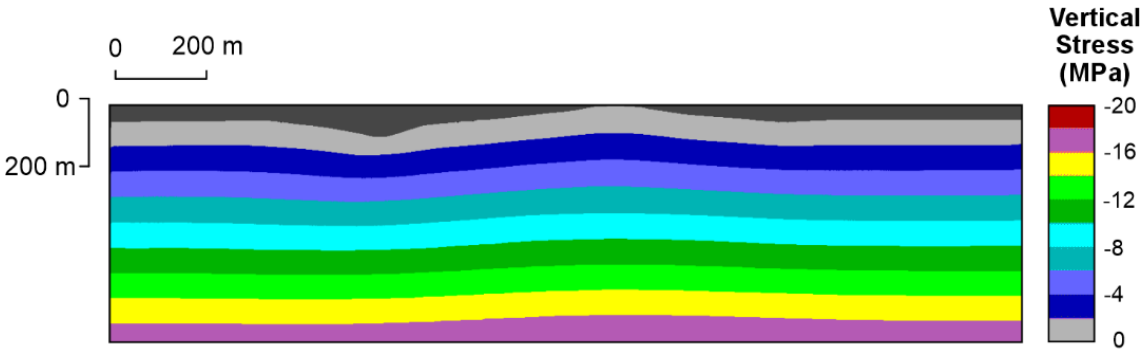

Vertical stress.

Figure A1.6: Pre-mining stress environment for 910 to 906 panel model.

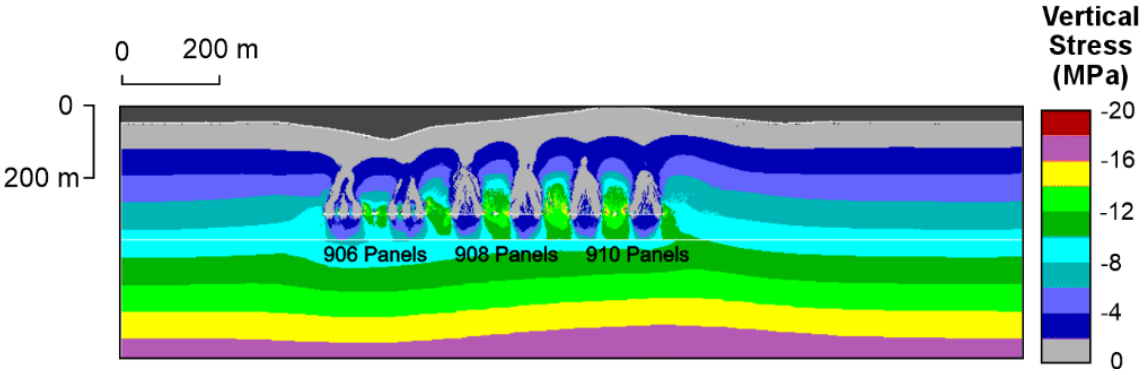

Vertical stress.

Figure A1.7: Post-mining stress environment for 910 to 906 panel model.

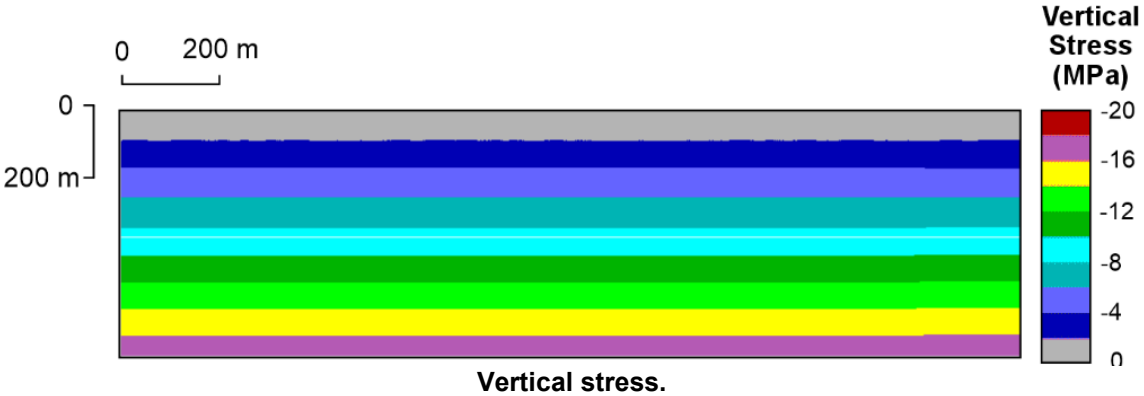

Vertical stress.

Figure A1.8: Pre-mining stress environment for 918 panel 280 m depth model.

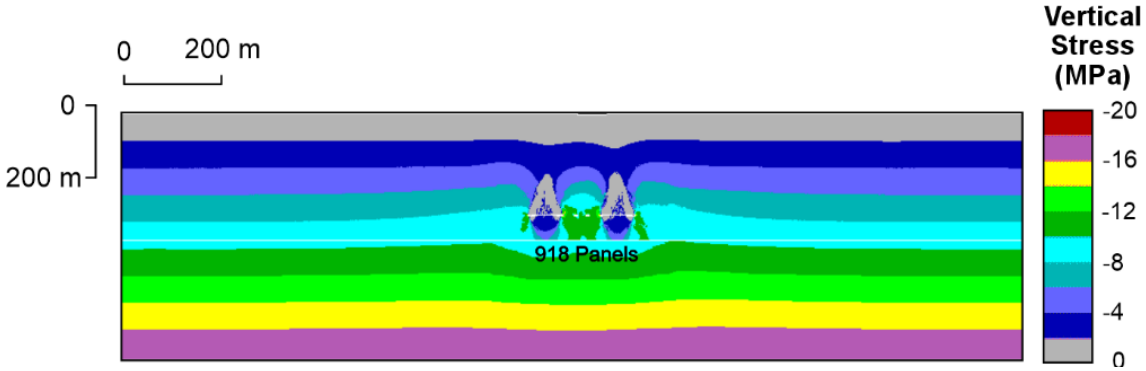

Vertical stress.

Figure A1.9: Post-mining stress environment for 918 panel 280 m depth model.

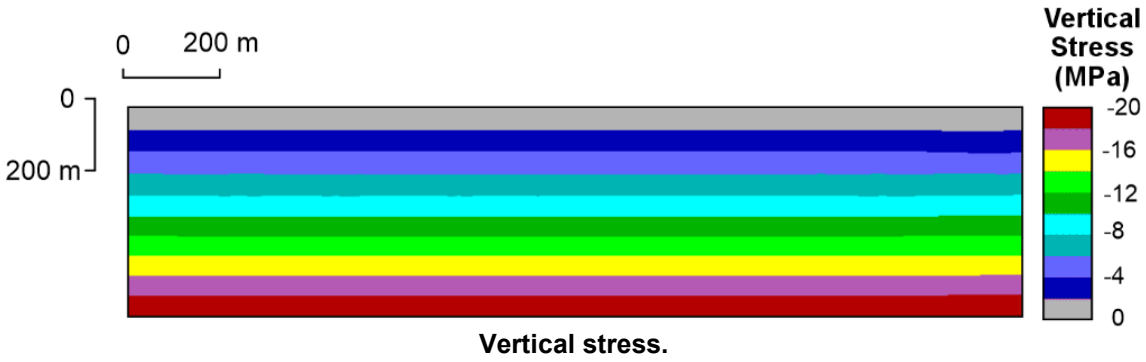

Vertical stress.

Figure A1.10: Pre-mining stress environment for 918 panel 180 m depth model.

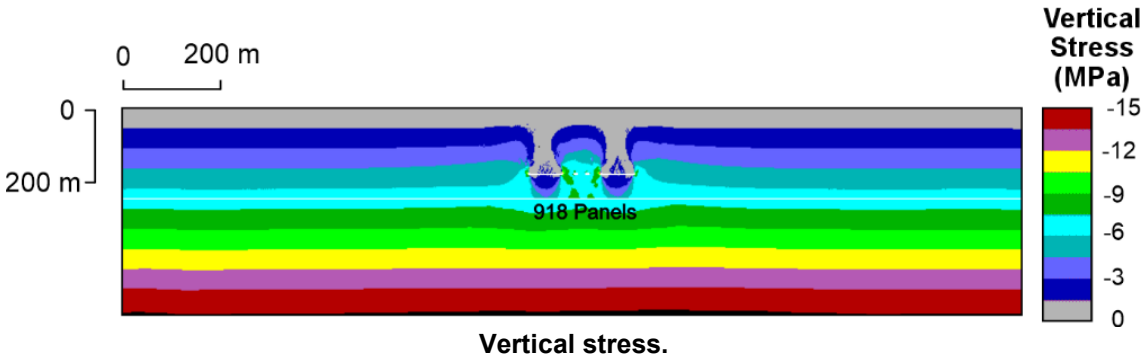

Vertical stress.

Figure A1.11: Post-mining stress environment for 918 panel 180 m depth model.

1.3 Post mining vertical displacement

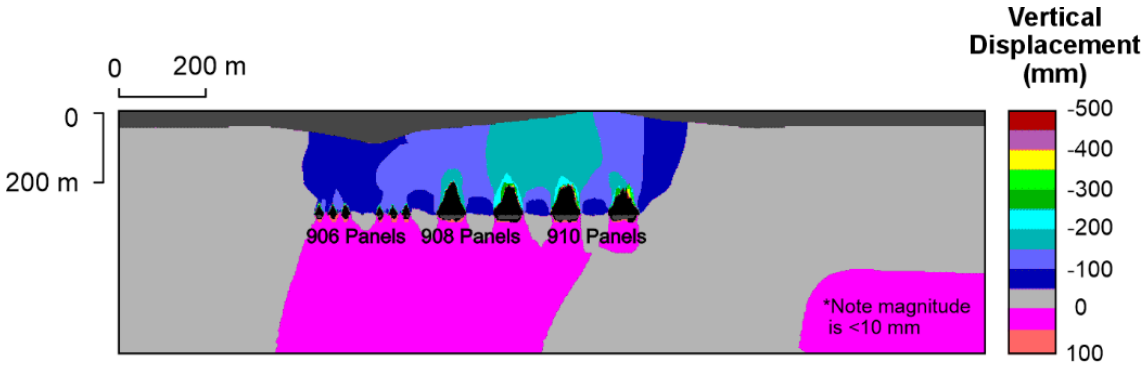

Figure A1.12: Vertical displacement post mining for 910-906 panel modelling.

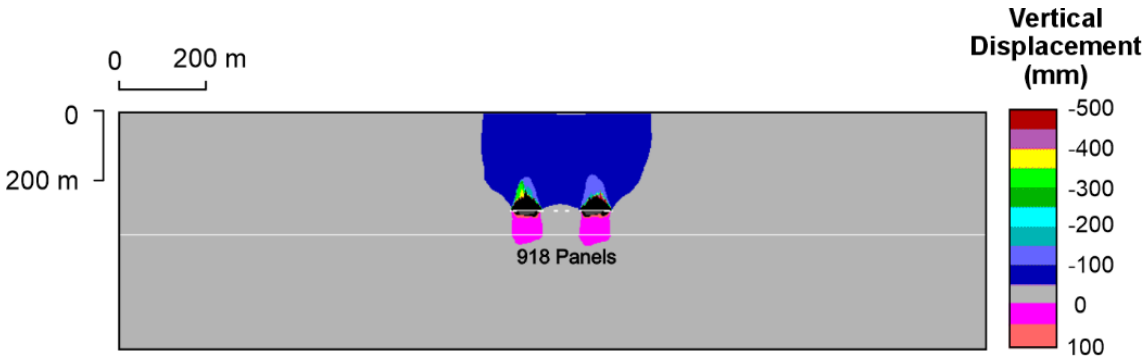

Figure A1.13: Vertical displacement post mining for 918 panel 280 m depth modelling.

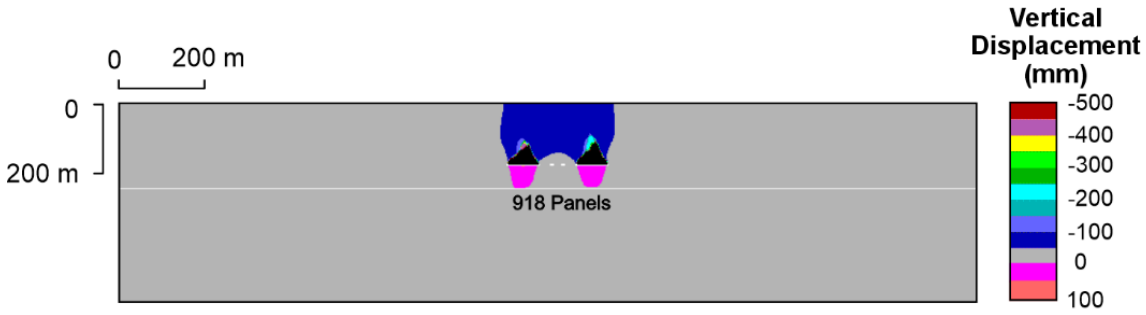

Figure A1.14: Vertical displacement post mining for 918 panel 180 m depth modelling.

1.4 Modelling Extraction Methodology

The model grid is generated using the extents and boundary conditions presented previously. The stresses are initialised, and the model is then stepped to in order to reach an initial steady state. Displacements are reset to zero providing an equilibrated pre mining model.

SCT's experience in simulating the nature of rock failure and caving in a 2D model has informed the panel extraction methodology. The 2D panel is extracted (by nulling the elements) from the centre out to the panel edge in 2 m increments to the predefined panel width. This approach is designed to simulate real-world out of plane caving fractures in the 2D model and experience has shown this approach provides a reasonable representation.

The extraction height is predefined based on the mining geometry. In the case of shortwall mining the shortwall is extracted using the methodology described above.

After each incremental excavation, the stress and strain is allowed to redistribute using standard FLAC computation. Once the top of the excavation boundary meets the floor elements, these elements are restricted from moving past the floor elements and goaf loading is transferred through to the floor.

References

Gale, W. and Sheppard, I., 2011. Investigation into abnormal increased subsidence above longwall panels at Tahmoor Colliery NSW. In Proceedings of the Eighth Triennial Conference on Management of Subsidence, Pokolbin, NSW: Mine Subsidence Technological Society, 2011: pp 63-79.

Nemcik, J., Gale, W. and Fabjanczyk, M., 2006. Methods for Interpreting Ground Stress Based on Underground Stress Measurements and Numerical Modelling. In Proceedings of Coal Operators Conference 2006.

APPENDIX 2 – MODELLING MODES OF ROCK FAILURE

Legend	Explanation
None	No rock failure has occurred.
Shear fracture and reactivation	The rock matrix has failed in shear. Conjugate failure planes can occur during this process. The two colours signify which general orientation, between the two (i.e. upper left to lower right or upper right to lower left), is most likely to occur.
Bedding shear and reactivation	The rock unit has either failed by shear of intact material along bedding or a previously failed bed has undergone further shear.
Tension fractures reactivated in shear	The rock unit which initially failed in tension has undergone shear movement.
Tension reactivation of shear fractures	A shear fracture that is opening under tension. The two colours are used depending on the most likely conjugate shear fracture that occurred on initial shear failure.
Tension fracture	The rock matrix has failed in tension.
Tensile failure of bedding and reactivation in tension	The rock unit has either failed by tension across the bedding or a previously failed bed has undergone further tensile opening.
Shear failure of intact rock	The rock matrix has failed in shear.
Pre-existing joint or cleat shear reactivation	A pre-existing joint or cleat has undergone shear movement along its joint or cleat surface.
Pre-existing joint or cleat tensile reactivation	A pre-existing joint or cleat has undergone tensile opening along its joint or cleat surface.
Mohr failure criteria	The Mohr failure criterion is initiated when the rock unit has the potential to fail by multiple modes (3 or more).

APPENDIX 3 – COMPOSITE LOG OF CLRP27

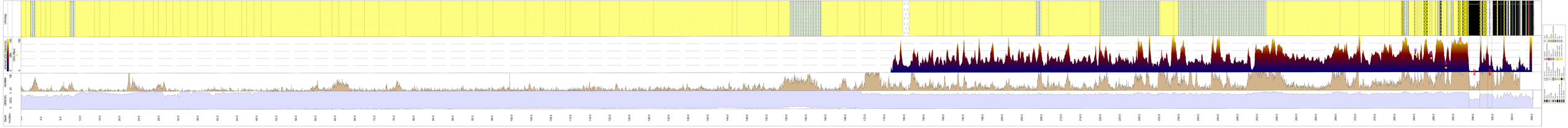
Libsvip
Sample 1 ATAC Fragments
Sample 1 ATAC Peaks
Sample 1 ATAC Coverage
Sample 1 ATAC Transcripts
Sample 1 ATAC Genes

APPENDIX 4 – TRIAXIAL STRENGTH TEST RESULTS FROM SPRINGVALE MINE

TABLE 4 Laboratory Rock Testing Results

Samples		UCS Test #			Triaxial Test ##					Brazil Test		Porosity	Dry Density	Bulk Density
Rock Type	Depth	UCS	Tangent Modulus	Moisture Content	Friction Angle	Cohesion	UCS	Modulus	Moisture Content	Tensile Strength	Moisture Content			
	metres	MPa	GPa	%	degrees	MPa	MPa	GPa	%	MPa	%	%	t/m^3	t/m^3
SS + STclasts	68.0 - 68.55	16.3	8.5	7.6						2.06	5.1	9.1	2.41	2.39
Congl SS	100.81 - 101.23				39	7	24	9.5	7.6	1.47	4.6	9.8	2.25	2.33
Congl SS	132.41 - 132.97				37	8	30	11.9	3.5	1.50	4.2	11.5	2.20	2.43
Claystone	152.4 - 152.77				26	12	38	8.2	2.2	3.56	2.1	5.1	2.59	2.67
Congl SS	166.88 - 167.59	39.4	5	2.1						2.66	5.1	5.1	2.53	2.57
SS f-m	192.47 - 192.9	48.5	14.9	2.6						4.29	3.1	7.8	2.41	2.53
SS f + ST lam.	234.05 - 234.37				32	13	46	8.4	1.8	5.31	1.9	4.6	2.59	2.62
SS f tuffaceous	251.16 - 251.71	51.6	8.4	4.7						4.77*	5.5	13.3	2.22	2.46
SS f-m lithic	287.06 - 287.36	43.6	11.6	3.3						1.32**	4.5	10.2	2.49	2.56
ST + SS lam.	314.96 - 315.24				19	23	64	10.4	3.4	3.87	4.2	8.7	2.41	2.57
SS f + ST lam.	339.19 - 339.66	141.6	21.6	2.9						14.65	2.7	6.5	2.44	2.50
ST + SS lam.	348.83 - 349.42				26	7	21	4.1	6.3	3.18	6.2	12.8	2.26	2.39
SS/ST disturbed bedding	369.62 - 370.04	35.6	8.8	4.8						5.43	4.0	10.4	2.30	2.45

SS - Sandstone ST - Siltstone Congl - Conglomeritic lam - laminations f - fine grained m - medium grained

\# Unconfined Compressive Strength (UCS) Test

Triaxial Test - UCS was calculated from stress plot and the Modulus was calculated from the reload curve at 2 MPa confining stress

* Three samples of finer grained part of sample were averaged at 4.77, and two coarser grained samples were 22.06 and 10.85

** 2 samples averaged. Normally 5 samples are tested and averaged for the Brazilian indirect tensile strength